The scaling of population growth of conifer invasions in New Zealand

---

A thesis
submitted in partial fulfilment
of the requirements for the Degree of
Doctor of Philosophy

at
Lincoln University
by
Rowan Ingram Sprague

Lincoln University
2018

Abstract of a thesis submitted in partial fulfilment of the requirements for the Degree of Doctor of Philosophy.

The scaling of population growth of conifer invasions in New Zealand

by

Rowan Ingram Sprague

In ecology, we often want to answer questions about how populations change at broad spatial scales, but we frequently lack data at these scales. To fill this knowledge gap we typically extrapolate from small-scale observations, but common methods ignore spatial processes such as the neighbourhood effects of density and dispersal which have a large effect on plant populations. In this thesis I will use aerial imagery to develop new methods to measure scaling population growth. I will use this approach to show that broad scale processes slow population growth of conifer invasions in New Zealand.

To do this, first I assessed the utility of using aerial imagery for detecting invasive conifers across different densities. Using data of trees measured in the field and detected from aerial imagery, I found that aerial imagery has a tendency to detect trees inconsistently across densities. However, for the mid-to-large-sized trees, this detection bias mostly disappeared and the imagery could reliably detect this size of trees. Due to this detection bias from density, I then examined the effects of detection bias on the estimates of scaling up population growth using simulations. I showed that even though there is a detection bias from aerial imagery, I am confident that this bias will not affect the estimates of population growth and scaling. Finally, using data collected from aerial imagery of eight conifer invasion sites across the South Island of New Zealand, I asked whether spatial processes have a large effect on the population growth of alien conifers. I expanded upon existing methodology to enable me to account for spatial processes in dynamic, rapidly changing systems. In doing so, I developed the method to factor in dispersal and the effects of density using a Bayesian spatial random effects model. I found that broad scale spatial processes slow population growth in conifer invasions.

This study is the first of its kind to link data from aerial imagery to population dynamics models to test for the effects of spatial processes. Furthermore, a dataset of this scale, detail, and timespan has never before been collected for alien conifer invasions. By the end of this thesis, I will prove that spatial processes have a large effect on the population dynamics of invasive conifer trees. I show that when

we scale up population growth from a small to broad spatial scale and we ignore the effects of space, we will vastly over-estimate the ability of a population to grow.

Keywords: spatial processes, wilding conifers, spatial scale, scale transition theory, mean field population growth, aerial imagery, detection bias, observation error, density dependence, intrinsic growth rate, spatial structure, landscape demography, in-filling

Acknowledgements

I first would like to thank my supervisors, Will Godsoe and Phil Hulme. You were a great team and offered me so many hours of guidance and advice. You both helped me become a better scientist, critical thinker, and writer. Will, thank you for all of the whiteboard sessions and fun ideas. You taught me the value of looking at a question with a different perspective and to remember that science should be fun. Phil, thank you for encouraging me to think about the biological significance of my work and teaching me how to formulate a good research question and place my project in a wider context. Thank you also for putting up with Will and I getting excited about equations and math! To both of you, I appreciated all of your insights, whether they were about one of my drafts or a discussion in lab group. Thank you both for supporting me through this journey!

I would also like to thank all of the people who helped me with figuring out the details and execution of my PhD. Thank you, Duane Peltzer, for assessing my work earlier on and offering so many great insights and ideas. These really helped form my questions and research direction. Thank you, Stella Belliss and Steven McNeill, for lending me the Manaaki Whenua Landcare Research GPS and giving me advice on spatial analyses. Thank you, Larry Barrows, for your knowledge of wilding conifers in New Zealand and for providing advice on sites for my image analyses. Thank you, Steve Palmer, for more advice on sites and wilding pine invasions in Canterbury. I also received great feedback and ideas from the Ecological Modeling group at Manaaki Whenua Landcare Research for my population growth models in Chapter 4; thank you all for your suggestions. A big thank you to Elena Moltchanova from the University of Canterbury for your help and ideas with my population growth models and confirming my interpretation of the statistics. Thank you to Pete Raal from the Department of Conservation for ideas about how to connect my research, particularly in Chapter 2, to the management of wilding conifers. I would also like to thank Peter Willemse from the Department of Conservation for information about conifer invasion sites, particularly in the Mackenzie Basin.

Thank you to the aerial imagery team at Land Information New Zealand for providing the fantastic resource of orthorectified aerial imagery. Thank you also to the imagery team at Google Earth for providing all of the satellite imagery as well. I think it is safe to say that my PhD would be quite different without these data!

A huge thanks as well to all the people who helped me complete my fieldwork. Thank you so much to Nick Ledgard and Gordon Baker for providing me with access to the Mt Barker site and for sharing with me your knowledge about the site and the invasion. Thank you so much to Johnathon and Brendon Ridden for sacrificing your weekends and assisting me with my fieldwork. I really appreciate you giving so much of your time to help me measure all of those trees.

I could not have completed my PhD without the financial support I received. A big thank you to the Bio-Protection Research Centre for my PhD scholarship which paid for my fees and stipend as well as

provided me with research funds. Another big thank you to the Hellaby Trust for their financial support which paid for my fieldwork.

Thank you to the Bio-Protection Research Centre operations and administration team, Andrew Holyoake, Sandy Wilson, Dianne Fyfe, Claire Tee, Michelle Boyle, and Ashley Campbell. You all made sure that everything ran smoothly and were always so prompt with answering my questions, even if I probably had already asked the question before.

I am also very grateful for the wonderful community of students and staff in the Bio-Protection Research Centre. I would like to say a great giant thank you to my officemates, Tyler Brummer, Tom Carlin, Andrei Costan, and Sandra Savinen. Thank you for all of the many laughs- even when I was feeling unmotivated and stressed, you all could always make me laugh and smile. I cannot tell you how much that meant to me and helped me. Thank you also for always being so understanding and kind even when I was grumpy – thank you for being great friends! I am very grateful to the wonderful people of Twisted Minds as well. Thank you all for your friendship and all the adventures.

Thank you so much to the Ridden Family, Jillian, Craig, Brendon, and Snow. You all welcomed me into your family with such open arms and supported me through all of this. You helped me remind myself why I was working on wilding conifers and offered a home away from home for me.

A gigantic thank you to my family back in beautiful Virginia, Mama, Papa, Mary, Nick, Lucy, Eliza, and little Leona. Even though you were miles away, you still made me feel like you were close. You provided my work and challenges with context and always asked me how things were going and listened to my excitements and obstacles. All of your notes of encouragement in the last few months helped me so much to push through all of the work and finish this thesis. I cannot thank you enough for those notes and for your support! Thank you all to the group family chat for sending me love and thoughts as well as happy photos. I love you all so much and thank you for your encouragement!

Finally, I could not have finished this PhD without the never-ending support of my partner, Johnathon Ridden. You believed in me even when I didn't, and you were there with me every step of the way. You were there with me to celebrate the small victories and were there when I felt crushed, overwhelmed, and way too stressed. Especially near the end of my PhD, you found new and creative ways to show me how much you cared for me and knew that I could finish. Thank you for putting up with my craziness of signing up for probably too many extra side projects to do and thank you for supporting me through all of them. Every day you were there to listen, bounce ideas off of, and read drafts. Thank you for sacrificing your evenings and weekends to brainstorming or discussing how to reframe an introduction. Thank you for pulling me away from the computer when I needed to put work down, thank you for reminding me to look after myself, thank you for creating a place of calm in the middle of some tough challenges! Thank you for being the best partner for me and my #1 cheerleader!

Table of Contents

List of Tables

List of tables in Appendices

List of Figures

List of Figures in Appendices

Chapter 1
Introduction

Some of the most pressing ecological issues we face today occur at large spatial scales (Gurevitch, Fox, Fowler, & Graham, 2016). With the climate rapidly changing, we want to know how species will respond and how these responses might vary globally (Clark, Bell, Hersh, & Nichols, 2011; Cotto et al., 2017; Jump & Peñuelas, 2005). Furthermore, as the number of species introductions to new areas increases, we want to know which drivers lead to species establishment success and how the local communities will respond (Early et al., 2016; Mesgaran et al., 2016; Yokomizo, Takada, Fukaya, & Lambrinos, 2017). These large-scale phenomena can have cascading and very varied effects down to the local scale (Castorani et al., 2015; Queenborough, Burnet, Sutherland, Watkinson, & Freckleton, 2011). However, we do not know how population dynamics of species translate between local to regional scales (Griffith, Salguero-Gómez, Merow, & McMahon, 2016).

Scaling up population growth from a small to large scale is difficult because of the potential influence of spatial processes (Freckleton & Watkinson, 2002; Griffith et al., 2016; Gurevitch et al., 2016). Spatial processes can be defined as those mechanisms or factors which affect a population's growth and vary across space (Tilman, Lehman, & Kareiva, 1997). In this thesis, the main spatial processes of concern are dispersal, variation in density, and the effects of density on a population's growth (Law, Murrell, & Dieckmann, 2003; Nathan & Muller-Landau, 2000). Therefore, we need a robust method to estimate how spatial processes change population growth.

Ambiguities due to the scaling of population growth in ecology are well documented (Levin, 1992; Levin & Pacala, 1997; Wiens, 1989). Ecologists have long known that a study's scale of observation affects the findings on population growth (Dorken, Freckleton, & Pannell, 2017; Levin, 1992; Paradis, Baillie, Sutherland, & Gregory, 1999). While the scale dependence of population growth has been recognised, many studies have speculated about scaling up population growth. For example, Bocedi et al. (2012) tested what happened to estimates of dispersal and population growth when the plot size was increased from a fine to a coarse resolution. The authors found that when they attempted to scale up population growth estimates by simply looking at a coarser resolution, they tended to over-estimate the population abundance as well as the dispersal distances (Bocedi et al., 2012). In a similar message, Turnbull et al. (2007) found that the spatial arrangement of individuals can affect the population growth and therefore upscaling population parameter estimates is complicated. Time and time again, studies have identified both the importance of scaling up population growth and the complexity of doing so (Bocedi et al., 2012; Freckleton & Watkinson, 2002; North & Ovaskainen, 2007; Pagel & Schurr, 2012).

Few studies have actually attempted to scale up population growth data. Therefore, there is a disconnect between the scale at which ecologists often collect data and the scale at which ecologists want to study and answer questions about broad-scale phenomena (Hirt et al., 2018; Sandel & Smith, 2009). Often because of limited cost and time, most studies are only conducted at a small spatial scale (less than one hectare) even when they aspire to be relevant for regional spatial scales (Dunham & Beaupre, 2001; Estes et al., 2018; Salguero-Gómez et al., 2015). Additionally there is a growing demand for studies examining phenomena occurring over vast spatial scales (Hampton et al., 2013; Hogg, Huvenne, Griffiths, & Linse, 2018; Soranno & Schimel, 2014).

In this thesis, I will address this emerging opportunity of improving the link between broad scale demography and local scale population growth. In order to do this, we need to first understand the effect of spatial processes on demography. I will focus this introduction on plants because these taxa are the focus of the rest of the thesis. As sessile organisms, it is likely that spatial processes could have interesting and variable effects on a plant population's growth (Law & Dieckmann, 2000; Law et al., 2003).

1.1 How spatial processes affect the scaling of plant population growth

The following mechanisms affect the spatial structure and thus the scaling of plant population growth: biotic interactions, environmental factors, seed dispersal, and density dependence (Dieckmann, Law, & Metz, 2000; Nathan & Muller-Landau, 2000; Turnbull et al., 2007). Biotic interactions, or those interactions which occur between species or communities, affect the success of a population through the positive (such as mutualist or commensalist) or negative (competition or amensalist) effects (Bolker, Pacala, & Neuhauser, 2003; Wisz et al., 2013). Environmental factors such as soil type or climate will alter where a population will grow as well as how quickly it will grow (Dale, 1999). Seed dispersal is an inherently spatial process and a key component of population growth (Cousens, Dytham, & Law, 2008; Dieckmann, O'Hara, & Weisser, 1999). It determines the area where plant recruitment will occur, thus influencing the subsequent spatial arrangement of individuals (Nathan & Muller-Landau, 2000). Another reason why spatial processes can affect population growth across spatial scales is because an individual plant can grow differently in response to its neighbourhood density. When a plant's per-capita growth rate changes with density of surrounding trees or its neighbourhood, this is known as density dependence (Peters, 2003; Zhu, Woodall, Monteiro, & Clark, 2015). Each of these mechanisms acts at different spatial scales, thereby changing the scaling of population growth (Gurevitch et al., 2016).

To simplify the scope of this thesis, I will only focus on single, separate populations and will not focus on communities. Therefore, while biotic interactions are an important spatial process which shape population growth across spatial scales, I will not include them in this thesis. The other three mechanisms can be organised into two broad categories, dispersal and the effects of density (i.e.,

nonlinear growth) (Chesson, Donahue, Melbourne, & Sears, 2005; Nathan & Muller-Landau, 2000; Svenning et al., 2014).

As a main component of demography, seed dispersal governs the future growth of a population because it shapes a population's future spatial structure (Beckman & Rogers, 2013; Howe & Miriti, 2004). Dispersal is a localised process because it depends on the location of the parent plant and the surrounding environment (Cousens et al., 2008). Furthermore, dispersal also interacts with local competition between individuals to form a trade-off for plants in which if local competition is high, then long distance dispersal can be favoured at the risk of less suitable habitat (North & Ovaskainen, 2007; Starrfelt & Kokko, 2010). However, dispersal can be both short and long distance, thereby driving spatial structure at both local and regional scales (Beckman, Bullock, & Salguero-Gómez, 2018; Fletcher & Westcott, 2013). Dispersal therefore is affected by the current spatial structure of a plant population and it shapes the future spatial structure of a population across scales (Beckman & Rogers, 2013; Caughlin, Elliott, & Lichstein, 2016). Thus the spatial process of dispersal affects the scaling of population growth.

A major reason that broad scale processes alter population growth is that organisms respond to variation in population density (Chesson, 2012; Gravel, Guichard, & Hochberg, 2011). The density of a plant population often differs greatly across a region. Environmental variables make some areas more suitable for plant growth than others, causing some areas in a landscape to have dense areas of plants while others have few or no plants (Dale, 1999).

The spatial process of density dependence also affects the scaling of population growth. Density dependence can be negative, in which case per-capita growth rate declines at higher densities of other individuals. This is often described as intraspecific competition (Casper & Jackson, 1997). Some examples of types of negative density dependence are lower rates of seedling establishment close to parent trees due to pathogens and pests (Connell, 1971; Janzen, 1970), competition between saplings and adults (Hubbell, Condit, & Foster, 1990), and higher rates of adult mortality in denser stands (Castagneri, Lingua, Vacchiano, Nola, & Motta, 2010).

Density dependence can also be positive, in which case per-capita growth increases at higher densities of individuals (Holmgren, Scheffer, & Huston, 1997). Some examples of positive density dependence are ectomycorrhizal infection increasing the growth of seedlings at intermediate distances from adults (Dickie, Schnitzer, Reich, & Hobbie, 2005), frugivorous birds dispersing trees' seeds in aggregated areas (Spiegel & Nathan, 2012), and higher densities of a tropical forest tree attracting more bee pollinators to their flowers (Ghazoul, Liston, & Boyle, 1998). These density dependence trends in plant growth cause spatial patterns such as aggregation and over-dispersion (Dieckmann et al., 2000). These changes in spatial structure can then affect dispersal, feeding into more changes in future spatial structure at varying spatial scales.

The regional population growth rate is a result of the processes of dispersal, the variation of density, and density dependence (Chesson et al., 2005). However, averaging the effects of these processes across a region does not necessarily equate to their effect at the broad scale (Chesson, 2012). This is because the average is not the same as the components themselves at fine scales (known as the 'fallacy of the averages' or Jensen's inequality (Chesson, 1998; Rastetter et al., 1992)). As such, the average dispersal and effects of density on an individual would not be the same as they are at a local scale (Ovaskainen & Cornell, 2006). This is because averaging density and the effects of density across a large area effectively ignores the effect these spatial processes have on population growth (Murrell, Dieckmann, & Law, 2004). Therefore we need a way to account for these spatial processes in order to properly scale up population growth.

1.2 Ways to account for spatial processes

Several methods have been proposed which seek to capture and scale up population growth. One method uses mechanistic Individual Based Models (IBMs) scaled between a local and regional scale and populated with specific life history data (e.g., (Vance, Steele, & Forrester, 2010)). A similar approach uses IBMs and transition matrices with mechanistic data of populations to scale IBMs at a fine-scale using transition probability matrices (Cipriotti, Wiegand, Pütz, Bartoloni, & Paruelo, 2016). Another method uses patch occupancy models in which patches can be occupied or unoccupied and are linked by dispersal (e.g., (Caughlin et al., 2016; Hanski & Ovaskainen, 2003; Ovaskainen, 2002)). A fourth method uses moment closure models to approximate the distribution of individuals over space, and density dependent effects among these individuals (e.g., (Barraquand & Murrell, 2013; Murrell et al., 2004; Ovaskainen & Cornell, 2006; Raghib, Hill, & Dieckmann, 2011)). Table 1.1 summarises examples of these methods along with their limitations.

Table 1.1 Examples and limitations of population growth scaling methods.

Method	Examples	Limitations
Mechanistic IBMs	Vance et al. (2010) created an IBM of density dependent death of a coral reef fish species, with the model variables based on field data	Dispersal can only occur at a low rate; substantial amount of life history data or assumptions are required (Urban et al., 2016)
Transition matrices coupled with IBMs	Cipriotti et al. (2016) simulated scaling up the spatiotemporal dynamics of a grass species in Argentina between a 0.15ha area to a 2500ha area	Requires a substantial amount of mechanistic data; method does not directly quantify density dependence; model has not been tested yet using field data (Cipriotti et al., 2016)
Patch occupancy models	Ovaskainen (2002) modelled the changing occupancy of butterflies over time in a heterogeneous habitat Caughlin et al. (2016) looked at how landscape features alter forest regeneration	Only suited for populations with metapopulation structure and if habitat patch number is reasonably large (Ovaskainen, 2002; Purves, Zavala, Ogle, Prieto, & Rey Benayas, 2007); method does not explicitly account for effects of density on growth (i.e., density dependence)
Moment Closure models	Law et al. (2003) used an IBM to simulate the population dynamics of a single-species population and examined effects of dispersal and competition on population dynamics Adams, Holland, Law, Plank, & Raghib (2013) used birth, growth, death IBMs to study scaling between individual tree to forest stand level Barraquand & Murrell (2013) modelled predator-prey dynamics including functions for movement, births, and deaths	Challenging to implement (Purves et al., 2007); involves complicated mathematics making it difficult to include environmental variation changing over time (Vance et al., 2010)

As shown in Table 1.1, all of these methods have limitations, and furthermore, each of them requires a great deal of data, making them difficult to implement (Barraquand & Murrell, 2013; Caughlin et al., 2016).

A method developed by Chesson et al. (2005) known as on scale transition theory simplifies the problem by focusing on how demographic processes change at broad spatial scales rather than a complete description of the mechanisms shaping population growth. A disadvantage of the STT is that we cannot tease apart interactions between mechanisms shaping population growth because it does not gather data of individuals and complete life histories (Law et al., 2003). However, this simplification makes the methodology of the STT more straight-forward and accessible. The approach of STT uses Jensen's inequality to approximate the difference between broad scale population growth and growth

assuming an average density across a region. The result is a series of scale transition terms (STT). The most fundamental of these terms (and the one I will focus on) accounts for the spatial variation in density and the density dependence of population growth to scale up population growth data (Chesson, 2012; Chesson et al., 2005; Melbourne & Chesson, 2006).

By accounting for these factors, spatial processes from density are thereby explained and the fallacy of the averages is avoided. Once the components are calculated, the method is not computationally demanding and estimating the STT is straightforward. Furthermore, this method can be adapted to a range of metapopulation structures (patch models and single populations) (Chesson et al., 2005). In the framework of this method, dispersal is only considered to be local, and it is assumed that the mixing effects of dispersal cancel out at a regional scale (Melbourne & Chesson, 2006).

However, this method has not been tested for rapidly changing systems, such as populations which are expanding or those which are declining. Therefore, while the findings of previous studies which have estimated the STT for stable systems are useful, they cannot be assumed to be valid for systems with transient dynamics. This thesis will address this knowledge gap by validating this method in order to test how spatial processes influence population growth for unstable systems.

Many studies have already estimated the components of this scale transition term (see Baguette, Blanchet, Legrand, Stevens, & Turlure, (2013); Comita, Muller-Landau, Aguilar, & Hubbell, (2010); Wu et al., (2016)). From these studies, we know that we will need to get a substantial amount of data on population densities and density dependence across time and space in order to quantify how growth changes with scale (Royle, Fuller, & Sutherland, 2018). Therefore to properly estimate the effect of spatial processes on population growth, I first need to gather and explore data at a large scale.

1.3 Using remote sensing imagery to gather large-scale data

Remote sensing technology offers unexplored opportunities to quantify population growth at multiple spatial scales. Remote sensing imagery is collected from instruments such as satellites and aircrafts, and these data can be gathered across large regions (i.e., 10s of square kilometers) at fine spatial resolutions (under a meter in pixel size) (Warner, Nellis, & Foody, 2009) and over multiple time steps. These imagery have spatial and spectral resolutions; spatial resolution refers to pixel size and spectral resolution refers to how many spectral bands an image has (relating to the spectrum of light) (Warner et al., 2009).

Aerial photography is a subset of remote sensing imagery in which the imagery data has been gathered from an aircraft or type of airborne vehicle such as a drone. Aerial photography often has high spatial resolution (pixel sizes are usually one meter or smaller), but it does not have a high spectral resolution (Bradley, 2014; Müllerová, Pergl, & Pyšek, 2013). Due to its ability to gather fine-scale data across broad areas, its relative low cost, and its availability, it is well suited to study changing systems or environments (Brook & Bowman, 2006; Huang & Asner, 2009; Müllerová et al., 2013). Table 1.2

summaries several studies which have used aerial photography to estimate and monitor population dynamics through time.

Table 1.2 Example studies which use aerial photography to examine population dynamics.

Purpose of Study	Study and system examined	Type of imagery used	Reference
Mapping and monitoring the spread of invading populations	Ponderosa pine invading into grasslands in Colorado Front Range	Digitized aerial photography (historic from 1937-1990)	(Mast, Veblen, & Hodgson, 1997
	Pinyon and Juniper encroaching in rangelands of western USA	High-resolution aerial imagery (RGB)	(Hulet, Roundy, Petersen, Jensen, & Bunting, 2013; Poznanovic, Falkowski, Maclean, Smith, & Evans, 2014)
	Invasion of *Heracleum mantegazzianum* in the Czech Republic	Historic high resolution aerial imagery (panchromatic and multispectral), from 1947-1996	(Müllerová, Pyšek, Jarošík, & Pergl, 2005)
Estimating the population abundances of threatened species	Three tree species in Cambodia near the Bayon and Baphuon temples	High resolution aerial imagery (RGB)	(Singh, Evans, Tan, & Nin, 2015)
	A species of red seaweed (*Chondrus crispus*) in eastern Canada	Historic high resolution aerial imagery	(Sharp et al., 2010)
Estimating the densities/locations of individuals for population dynamics models	Modelling shrub encroachment onto savannahs in Swaziland	Historic high resolution aerial photographs	(Roques, O'Connor, & Watkinson, 2001)
	Modelling demographic dynamics and spread of two species invading into South African shrublands (*Acacia cyclops* and *Pinus pinaster*)	Historic high resolution aerial photographs	(Higgins, Richardson, & Cowling, 2001)

As seen in the example studies (Table 1.2), aerial imagery is often used for studying dynamic systems such as species invasions or declines. Furthermore, remote sensing imagery has been used to estimate population parameters such as density dependence (Van Gunst, Weisberg, Yang, & Fan, 2016), population growth rate (Lamar & McGraw, 2005), dispersal (Buckley et al., 2005), and spatial patterns (Franklin, Michaelsen, Strahler, & Barbara, 1985).

However, aerial imagery and other types of big data have not yet been applied to the issue of scaling up population growth. Many of the studies listed in Table 1.1 were for a limited number of sites and thus did not capture the complexity and intricacy which broad scale datasets contain (Mouquet et al., 2015). There is much value in using big data to examine the issue of scaling (Hampton et al. 2013; Soranno & Schimel, 2014), and aerial imagery offers a method to acquire that data.

There are still several unknowns with using aerial photography for gathering fine-resolution large-scale population dynamics data. Because not all individuals in a population are detected when using remote sensing imagery (Franklin et al., 1985; Xie, Sha, & Yu, 2008), the limitations of using these imagery needed to be determined in order to study the scaling of population dynamics. Additionally, we need to be able to accurately quantify the density of individuals across a region and be able to do this consistently across different densities as well. I would also like to determine the limitations of what age structure aerial photography can detect. Before I can confidently use aerial imagery to study scaling population growth, I will first need to confirm that aerial photography can accurately capture the density and age structure of a population.

1.4 Potential error and biases in large-scale datasets

To leverage the opportunity presented by aerial photography to estimate how population growth changes with spatial scale I must first confront some of these data's shortcomings. When collecting large datasets on populations, especially those which occur over large spatial areas, there will be inevitable errors in the data (Kellner & Swihart, 2014; Queenborough et al., 2011). Observation or detection errors are when individuals in a sampling area are missed and are due to sampling or random chance (Ahrestani, Hebblewhite, & Post, 2013; Wright, Irvine, Warren, & Barnett, 2017). These errors are common in population abundance and density data (Kéry & Schmidt, 2008; Royle, Nichols, & Kéry, 2005), and surveys of plants are not immune to errors in detection (Clarke, Lewis, Brandle, & Ostendorf, 2012; Wright et al., 2017). For example, Chen et al. (2013) found that in surveys of plant species along transect lines, the season in which the survey was conducted and the elevation of the survey could lead to errors in the detection of plant species. Ng and Driscoll (2015) found that a common herbaceous weed was more difficult to detect when it was not in flower and when the leaf litter height was high.

While the presence of detection error in plant population surveys is known, we are not sure how these errors could propagate and introduce potential biases in parameter estimates, particularly when we are scaling up population growth data. Uncertainty and bias can have a large influence on population parameter estimates (Clark, 2003; Elderd & Miller, 2016; McCallum, 2008). We need to know the variation in population parameter estimates because even small changes in population parameters can have big implications for predictions of species (Ludwig, 1996; Ramula & Buckley, 2009). Additionally, error in population densities and abundances can in turn lead to incorrectly detecting processes such as density dependence (Freckleton, Watkinson, Green, & Sutherland, 2006; Lebreton

& Gimenez, 2013). Therefore I will need to assess whether errors in population densities could introduce biases in the estimates of population growth across spatial scales.

1.5 Value of looking at conifer invasions for studying scale issues

To estimate population growth across spatial scales and understand the effects of detection error on the parameter estimates, I need a system where change is rapid enough to be observed across broad scales. I also need a system where I could detect individuals and densities using aerial photography.

An ideal model system for this work is biological invasions, which occur when a species is intentionally, accidentally, or self- introduced, and it establishes and spreads at the harm of the local environment (Mack et al., 2000; Vitousek, Dantonio, Loope, Rejmánek, & Westbrooks, 1997). Spatial processes such as dispersal and biotic interactions are key drivers of biological invasions (Hastings et al., 2005; Levine et al., 2003). Invasions also occur over large scales and relatively rapid timespans; therefore population dynamics could likely be detected using aerial photography provided the data was available at multiple time steps for the region (Bradley, 2014; Vitousek et al., 1997). Additionally, biological invasions can harm the surrounding ecological communities and negatively impact economies (Hejda, Pyšek, & Jarošík, 2009; Mack et al., 2000; McCary, Mores, Farfan, & Wise, 2016; Pimentel et al., 2001). Therefore, a better understanding of population growth across spatial scales would contribute to counteracting the harmful effects of invasions and benefit their management strategies (Early et al., 2016).

Wilding conifer invasions in New Zealand exemplify many of the desirable characteristics of biological invasions. The term wilding conifers refers to conifers that have naturalised and self-established from intentionally-planted or self-seeded individuals (Froude, 2011; Ledgard, 2004). These invasions affect a large area in New Zealand (Ministry of Primary Industries, 2014), occur over rapid timespans (Froude, 2011), and threaten biodiversity and productive land (Dickie et al., 2014; Mark & Dickinson, 2008; Pawson, McCarthy, Ledgard, & Didham, 2010; Rundel, Dickie, & Richardson, 2014).

Many species of wilding conifers are highly invasive in New Zealand (Richardson, 1998), with the most invasive species identified by the Department of Conservation as the following, in order from most invasive to least invasive: *Pinus contorta* (Lodgepole pine), *Pinus sylvestris* (Scots pine), *Pinus mugo* subsp mugo (Dwarf mountain pine), *Pinus mugo* subsp uncinata (Dwarf mountain pine), *Pseudotsuga menziesii* (Douglas fir), *Pinus nigra* (Corsican pine), *Larix decidua* (European larch), *Pinus ponderosa* (Ponderosa pine), *Pinus muricata* (Bishop pine), and *Pinus radiata* (Radiata or Monterey pine) (Froude, 2011; Harding, 2001).

Both human mediated factors such as forestry use and area planted as well as biogeographic factors such as climate match have contributed to the introductions and success of these species (Hunter & Douglas, 1984; McGregor, Watt, Hulme, & Duncan, 2012). In part due to their ability to mature early,

produce smaller seeds, and have more frequent large seed crops (Richardson, Williams, & Hobbs, 1994), these wilding conifer species have invaded vast amounts of land in New Zealand. In 2011, an estimated 1.1 million hectares of land were found to be affected by wilding conifers (Froude, 2011). In 2014, these conifers affected over 1.8 million hectares of land and the government now spends $16 million per year on control efforts (Ministry of Primary Industries, 2014).

1.5.1 Spatial processes in wilding conifer invasions

The spatial processes in wilding conifer invasions could likely affect the scaling of population growth. Dispersal by wind is a key driver of the areal spread of these species (Froude, 2011). While many seeds fall and establish close to the parent trees, seeds can disperse several kilometres in high wind events (Hunter & Douglas, 1984). Furthermore, density dependence is suspected to affect the growth of conifer populations. The competition from the existing vegetation can hinder or sometimes even aid the growth of conifers through sheltered microsites (Ledgard, 2004; Richardson et al., 1994). Pines in particular have been found to invade grasslands and shrublands well because in these systems the pines can out-compete the surrounding vegetation (Richardson & Bond, 1991; Rundel et al., 2014). There have been few studies on the intraspecific competition between individual conifers; however, self-thinning has been found in even-aged stands of some pine species (del Río, Montero, & Bravo, 2001; Kenkel, 1988). The presence of ectomycorrhizal fungi in the soil is also thought to improve the growth of individuals once they are inoculated (Davis, Grace, & Horrell, 1996). In fact, it is believed that ectomycorrhizal fungi from mature, established conifers can aid the establishment and growth of seedlings and saplings as a form of positive density dependence (Dickie, Bolstridge, Cooper, & Peltzer, 2010; Nuñez, Horton, & Simberloff, 2009; Rundel et al., 2014). Since the density of these trees can vary across a region, the effects of density on the growth of a population are scale-dependent and will affect scaling.

Previous work on conifer invasions points to the importance of spatial processes, although this has never been explicitly tested. Dispersal has been found to be a key component of the spread of populations (Buckley et al., 2005; Caplat, Nathan, & Buckley, 2012; Hastings et al., 2005). For example, (Caplat et al., 2012) developed a mechanistic wind dispersal model and found that seed terminal velocity was a significant driver of spread rate. Additionally, there is evidence that density dependence could affect the scaling of population growth as well. For example, Schurr, Steinitz, & Nathan (2008) found that tree density affects both dispersal and fecundity for an invasion of *Pinus halepensis*. Higgins et al. (2001) found that the density of pine invasions tended to become more aggregated over time, implying that spatial processes arising from density could have a stronger effect as an invasion progresses. More generally, studies recognise the effects of local density dependence on population range expansions and contractions (Svenning et al., 2014; Urban, Tewksbury, & Sheldon, 2012). While this evidence points to the importance of spatial processes in the population growth of conifer invasions, so far in projections of population growth for conifer invasions in New Zealand,

spatial processes have not been taken into account. Therefore the findings of this thesis will contribute to our understanding of the population growth of conifer invasions.

1.5.2 Practical reasons why wilding conifers are an exemplar study system

Due to the vast amount of research and management of these conifers, we know many areas where populations are spreading (i.e., the Wilding Conifer Information System (Land Information New Zealand, 2018b)). Therefore, the availability of sites will not be a limiting factor for this thesis. Additionally, these trees are relatively easy to distinguish using aerial imagery because some species often spread into grasslands (Allen & Lee, 1989) which contrast highly against the dark conifer foliage. Furthermore, the invasions occur over timespans which are appropriate for using aerial imagery (Mast et al., 1997), and there is a substantial amount of aerial imagery available for these timespans (see Land Information New Zealand (2018a)). Studies using aerial imagery of conifer invasions have been done before as well (Mast et al., 1997; Sahara, Sarr, Van Kirk, & Jules, 2015). Dash et al. (2017) used aerial imagery and airborne laser scanning technology to detect wilding conifers invading in grasslands and mixed shrub vegetation. These results are promising for using aerial imagery to detect densities of these trees. However, the utility of free or low-cost aerial imagery has not yet been explored or maximised.

1.6 Thesis purpose and objectives

My thesis seeks to understand how spatial processes can affect the scaling of population growth. To do this, first I will evaluate the utility of using broad-scale aerial imagery data to detect the densities, age structure, and spatial patterns of conifer invasions (Chapter 2). In this assessment, I aim to document substantial bias in detecting densities of conifer trees and the effects of this bias on estimating population growth across scales was not known. In Chapter 3, I will address this by testing for synergistic effects of observation error and detection bias on the estimates of the scaling of population growth. Finally in Chapter 4, using insights from the previous chapters, I will extend the methods of the scale transition theory to estimate the scaling of growth for broad-scale, dynamic conifer invasions.

Together, my work highlights the importance of broad scale processes in shaping population growth and hence the need to obtain new data sources to estimate its impact. The findings of this thesis will not only contribute to the population ecology literature on spatial scales and processes, but they will also contribute to the knowledge and management of invasive conifers.

1.7 Thesis Structure

Chapters 2-4 are written to be stand-alone publications; therefore there is a small amount of repetition between them. Chapter 2 has been submitted to *Biological Invasions* and is currently being reviewed. I plan to submit Chapter 3 to *Ecological Modelling* and Chapter 4 to *Journal of Ecology*.

1.8 References

Adams, T. P., Holland, E. P., Law, R., Plank, M. J., & Raghib, M. (2013). On the growth of locally interacting plants: Differential equations for the dynamics of spatial moments. *Ecology*, 94(12), 2732–2743. https://doi.org/10.1890/13-0147.1

Ahrestani, F. S., Hebblewhite, M., & Post, E. (2013). The importance of observation versus process error in analyses of global ungulate populations. *Scientific Reports*, 3. https://doi.org/10.1038/srep03125

Allen, R. B., & Lee, W. G. (1989). Seedling establishment microsites of exotic conifers in *Chinochloa rigida* tussock grassland, Otago, New Zealand. *New Zealand Journal of Botany*, 27, 491–498.

Baguette, M., Blanchet, S., Legrand, D., Stevens, V. M., & Turlure, C. (2013). Individual dispersal, landscape connectivity and ecological networks. *Biological Reviews*, 88(2), 310–326. https://doi.org/10.1111/brv.12000

Barraquand, F., & Murrell, D. J. (2013). Scaling up predator-prey dynamics using spatial moment equations. *Methods in Ecology and Evolution*, 4(3), 276–289. https://doi.org/10.1111/2041-210X.12014

Beckman, N. G., Bullock, J. M., & Salguero-Gómez, R. (2018). High dispersal ability is related to fast life-history strategies. *Journal of Ecology*, 106(4), 1349–1362. https://doi.org/10.1111/1365-2745.12989

Beckman, N. G., & Rogers, H. S. (2013). Consequences of seed dispersal for plant recruitment in tropical forests: Interactions within the seedscape. *Biotropica*, 45(6), 666-681. https://doi.org/10.1111/btp.12071

Bocedi, G., Pe'er, G., Heikkinen, R. K., Matsinos, Y., & Travis, J. M. J. (2012). Projecting species' range expansion dynamics: Sources of systematic biases when scaling up patterns and processes. *Methods in Ecology and Evolution*, 3(6), 1008–1018. https://doi.org/10.1111/j.2041-210X.2012.00235.x

Bolker, B. M., Pacala, S. W., & Neuhauser, C. (2003). Spatial dynamics in model plant communities: What do we really know? *The American Naturalist*, 162(2), 135–48. https://doi.org/10.1086/376575

Bradley, B. A. (2014). Remote detection of invasive plants: A review of spectral, textural and phenological approaches. *Biological Invasions*, 16(7), 1411–1425. https://doi.org/10.1007/s10530-013-0578-9

Brook, B. W., & Bowman, D. M. J. S. (2006). Postcards from the past: Charting the landscape-scale conversion of tropical Australian savanna to closed forest during the 20th century. *Landscape Ecology*, 21(8), 1253–1266. https://doi.org/10.1007/s10980-006-0018-7

Buckley, Y. M., Brockerhoff, E., Langer, L., Ledgard, N. J., North, H., & Rees, M. (2005). Slowing down a pine invasion despite uncertainty in demography and dispersal. *Journal of Applied Ecology*, 42(6), 1020–1030. https://doi.org/10.1111/j.1365-2664.2005.01100.x

Caplat, P., Nathan, R., & Buckley, Y. M. (2012). Seed terminal velocity, wind turbulence, and demography drive the spread of an invasive tree in an analytical model. *Ecology*, 93(2), 368–377. https://doi.org/10.1890/11-0820.1

Casper, B. B., & Jackson, R. B. (1997). Plant competition underground. *Annual Review of Ecology and Systematics*, 28, 545–70. https://doi.org/10.1146/annurev.ecolsys.28.1.545

Castagneri, D., Lingua, E., Vacchiano, G., Nola, P., & Motta, R. (2010). Diachronic analysis of individual-tree mortality in a Norway spruce stand in the eastern Italian Alps. *Annals of Forest Science*, 67(3), 304. Retrieved from http://www.afs-journal.org/10.1051/forest/2009111

Castorani, M. C. N., Reed, D. C., Alberto, F., Bell, T. W., Simons, R. D., Cavanaugh, K. C., Siegel, D. A., & Raimondi, P. T. (2015). Connectivity structures local population dynamics: A long-term empirical test in a large metapopulation system. *Ecology*, *96*(12), 3141–3152. https://doi.org/10.1890/15-0283.1

Caughlin, T. T., Elliott, S., & Lichstein, J. W. (2016). When does seed limitation matter for scaling up reforestation from patches to landscapes? *Ecological Applications*, 26(8), 2437–2448. https://doi.org/10.1002/eap.1410

Chen, G., Kéry, M., Plattner, M., Ma, K., & Gardner, B. (2013). Imperfect detection is the rule rather than the exception in plant distribution studies. *Journal of Ecology*, 101(1), 183–191. https://doi.org/10.1111/1365-2745.12021

Chesson, P. (1998). Recruitment limitation: A theoretical perspective. *Australian Journal of Ecology*, 23(3), 234–240. https://doi.org/10.1111/j.1442-9993.1998.tb00725.x

Chesson, P. (2012). Scale transition theory: Its aims, motivations and predictions. *Ecological Complexity*, 10, 52–68. https://doi.org/10.1016/j.ecocom.2011.11.002

Chesson, P., Donahue, M. J., Melbourne, B. A., & Sears, A. L. W. (2005). Scale transition theory for understanding mechanisms in metacommunities. In M. Holyoak, M. A. Leibold, & R. D. Holt (Eds.), *Metacommunities: Spatial Dynamics and Ecological Communities* (pp. 279–306). Chicago: University of Chicago Press.

Cipriotti, P. A., Wiegand, T., Pütz, S., Bartoloni, N. J., & Paruelo, J. M. (2016). Nonparametric upscaling of stochastic simulation models using transition matrices. *Methods in Ecology and Evolution*, 7(3), 313–322. https://doi.org/10.1111/2041-210X.12464

Clark, J. S. (2003). Uncertainty and variability in demography and population growth: A hierarchical approach. *Ecology*, 84(6), 1370-1381. https://doi.org/10.1890/0012-9658(2003)084[1370:UAVIDA]2.0.CO;2

Clark, J. S., Bell, D. M., Hersh, M. H., & Nichols, L. (2011). Climate change vulnerability of forest biodiversity: Climate and competition tracking of demographic rates. *Global Change Biology*, 17(5), 1834–1849. https://doi.org/10.1111/j.1365-2486.2010.02380.x

Clarke, K. D., Lewis, M., Brandle, R., & Ostendorf, B. (2012). Non-detection errors in a survey of persistent, highly-detectable vegetation species. *Environmental Monitoring and Assessment*, 184(2), 625–635. https://doi.org/10.1007/s10661-011-1991-0

Comita, L. S., Muller-Landau, H. C., Aguilar, S., & Hubbell, S. P. (2010). Asymmetric density dependence shapes species abundances in a tropical tree community. *Science*, 329(5989), 330–332. https://doi.org/10.1126/science.1190772

Connell, J. H. (1971). On the role of natural enemies in preventing competitive exclusion in some marine animals and in rain forest trees. In P. J. D. Boer, & G. R. Gradwell (Eds). *Dynamics of Populations* (pp .298-312). Wagningen, Netherlands: Centre for Agricultural Publication and Documentation. https://doi.org/10.1890/07-2056.1.

Cotto, O., Wessely, J., Georges, D., Klonner, G., Schmid, M., Dullinger, S., Thuiller, W., & Guillaume, F. (2017). A dynamic eco-evolutionary model predicts slow response of alpine plants to climate warming. *Nature Communications*, 8(15399). https://doi.org/10.1038/ncomms15399

Cousens, R., Dytham, C., & Law, R. (2008). *Dispersal in Plants: A Population Perspective*. Oxford, UK: Oxford University Press. https://doi.org/10.1093/acprof:oso/9780199299126.001.0001

Dale, M. R. T. (1999). *Spatial Pattern Analysis in Plant Ecology*. Cambridge: Cambridge University Press.

Dash, J. P., Pearse, G. D., Watt, M. S., & Paul, T. (2017). Combining airborne laser scanning and aerial imagery enhances echo classification for invasive conifer detection. *Remote Sensing*, 9(2), 156-177. https://doi.org/10.3390/rs9020156

Davis, M. R., Grace, L. J., & Horrell, R. F. (1996). Conifer establishment in South Island high country: Influence of mycorrhizal inoculation, competition removal, fertiliser application, and animal exclusion during seedling establishment. *New Zealand Journal of Forestry Science*, 26(3), 380–394.

del Río, M., Montero, G., & Bravo, F. (2001). Analysis of diameter-density relationships and self-thinning in non-thinned even-aged Scots pine stands. *Forest Ecology and Management*, 142(1–3), 79–87. https://doi.org/10.1016/S0378-1127(00)00341-8

Dickie, I. A., Bolstridge, N., Cooper, J. A., & Peltzer, D. A. (2010). Co-invasion by *Pinus* and its mycorrhizal fungi. *New Phytologist*, 187(2), 475–484. https://doi.org/10.1111/j.1469-8137.2010.03277.x

Dickie, I. A., Schnitzer, S. A., Reich, P. B., & Hobbie, S. E. (2005). Spatially disjunct effects of co-occurring competition and facilitation. *Ecology Letters*, 8(11), 1191–1200. https://doi.org/10.1111/j.1461-0248.2005.00822.x

Dickie, I. A., St John, M. G., Yeates, G. W., Morse, C. W., Bonner, K. I., Orwin, K., & Peltzer, D. A. (2014). Belowground legacies of *Pinus contorta* invasion and removal result in multiple mechanisms of invasional meltdown. *AoB Plants*, 1–15. https://doi.org/10.1093/aobpla/plu056

Dieckmann, U., Law, R., & Metz, J. A. J. (2000). *The Geometry of Ecological Interactions*. Cambridge Studies in Adaptive Dynamics (Vol. 1). Cambridge, United Kingdom: Cambridge University Press. https://doi.org/10.1017/CBO9780511525537

Dieckmann, U., O'Hara, B., & Weisser, W. (1999). The evolutionary ecology of dispersal. *Trends in Ecology and Evolution*, 14(3), 88–90. https://doi.org/10.1016/S0169-5347(98)01571-7

Dorken, M. E., Freckleton, R. P., & Pannell, J. R. (2017). Small-scale and regional spatial dynamics of an annual plant with contrasting sexual systems. *Journal of Ecology*, 105(4), 1044–1057. https://doi.org/10.1111/1365-2745.12719

Dunham, A. E., & Beaupre, S. J. (2001). Ecological experiments: Scale, phenomenology, mechanism, and the illusion of generality. In W. J. J. Resetarits & J. Bernardo (Eds.), *Experimental Ecology: Issues and Perspectives* (pp. 27–49). Oxford, UK: Oxford University Press.

Early, R., Bradley, B. A., Dukes, J. S., Lawler, J. J., Olden, J. D., Blumenthal, D. M., Gonzalez, P., Grosholz, E. D., Ibañez, I., Miller, L. P., Sorte, C. J. B., & Tatem, A. J. (2016). Global threats from invasive alien species in the twenty-first century and national response capacities. *Nature Communications,* 7(12485). https://doi.org/10.1038/ncomms12485

Elderd, B. D., & Miller, T. E. X. (2016). Quantifying demographic uncertainty: Bayesian methods for integral projection models. *Ecological Monographs*, 86(1), 125–144. https://doi.org/10.1890/15-1526.1

Estes, L., Elsen, P. R., Treuer, T., Ahmed, L., Caylor, K., Chang, J., Choi, J. J., & Ellis, E. C. (2018). The spatial and temporal domains of modern ecology. *Nature Ecology and Evolution*, 2(5), 819–826. https://doi.org/10.1038/s41559-018-0524-4

Fletcher, C. S., & Westcott, D. A. (2013). Dispersal and the design of effective management strategies for plant invasions: Matching scales for success. *Ecological Applications*, 23(8), 1881–1892. https://doi.org/10.1890/12-2059.1

Franklin, J., Michaelsen, J., Strahler, A. H., & Barbara, S. (1985). Spatial analysis of density dependent pattern in coniferous forest stands. *Vegetatio*, 64, 29–36. https://doi.org/10.1007/BF00033451

Freckleton, R. P., & Watkinson, A. R. (2002). Large-scale spatial dynamics of plants: Metapopulations, regional ensembles and patchy populations. *Journal of Ecology*, 90(3), 419–434. https://doi.org/10.1046/j.1365-2745.2002.00692.x

Freckleton, R. P., Watkinson, A. R., Green, R. E., & Sutherland, W. J. (2006). Census error and the detection of density dependence. *Journal of Animal Ecology*, 75(4), 837-851. https://doi.org/10.1111/j.1365-2656.2006.01121.x

Froude, V. A. (2011). Wilding conifers in New Zealand: Status report. Bay of Islands. https://doi.org/978-0-478-40010-6

Ghazoul, J., Liston, K. A., & Boyle, T. J. B. (1998). Disturbance-induced density-dependent seed set in *Shorea siamensis* (Dipterocarpaceae), a tropical forest tree. *Journal of Ecology*, 86(3), 462–473.

Gravel, D., Guichard, F., & Hochberg, M. E. (2011). Species coexistence in a variable world. *Ecology Letters*, 14(8), 828-839. https://doi.org/10.1111/j.1461-0248.2011.01643.x

Griffith, A. B., Salguero-Gómez, R., Merow, C., & McMahon, S. (2016). Demography beyond the population. *Journal of Ecology*, 104(2), 271–280. https://doi.org/10.1111/1365-2745.12547

Gurevitch, J., Fox, G. A., Fowler, N. L., & Graham, C. H. (2016). Landscape demography: Population change and its drivers across spatial scales. *The Quarterly Review of Biology*, 91(4), 459–485. https://doi.org/10.1086/689560

Hampton, S. E., Strasser, C. A., Tewksbury, J. J., Gram, W. K., Budden, A. E., Batcheller, A. L., Duke, C. S., & Porter, J. H. (2013). Big data and the future of ecology. *Frontiers in Ecology and the Environment*, 11(3), 156–162. https://doi.org/10.1890/120103

Hanski, I., & Ovaskainen, O. (2003). Metapopulation theory for fragmented landscapes. *Theoretical Population Biology*, 64(1) ,119-127. https://doi.org/10.1016/S0040-5809(03)00022-4

Harding, M. (2001). South Island Wilding Conifer Strategy. Christchurch. Retrieved 20 September 2018, from https://www.doc.govt.nz/about-us/science-publications/conservation-publications/threats-and-impacts/weeds/south-island-wilding-conifer-strategy/executive-summary/

Hastings, A., Cuddington, K., Davies, K. F., Dugaw, C. J., Elmendorf, S., Freestone, A., Harrison, S., Holland, M., Malvadkar, U., Melbourne, B., Moore, K., Taylor, C., & Thomson, D. (2005). The spatial spread of invasions: New developments in theory and evidence. *Ecology Letters,* 8(1), 91–101. https://doi.org/10.1111/j.1461-0248.2004.00687.x

Hejda, M., Pyšek, P., & Jarošík, V. (2009). Impact of invasive plants on the species richness, diversity and composition of invaded communities. *Journal of Ecology*, 97(3), 393–403. https://doi.org/10.HH/j.1365-2745.2009.01480.x

Higgins, S. I., Richardson, D. M., & Cowling, R. M. (2001). Validation of a spatial simulation model of a spreading alien plant population. *Journal of Applied Ecology*, 38(3), 571–584. https://doi.org/10.1046/j.1365-2664.2001.00616.x

Hirt, M. R., Grimm, V., Li, Y., Rall, B. C., Rosenbaum, B., & Brose, U. (2018). Bridging scales: Allometric random walks link movement and biodiversity research. *Trends in Ecology & Evolution*, 33(9), 701-712. https://doi.org/10.1016/j.tree.2018.07.003

Hogg, O. T., Huvenne, V. A. I., Griffiths, H. J., & Linse, K. (2018). On the ecological relevance of landscape mapping and its application in the spatial planning of very large marine protected areas. *Science of the Total Environment*, 626, 384–398. https://doi.org/10.1016/j.scitotenv.2018.01.009

Holmgren, M., Scheffer, M., & Huston, M. A. (1997). The interplay of facilitation and competition in plant communities. *Ecology*, 78(7), 1966-1975. https://doi.org/10.1890/0012-9658(1997)078[1966:TIOFAC]2.0.CO;2

Howe, H. F., & Miriti, M. N. (2004). When seed dispersal matters. *BioScience*, 54(7), 651–660. https://doi.org/10.1641/0006-3568(2004)054[0651:WSDM]2.0.CO;2

Huang, C.-Y., & Asner, G. P. (2009). Applications of remote sensing to alien invasive plant studies. *Sensors*, 9(6), 4869–89. https://doi.org/10.3390/s90604869

Hubbell, S. P., Condit, R., & Foster, R. B. (1990). Presence and absence of density dependence in a neotropical tree community. *Philosophical Transactions of the Royal Society of London Series B-Biological Sciences*, 330(1257), 269–281. https://doi.org/10.1098/rstb.1990.0198

Hulet, A., Roundy, B. A., Petersen, S. L., Jensen, R. R., & Bunting, S. C. (2013). Assessing the relationship between ground measurements and object-based image analysis of land cover classes in pinyon and juniper woodlands. *Photogrammetric Engineering & Remote Sensing*, 79(9), 799–808. https://doi.org/10.14358/PERS.79.9.799

Hunter, G. G., & Douglas, M. H. (1984). Spread of exotic conifers on South Island rangelands. *New Zealand Journal of Forestry*, 29(1), 78-96.

Janzen, D. H. (1970). Herbivores and the number of tree species in tropical forests. *The American Naturalist,* 104 (940), 501–528. https://doi.org/10.2307/2678832.

Jump, A. S., & Peñuelas, J. (2005). Running to stand still: Adaptation and the response of plants to rapid climate change. *Ecology Letters*, 8(9), 1010–1020. https://doi.org/10.1111/j.1461-0248.2005.00796.x

Kellner, K. F., & Swihart, R. K. (2014). Accounting for imperfect detection in ecology: A quantitative review. *PLoS ONE*, 9(10), e111436. https://doi.org/10.1371/journal.pone.0111436

Kenkel, N. C. (1988). Pattern of self-thinning in jack pine: Testing the random mortality hypothesis. *Ecology*, 69(4), 1017–1024. https://doi.org/10.2307/1941257

Kéry, M., & Schmidt, B. (2008). Imperfect detection and its consequences for monitoring for conservation. *Community Ecology*, 9(2), 207–216. https://doi.org/10.1556/ComEc.9.2008.2.10

Lamar, W. R., & McGraw, J. B. (2005). Evaluating the use of remotely sensed data in matrix population modeling for eastern hemlock (*Tsuga canadensis* L.). *Forest Ecology and Management*, 212(1–3), 50–64. https://doi.org/10.1016/j.foreco.2005.02.056

Land Information New Zealand. (2018a). Aerial Imagery. Retrieved 21 September 2018, from https://www.linz.govt.nz/data/linz-data/aerial-imagery

Land Information New Zealand. (2018b). Wilding Conifer Information System. Retrieved 21 September 2018, from https://www.linz.govt.nz/crown-property/using-crown-property/biosecurity/control-programmes/wilding-conifer-information-system

Law, R., & Dieckmann, U. (2000). A dynamical system for neighborhoods in plant communities. *Ecology*, 81(8), 2137–2148. https://doi.org/10.1890/0012-9658(2000)081{[}2137:ADSFNI]2.0.CO;2

Law, R., Murrell, D. J., & Dieckmann, U. (2003). Population growth in space and time: Spatial logistic equations. *Ecology*, 84(1), 252–262. https://doi.org/10.1890/0012-9658(2003)084[0252:PGISAT]2.0.CO;2

Lebreton, J.-D., & Gimenez, O. (2013). Detecting and estimating density dependence in wildlife populations. *The Journal of Wildlife Management*, 77(1), 12–23. https://doi.org/10.1002/jwmg.425

Ledgard, N. J. (2004). Wilding conifers – New Zealand history and research background. In S. M. Z. and C. M. B. R.L. Hill (Ed.), *Managing Wilding Conifers in New Zealand: Present and Future* (pp. 1–25). New Zealand Plant Protection Society.

Levin, S. A. (1992). The problem of pattern and scale in ecology: The Robert H. MacArthur Award Lecture. *Ecology*, 73(6), 1943–1967. https://doi.org/doi:10.2307/1941447

Levin, S. A., & Pacala, S. W. (1997). Theories of simplification and scaling of spatially distributed processes. In D. Tilman & P. Kareiva (Eds.), *Spatial Ecology: The Role of Space in Population Dynamics and Interspecific Interactions* (pp. 271–295). Princeton, New Jersey: Princeton University Press.

Levine, J. M., Vilà, M., D'Antonio, C. M., Dukes, J. S., Grigulis, K., & Lavorel, S. (2003). Mechanisms underlying the impacts of exotic plant invasions. *Proceedings of the Royal Society B: Biological Sciences*, 270(1517), 775–781. https://doi.org/10.1098/rspb.2003.2327

Ludwig, D. (1996). Uncertainty and the assessment of extinction probabilities. *Ecological Applications*, 6(4), 1067–1076. https://doi.org/10.2307/2269591

Mack, R. N., Simberloff, D., Mark Lonsdale, W., Evans, H., Clout, M., & Bazzaz, F. A. (2000). Biotic invasions: Causes, epidemiology, global consequence, and control. *Ecological Applications*, 10, 689–710. https://doi.org/10.1890/1051-0761(2000)010[0689:BICEGC]2.0.CO;2

Mark, A. F., & Dickinson, K. J. M. (2008). Maximising water yields with indigenous non-forest vegetation: A New Zealand perspective. *Frontiers in Ecology and the Environment*, 6(1), 25–34.

Mast, J. N., Veblen, T. T., & Hodgson, M. E. (1997). Tree invasion within a pine/grassland ecotone: An approach with historic aerial photography and GIS modeling. *Forest Ecology and Management*, 93(3), 181–194. https://doi.org/10.1016/S0378-1127(96)03954-0

McCallum, H. (2008). *Population Parameters: Estimation for Ecological Models*. Oxford, UK: Blackwell Science.

McCary, M. A., Mores, R., Farfan, M. A., & Wise, D. H. (2016). Invasive plants have different effects on trophic structure of green and brown food webs in terrestrial ecosystems: A meta-analysis. *Ecology Letters*, 19(3), 328–335. https://doi.org/10.1111/ele.12562

McGregor, K. F., Watt, M. S., Hulme, P. E., & Duncan, R. P. (2012). What determines pine naturalization: Species traits, climate suitability or forestry use? *Diversity and Distributions*, 18(10), 1013–1023. https://doi.org/10.1111/j.1472-4642.2012.00942.x

Melbourne, B. A., & Chesson, P. (2006). The scale transition: Scaling up population dynamics with field data. *Ecology*, 87(6), 1478–1488. https://doi.org/10.1890/0012-9658(2006)87[1478:TSTSUP]2.0.CO;2

Mesgaran, M. B., Lewis, M. A., Ades, P. K., Donohue, K., Ohadi, S., Li, C., & Cousens, R. D. (2016). Hybridization can facilitate species invasions, even without enhancing local adaptation. *Proceedings of the National Academy of Sciences,* 113(36), 10210–10214. https://doi.org/10.1073/pnas.1605626113

Ministry of Primary Industries. (2014). The right tree in the right place: New Zealand wilding conifer management strategy 2015-2030. Retrieved 20 September 2018, from http://www.wildingconifers.org.nz/about-us/programme-2/the-national-wilding/

Mouquet, N., Lagadeuc, Y., Devictor, V., Doyen, L., Duputié, A., Eveillard, D., Faure, D., Garnier, E., Gimenez, O., Huneman, P., Jabot, F., Jarne, P., Joly, D., Julliard, R., Kéfi, S., Kergoat, G. J., Lavorel, S., Le Gall, L., Meslin, L., Morand, S., Morin, X., Morlon, H., Pinay, G., Pradel, R., Schurr, F. M., Thuiller, W., & Loreau, M. (2015). Predictive ecology in a changing world. *Journal of Applied Ecology*, 52(5), 1293-1310. https://doi.org/10.1111/1365-2664.12482

Müllerová, J., Pergl, J., & Pyšek, P. (2013). Remote sensing as a tool for monitoring plant invasions: Testing the effects of data resolution and image classification approach on the detection of a model plant species *Heracleum mantegazzianum* (giant hogweed). *International Journal of Applied Earth Observations and Geoinformation*, 25, 55–65. https://doi.org/10.1016/j.jag.2013.03.004

Müllerová, J., Pyšek, P., Jarošík, V., & Pergl, J. (2005). Aerial photographs as a tool for assessing the regional dynamics of the invasive plant species *Heracleum mantegazzianum*. *Journal of Applied Ecology*, 42(6), 1042–1053. https://doi.org/10.1111/j.1365-2664.2005.01092.x

Murrell, D. J., Dieckmann, U., & Law, R. (2004). On moment closures for population dynamics in continuous space. *Journal of Theoretical Biology*, 229(3), 421–432. https://doi.org/10.1016/j.jtbi.2004.04.013

Nathan, R., & Muller-Landau, H. C. (2000). Spatial patterns of seed dispersal, their determinants and consequences for recruitment. *Trends in Ecology & Evolution*, 15(7), 278–285. https://doi.org/10.1016/S0169-5347(00)01874-7

Ng, K., & Driscoll, D. A. (2015). Detectability of the global weed *Hypochaeris radicata* is influenced by species, environment and observer characteristics. *Journal of Plant Ecology*, 8(4), 449–455. https://doi.org/10.1093/jpe/rtu032

North, A., & Ovaskainen, O. (2007). Interactions between dispersal, competition, and landscape heterogeneity. *Oikos*, 116(7), 1106–1119. https://doi.org/10.1111/j.0030-1299.2007.15366.x

Nuñez, M. A., Horton, T. R., & Simberloff, D. (2009). Lack of belowground mutualisms hinders Pinaceae invasions. *Ecology*, 90(9), 2352–2359. https://doi.org/10.1890/08-2139.1

Ovaskainen, O. (2002). The effective size of a metapopulation living in a heterogeneous patch network. *The American Naturalist*, 160(5), 612–628. https://doi.org/10.1086/342818

Ovaskainen, O., & Cornell, S. J. (2006). Space and stochasticity in population dynamics. *Proceedings of the National Academy of Sciences*, 103(34), 12781–12786. https://doi.org/10.1073/pnas.0603994103

Pagel, J., & Schurr, F. M. (2012). Forecasting species ranges by statistical estimation of ecological niches and spatial population dynamics. *Global Ecology and Biogeography*, 21(2), 293–304. https://doi.org/10.1111/j.1466-8238.2011.00663.x

Paradis, E., Baillie, S. R., Sutherland, W. J., & Gregory, R. D. (1999). Dispersal and spatial scale affect synchrony in spatial population dynamics. *Ecology Letters*, 2(2), 114–120. https://doi.org/10.1046/j.1461-0248.1999.22060.x

Pawson, S. M., McCarthy, J. K., Ledgard, N. J., & Didham, R. K. (2010). Density-dependent impacts of exotic conifer invasion on grassland invertebrate assemblages. *Journal of Applied Ecology*, 47(5), 1053–1062. https://doi.org/10.1111/j.1365-2664.2010.01855.x

Peters, H. A. (2003). Neighbour-regulated mortality: The influence of positive and negative density dependence on tree populations in species-rich tropical forests. *Ecology Letters*, 6(8), 757–765. https://doi.org/10.1046/j.1461-0248.2003.00492.x

Pimentel, D., McNair, S., Janecka, J., Wightman, J., Simmonds, C., O'Connell, C., Wong, E., Russel, L., Zern, J., Aquino, T., & Tsomondo, T. (2001). Economic and environmental threats of alien plant, animal, and microbe invasions. *Agriculture, Ecosystems and Environment*, 84(1), 1–20. https://doi.org/10.1016/S0167-8809(00)00178-X

Poznanovic, A. J., Falkowski, M. J., Maclean, A. L., Smith, A. M. S., & Evans, J. S. (2014). An accuracy assessment of tree detection algorithms in juniper woodlands. *Photogrammetric Engineering & Remote Sensing*, 80(5), 627–637. https://doi.org/10.14358/PERS.80.7.627

Purves, D. W., Zavala, M. A., Ogle, K., Prieto, F., & Rey Benayas, J. M. (2007). Environmental heterogeneity, bird-mediated directed dispersal, and oak woodland dynamics in Mediterranean Spain. *Ecological Monographs*, 77(1), 77–97. https://doi.org/10.1890/05-1923

Queenborough, S. A., Burnet, K. M., Sutherland, W. J., Watkinson, A. R., & Freckleton, R. P. (2011). From meso- to macroscale population dynamics: A new density-structured approach. *Methods in Ecology and Evolution*, 2(3), 289–302. https://doi.org/10.1111/j.2041-210X.2010.00075.x

Raghib, M., Hill, N. A., & Dieckmann, U. (2011). A multiscale maximum entropy moment closure for locally regulated space-time point process models of population dynamics. *Journal of Mathematical Biology*, 62(5), 605–653. https://doi.org/10.1007/s00285-010-0345-9

Ramula, S., & Buckley, Y. M. (2009). Multiple life stages with multiple replicated density levels are required to estimate density dependence for plants. *Oikos*, 118(8), 1164–1173. https://doi.org/10.1111/j.1600-0706.2009.17595.x

Rastetter, E. B., King, A. W., Cosby, B. J., Hornberger, G. M., O'Neill, R. V., & Hobbie, J. E. (1992). Aggregating fine-scale ecological knowledge to model coarser-scale attributes of ecosystems. *Ecological Applications*, 2(1), 55–70. https://doi.org/10.2307/1941889

Richardson, D. M. (1998). Forestry trees as invasive aliens. *Conservation Biology*, 12(1), 18–26. https://doi.org/10.1046/j.1523-1739.1998.96392.x

Richardson, D. M., & Bond, W. J. (1991). Determinants of plant distribution: Evidence from pine invasions. *The American Naturalist*, 137(5), 639-668.

Richardson, D. M., Williams, P. A., & Hobbs, R. J. (1994). Pine invasions in the Southern Hemisphere: Determinants of spread and invadability. *Journal of Biogeography*, 21(5), 511–527. https://doi.org/10.2307/2845655

Roques, K. G., O'Connor, T. G., & Watkinson, A. R. (2001). Dynamics of shrub encroachment in an African savanna: Relative influences of fire, herbivory, rainfall and density dependence. *Journal of Applied Ecology*, 38(2), 268–280. https://doi.org/10.1046/j.1365-2664.2001.00567.x

Royle, J. A., Fuller, A. K., & Sutherland, C. (2018). Unifying population and landscape ecology with spatial capture–recapture. *Ecography*, 41(3), 444-456. https://doi.org/10.1111/ecog.03170

Royle, J. A., Nichols, J. D., & Kéry, M. (2005). Modelling occurrence and abundance of species when detection is imperfect. *Oikos*, 110(2), 353–359. https://doi.org/10.1111/j.0030-1299.2005.13534.x

Rundel, P. W., Dickie, I. a., & Richardson, D. M. (2014). Tree invasions into treeless areas: Mechanisms and ecosystem processes. *Biological Invasions*, 16(3), 663–675. https://doi.org/10.1007/s10530-013-0614-9

Sahara, E. A., Sarr, D. A., Van Kirk, R. W., & Jules, E. S. (2015). Quantifying habitat loss: Assessing tree encroachment into a serpentine savanna using dendroecology and remote sensing. *Forest Ecology and Management*, 340, 9–21. https://doi.org/10.1016/j.foreco.2014.12.019

Salguero-Gómez, R., Jones, O. R., Archer, C. R., Buckley, Y. M., Che-Castaldo, J., Caswell, H., Hodgson, D., Scheuerlein, A., Conde, D.A., Brinks, E., de Buhr, H., Farack, C., Gottschalk, F., Hartmann, A., Henning A., Hoppe, G., Römer, G., Runge, J., Ruoff, T., Wille, J., Zeh, S., Davison, R., Vieregg, D., Baudisch, A., Altwegg, R., Colchero, F., Dong, M., de Kroon, H., Lebreton, J.-D., Metcalf, C. J. E., Neel, M. M., Parker, I. M., Takada, T., Valverde, T., Vélez-Espino, L. A., Wardle, G. M., Franco, M., & Vaupel, J. W. (2015). The Compadre Plant Matrix Database: An open online repository for plant demography. *Journal of Ecology*, 103(1), 202–218. https://doi.org/10.1111/1365-2745.12334

Sandel, B., & Smith, A. B. (2009). Scale as a lurking factor: Incorporating scale-dependence in experimental ecology. *Oikos*, 118(9), 1284–1291. https://doi.org/10.1111/j.1600-0706.2009.17421.x

Schurr, F. M., Steinitz, O., & Nathan, R. (2008). Plant fecundity and seed dispersal in spatially heterogeneous environments: Models, mechanisms and estimation. *Journal of Ecology*, 96(4), 628–641. https://doi.org/10.1111/j.1365-2745.2008.01371.x

Sharp, G., Semple, R., Vandermeulen, H., Wilson, M., LaRoque, C., & Nebel, S. (2010). The Basin Head Irish Moss (*Chondrus crispus*) population abundance and distribution 1980 to 2008. Canadian Scientific Advisory Secretariat Science Research Document, 2010/054, vi + 32 p.

Singh, M., Evans, D., Tan, B. S., & Nin, C. S. (2015). Mapping and characterizing selected canopy tree species at the Angkor world heritage site in Cambodia using aerial data. *PLoS ONE*, 10(4). https://doi.org/10.1371/journal.pone.0121558

Soranno, P. A., & Schimel, D. S. (2014). Macrosystems ecology: Big data, big ecology. *Frontiers in Ecology and the Environment*, 12(1), 3–3. https://doi.org/10.1890/1540-9295-12.1.3

Spiegel, O., & Nathan, R. (2012). Empirical evaluation of directed dispersal and density-dependent effects across successive recruitment phases. *Journal of Ecology*, 100(2), 392–404. https://doi.org/10.1111/j.1365-2745.2011.01886.x

Starrfelt, J., & Kokko, H. (2010). Parent-offspring conflict and the evolution of dispersal distance. *The American Naturalist,* 175(1), 38–49. https://doi.org/10.1086/648605

Svenning, J.-C., Gravel, D., Holt, R. D., Schurr, F. M., Thuiller, W., Münkemüller, T., Schiffers, K. H., Dullinger, S., Edwards, T. C., Hickler, T., Higgins, S. I., Nabel, J. E. M. S., Pagel, J., & Normand, S. (2014). The influence of interspecific interactions on species range expansion rates. *Ecography*, 37(12), 1198–1209. https://doi.org/10.1111/j.1600-0587.2013.00574.x

Tilman, D., Lehman, C. L., & Kareiva, P. (1997). Population dynamics in spatial habitats. In D. Tilman & P. Kareiva (Eds.), *Spatial Ecology: The Role of Space in Population Dynamics and Interspecfic Interactions* (pp. 3–20). Princeton, New Jersey: Princeton University Press.

Turnbull, L. A., Coomes, D. A., Purves, D. W., & Rees, M. (2007). How spatial structure alters population and community dynamics in a natural plant community. *Journal of Ecology*, 95(1), 79–89. https://doi.org/10.1111/j.1365-2745.2006.01184.x

Urban, M. C., Bocedi, G., Hendry, A. P., Mihoub, J.-B., Pe'er, G., Singer, A., Bridle, J. R., Crozier, L. G., De Meester, L., Godsoe, W., Gonzalez, A., Hellmann, J. J., Holt, R. D., Huth, A., Johst, K., Krug, C. B., Leadley, P. W., Palmer, S. C. F., Pantel, J. H., Schmitz, A., Zollner, P. A., & Travis, J. M. J. (2016). Improving the forecast for biodiversity under climate change. *Science*, 353(6304), aad8466-1 –aad8466-9. https://doi.org/ 10.1126/science.aad8466

Urban, M. C., Tewksbury, J. J., & Sheldon, K. S. (2012). On a collision course: Competition and dispersal differences create no-analogue communities and cause extinctions during climate change. *Proceedings of the Royal Society B: Biological Sciences,* 279(1735), 2072–2080. https://doi.org/10.1098/rspb.2011.2367

Van Gunst, K. J., Weisberg, P. J., Yang, J., & Fan, Y. (2016). Do denser forests have greater risk of tree mortality: A remote sensing analysis of density-dependent forest mortality. *Forest Ecology and Management*, 359, 19–32. https://doi.org/10.1016/j.foreco.2015.09.032

Vance, R. R., Steele, M. A., & Forrester, G. E. (2010). Using an individual-based model to quantify scale transition in demographic rate functions: Deaths in a coral reef fish. *Ecological Modelling*, 221(16), 1907–1921. https://doi.org/10.1016/j.ecolmodel.2010.04.014

Vitousek, P. M., Dantonio, C. M., Loope, L. L., Rejmánek, M., & Westbrooks, R. (1997). Introduced species: A significant component of human-caused global change. *New Zealand Journal of Ecology*, 21(1), 1–16. https://doi.org/10.1890/02-0571

Warner, T. A., Nellis, M. D., & Foody, G. M. (2009). Remote sensing scale and data selection issues. In T. A. Warner, M. D. Nellis, & G. M. Foody (Eds.), *The SAGE Handbook of Remote Sensing* (pp. 3–17). Los Angeles, USA: SAGE Publications.

Wiens, J. A. (1989). Spatial scaling in ecology. *Functional Ecology*, 3(4), 385. https://doi.org/10.2307/2389612

Wisz, M. S., Pottier, J., Kissling, W. D., Pellissier, L., Lenoir, J., Damgaard, C. F., Dormann, C. F., Forchhammer, M. C., Grytnes, J. A., Guisan, A., Heikkinen, R. K., Høye, T. T., Kühn, I., Luoto, M., Maiorano, L., Nilsson, M. C., Normand, S., Öckinger, E., Schmidt, N. M., Termansen, M., Timmermann, A., Wardle, D. A., Aastrup, P., & Svenning, J. C. (2013). The role of biotic interactions in shaping distributions and realised assemblages of species: Implications for species distribution modelling. *Biological Reviews*, 88(1), 15–30. https://doi.org/10.1111/j.1469-185X.2012.00235.x

Wright, W. J., Irvine, K. M., Warren, J. M., & Barnett, J. K. (2017). Statistical design and analysis for plant cover studies with multiple sources of observation errors. *Methods in Ecology and Evolution*, 8(12), 1832–1841. https://doi.org/10.1111/2041-210X.12825

Wu, J., Swenson, N. G., Brown, C., Zhang, C., Yang, J., Ci, X., Li, J., Sha, L., Cao, M., & Lin, L. (2016). How does habitat filtering affect the detection of conspecific and phylogenetic density dependence? *Ecology*, 97(5), 1182–1193. https://doi.org/10.1890/14-2465.1

Xie, Y., Sha, Z., & Yu, M. (2008). Remote sensing imagery in vegetation mapping: A review. *Journal of Plant Ecology*, 1(1), 9–23. https://doi.org/10.1093/jpe/rtm005

Yokomizo, H., Takada, T., Fukaya, K., & Lambrinos, J. G. (2017). The influence of time since introduction on the population growth of introduced species and the consequences for management. *Population Ecology*, 59(2), 89–97. https://doi.org/10.1007/s10144-017-0581-6

Zhu, K., Woodall, C. W., Monteiro, J. V. D., & Clark, J. S. (2015). Prevalence and strength of density-dependent tree recruitment. *Ecology*, 96(9), 2319–2327. https://doi.org/10.1890/14-1780.1

Chapter 2

Assessing the utility of aerial imagery to quantify the density, age structure and spatial pattern of alien conifer invasions

2.1 Introduction

Alien conifer invasions pose a threat to native biodiversity, ecosystem functions, and productive agricultural landscapes in the Southern Hemisphere (Higgins & Richardson, 1998; Nuñez et al., 2017; Richardson, Williams, & Hobbs, 1994; Simberloff et al., 2010). Conifer trees established in plantations and along the edges of pastures have naturalised and spread rapidly to new, and often isolated areas (Ledgard 2001; Richardson et al. 2008; Froude 2011). To combat their spread, land managers need cost-effective and time-efficient methods to locate sparse trees present across extensive landscapes, assess the rate of spread to prioritise management, and quantify the density of the invasion to determine appropriate management techniques (e.g., boom-spraying from helicopters vs. on the ground tree-felling).

Free aerial imagery (orthophotography) offers a promising solution to these problems. Aerial imagery can acquire data across large spatial scales, be repeated in both time and space, and costs less per unit area than field-based methods (Asner, Jones, Martin, Knapp, & Hughes, 2008; Bradley, 2014; Huang & Asner, 2009; Visser, Langdon, Pauchard, & Richardson, 2014). Similar low-cost high-resolution imagery, such as those data acquired from Google Earth, has been found to be useful for mapping canopy cover and monitoring spread of invasive alien trees (Visser et al., 2014). Furthermore, aerial imagery often has a high pixel resolution (<0.5m), which is needed to determine the locations of individual trees; whereas freely available satellite imagery such as captured by the LandSAT (30m resolution) and Sentinel (10m resolution) satellites is too coarse for this purpose (Huang & Asner, 2009; Ke & Quackenbush, 2011). For these reasons, aerial imagery has previously been used to map conifers and woody shrubs encroaching into grasslands and savannahs in the western US (Hulet, Roundy, Petersen, Jensen, & Bunting, 2013; Poznanovic, Falkowski, Maclean, Smith, & Evans, 2014; Sahara, Sarr, Van Kirk, & Jules, 2015), estimate tree and woody shrub cover and biomass (Madsen, Zvirzdin, Davis, Petersen, & Roundy, 2011; Mirik, Chaudhuri, Surber, Ale, & Ansley, 2013), and monitor encroachment over time (Mast, Veblen, & Hodgson, 1997).

Because of its increased use and interest, it is essential to carefully evaluate the accuracy of aerial imagery using ground-truthing (Bradley, 2014; Congalton, 1991). In ground-truthing, canopy cover and/or the locations of tree species are measured in the field and compared to what was detected from the aerial imagery to derive suitable measures of accuracy (Congalton, 1991). However, measures of accuracy are likely to be a function of tree density, since at high density, individual trees and size classes may be difficult to discern (Carreiras, Pereira, & Pereira, 2006; Strand, Robinson, & Bunting,

2007). This poses a considerable challenge in that it is particularly important to distinguish different life-stages, especially the mature, reproducing trees since they contribute to spread and are often the top priority for management (Buckley et al., 2005; Caplat, Coutts, & Buckley, 2012; Sykes, 2001). What is missing from past studies and current ground-truthing protocols is an understanding of how well aerial imagery can detect and quantify age structure, densities, and spatial patterns.

Since the future rate of spread will be determined by current tree density, it is essential to understand how density varies from one location to another. Sparse densities of trees spreading well ahead of the population invasion front can accelerate the rate of invasion (J. S. Clark, Lewis, & Horvath, 2001; Dovčiak, Hrivnák, Ujházy, & Gömöry, 2014; Shigesada, Kawasaki, & Takeda, 1995). Mid-to-high densities give rise to spatial patterns such as clustering and over-dispersion (Dieckmann, Law, & Metz, 2000; Law & Dieckmann, 2000). These patterns may have a key role in the rate of infilling behind the invasion front as they determine the strength of biotic interactions (Bolker & Pacala, 1997; Dieckmann et al., 2000), particularly by affecting the individual growth rate of trees through both competition and facilitation (Peters, 2003; Zhu, Woodall, Monteiro, & Clark, 2015).

I have focused this study on conifer invasions in New Zealand. In New Zealand, alien conifer trees affect over 1.7 million hectares of land and the government has spent upwards of $16 million (or $11 million USD) on control efforts (Ministry of Primary Industries, 2014). Given the scale of the problem in New Zealand, understanding the detection limitations of using freely available aerial imagery to study these conifer invasions is a management priority. In particular it is essential to assess how well aerial imagery performs at detecting trees at both low and high density, and the degree that it captures the age structure and spatial pattern of an invasion. This knowledge of the accuracy of aerial imagery can then be used to identify under what circumstances such orthophotography might be valuable in supporting the management of conifer invasions.

2.2 Methods

2.2.1 Study System and Site

The study site was located at Mt Barker (171°35′15″ E, 43°21′30″ S) in the South Island of New Zealand. The predominant species found at the site was *Pinus nigra* (Corsican pine), but there was also some *P. contorta* (Lodgepole pine), *P. sylvestris*, *P. ponderosa*, and *Pseudotsuga menziesii* (Douglas fir). The site (602 ha) was originally a mixture of alien and native grasslands. The alien conifers originate from a row of *P. nigra* planted around 1910, and the invasion has since spread into the tussock grasslands following the prevailing northwest winds. The other species arrived by wind from other intentionally plantings in the area. The invasion exhibits a wide range of tree densities up to over 1 tree/m^2 and occupies an area of about 6 km^2.

2.2.2 Data collection and image classification

Aerial imagery taken from an aircraft in late summer 2016 was retrieved from the Land Information New Zealand (LINZ) archive (Fig. 2.1). The imagery had three spectral bands (Red, Green, and Blue) and a pixel size of 0.3m. To identify the point locations of conifer trees, I used an automated, unsupervised image classification methodology based on methods used by Gougeon (1995), Wang et al. (2004), and Lamar et al. (2005). An automated procedure allowed me to run the image classification quickly and without human input, making it easy to run for non-experts. I also chose to use an unsupervised method as it did not require training data.

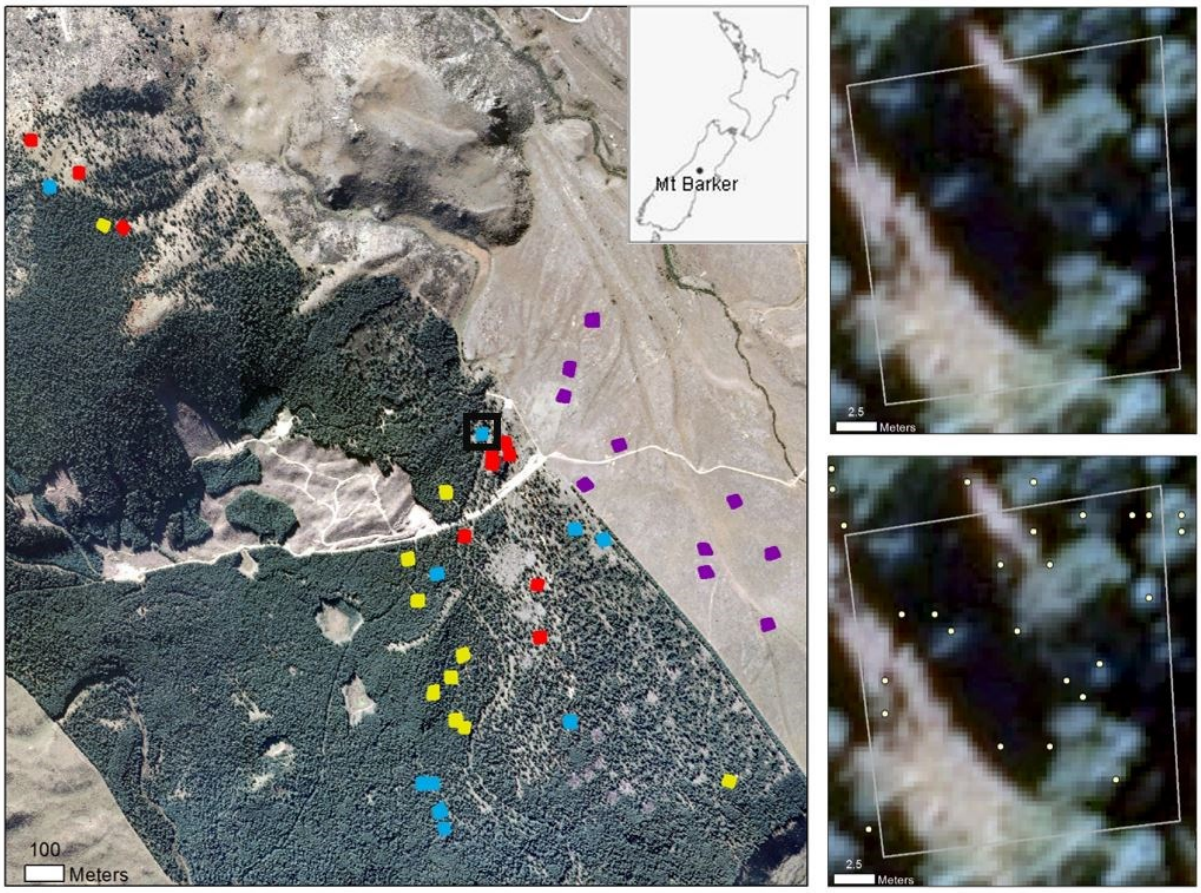

Figure 2.1 Aerial photo (left) of the study site with ground-truthing plots. Dark purple plots represent the plots in the sparse density, red plots represent low density, blue plots represent mid density, and yellow plots represent high density. The aerial photo was taken in late summer 2016 and access to the imagery was provided by Land Information New Zealand. The plot with the black outline is zoomed in to show an example of a ground-truthing plot in mid density (right two photos). The top right photo shows the plot with unclassified aerial imagery, and the bottom right photo shows the plot with the points of trees detected overlaid on the imagery.

The image classification procedure used intensity thresholds of the pixels of the three bands to separate the dark-coloured conifer trees from the light-coloured background vegetation (Ke & Quackenbush, 2011). I was able to do this because the dark-coloured conifer trees were easily distinguished against the light-coloured grassland vegetation, and there were very few other trees or shrubs in the area other than the species of interest. Using the distinct conifer tree pixels and the pixels

of the conifer shadows, I then applied a watershedding technique (following methods by Komura et al. (2004), Wang et al. (2004), and Deng et al. (2016)). This technique delineates objects according to changes in pixel colour intensity by following the shadows, or lower intensity areas, to segment individual tree-canopy objects. I adjusted the extent of the observation windows to be the smallest possible setting on the watershedding function so that it was more sensitive to changes in intensity of the pixels. This allowed me to segment and separate more trees in dense areas. All of these steps were done using the R package EBImage (Pau, Fuchs, Sklyar, Boutros, & Huber, 2010). Once the watershedding method was completed, I converted the resulting objects (trees) into polygons. I discarded the polygons which had an area of only one pixel ($0.09m^2$) to decrease the possible pixel noise in the imagery (Kelcey & Lucieer, 2012; Tomljenovic, Tiede, & Blaschke, 2016). I then converted the polygons to points using the centroid of each polygon, assuming that each polygon represented one tree. To do these steps I used the following R packages: raster (Hijmans, 2016), rgdal (Bivand, Keitt, & Rowlingson, 2017), and sp (Pebesma & Bivand, 2005). All of the image classification was done in R (R Core Team, 2017).

2.2.3 Field estimates of tree locations across densities

To ground-truth aerial imagery, forty 20m x 20m plots were distributed across the flat areas of the study site in a stratified random design (Congalton, 1991) to locate ten sample plots in each of the following densities: sparse density of trees (invasion front), low density, mid density, and high density (see Fig. 2.1 for locations of plots). These plots were placed at random within each density stratum at the Mt Barker site using the classified aerial imagery, so the groups of sparse, low, mid, and high densities were based on the number of trees that were predicted to be present in the plots. The coordinates of each of the four corners of the plots were determined, and a high-precision GPS (Trimble GeoExplorer 6000 series GeoXH with real-time and post processing differential correction) was used to locate the corners and set up the plots in the field. This handheld GPS unit had an average horizontal precision of 0.13m in very low density plots and 1.58m in high density plots (overall mean was 1.19m).

Within each plot, the following measurements were recorded on each tree over 0.5m in height: maximum size of the tree's canopy diameter, age class (determined by height), species, and whether the tree was coning (similar to methods of Haby, Tunn, & Cameron (2010) and Visser et al. (2014)). Additionally, each tree measured had its location recorded with the GPS, one GPS point per tree. The age classes were divided as follows: adults were those trees over 3m in height, sub-adults were 2-3m in height, old saplings were 1.5-2m in height, saplings were 1-1.5m in height, and young saplings were 0.5-1m in height. Trees under 0.5m in height were not measured as most of these trees had canopy diameters less than the size of the imagery's pixels (i.e., less than 0.3m in width).

2.2.4 Analyses

Due to the precision error from the GPS, I was not able to match up exactly the trees I measured in the field with the trees detected by the aerial imagery. Therefore, I conducted the analyses on a per plot basis to examine how many trees were detected in each plot and how many trees were measured in the field. This approach relied on the assumption that I was able to detect the largest tree canopies first and then progressively detect the smaller canopies. Other studies have found this assumption to be valid (Falkowski et al., 2008; Yu, Hyyppä, Vastaranta, Holopainen, & Viitala, 2011).

Relating canopy diameter size to reproductive stage

In the analyses assessing the detection of age structure, I focused on examining the mature, reproducing trees (coning trees) in the invaded landscape that were recorded from the ground-truthing assessment. To relate the canopy diameter size of trees to coning ability, I generated a distribution based on the proportion of trees coning at incremental sizes. I calculated the number of trees with canopy diameters between 0 – 8m by 0.5m increments (e.g., groups were 0-0.5m, 0.5-1m, 1-1.5m, etc.), and for each of these size groups, I calculated the proportion of trees which were coning. From these calculations, I fitted a logistic regression model to the proportions of trees coning. I also examined whether a tree's reproductive stage was related to its canopy size and the surrounding density using a generalised linear mixed effects regression with field plots as a random effect in the model.

Detection of tree diameter sizes across densities

I tested the effect of different size thresholds by first subsetting the field data based on canopy diameter sizes. The size classes were as follows: canopy diameter 1m and over, 1.5m and over, 2m and over, 2.5m and over, and 3m and over. Size classes were nested such that all trees in a particular size class included trees in the larger size classes. This approach was taken because I did not estimate the canopy diameter of each tree in the image classification of the aerial imagery and nor did I match up the tree I detected remotely with the trees I measured in the field due to precision errors with the GPS.

I next examined how the errors of commission and omission varied with canopy diameter size and determined the size classes with the lowest total error rates. Errors of commission mean that the aerial imagery detected a tree when there was not a tree present (false positive), and errors of omission mean that the aerial imagery failed to detect a tree that was recorded in the ground survey (false negative) (Congalton, 1991). I also examined how these commission and omission errors changed with density by comparing the mean errors at low, mid, and high densities of trees.

I compared the number of trees in a particular size class in the field plots with the number of trees detected per plot by the aerial imagery using linear regressions. By plotting each regression line against a 1:1 line with an intercept of zero and slope of one, I determined at which densities I was

under- or over-estimating the number of trees of that size class. Additionally, for each regression line, I tested if the intercept was different from zero using the offset term in the linear model in R. I also tested if the slope was different from one using the offset term in the linear model. An intercept significantly greater than zero indicated that particularly at low densities, the aerial imagery over-estimated the true number of trees in that size class. A slope significantly different from one indicated that the aerial imagery did not consistently estimate the true number of trees across densities.

Spatial patterns

To compare the spatial patterns of the trees which I detected to the trees which I measured in the field, I used Clark and Evans' indices of spatial randomness. These indices are based on the nearest neighbour distances and the density of trees in a plot (Clark & Evans, 1954) (Equation 2.1).

$$Index\ of\ Randomness = \frac{2\,\bar{r}}{\sqrt{\rho}} \qquad \text{(Equation 2.1)}$$

Where $\bar{r}$ is the mean nearest neighbour distance and ρ is the density of trees/plot

We can think of these indices as being indicators of the type of spatial pattern within a plot. Indices less than one indicate a clustered spatial pattern within a plot, indices equal to one indicate a random spatial pattern, and indices larger than one indicate an over-dispersed pattern. Other commonly calculated measures of spatial patterns such as Ripley's K and Pair Correlation Functions were not suitable because these methods required a much higher number of trees per plot than I found (Illian, Penttinen, Stoyan, & Stoyan, 2008).

For each plot, first the nearest neighbour distance for each tree was determined from both the aerial imagery and ground-truth data. Edge effects were accounted for by not calculating nearest neighbour distances for trees which were closer to an edge of a plot than to a neighbouring tree. Once calculated, the mean nearest neighbour distances were used to derive an index of spatial randomness for each plot for the pre-determined size class of trees. I tested for a difference between the indices of spatial randomness for the field and aerial imagery datasets across the plots using a paired t-test. When the comparisons yielded a non-significant result, polynomial regressions examining how the mean index per plot changed with density were modelled. These indices were plotted across plot densities, and the regression curves of these lines were compared to determine whether there was a difference in spatial patterns according to density.

2.3 Results

A total of 3952 trees over 0.5m in height were measured in the field, 1218 of which were over 1m in canopy diameter and 520 of which were over 2.5m in canopy diameter. The analysis of aerial imagery detected 802 trees across the plots, approximately only 20% of the trees surveyed in the field.

2.3.1 Relating canopy diameter size to reproductive tree stage

As tree canopy diameter size increased, so did the proportion of trees coning (Fig. 2.2). From the cumulative percentages of trees coning for size thresholds, almost 80% of trees with a canopy greater than 2.5m were coning compared to only a small proportion of trees (0.5%) below 2m.

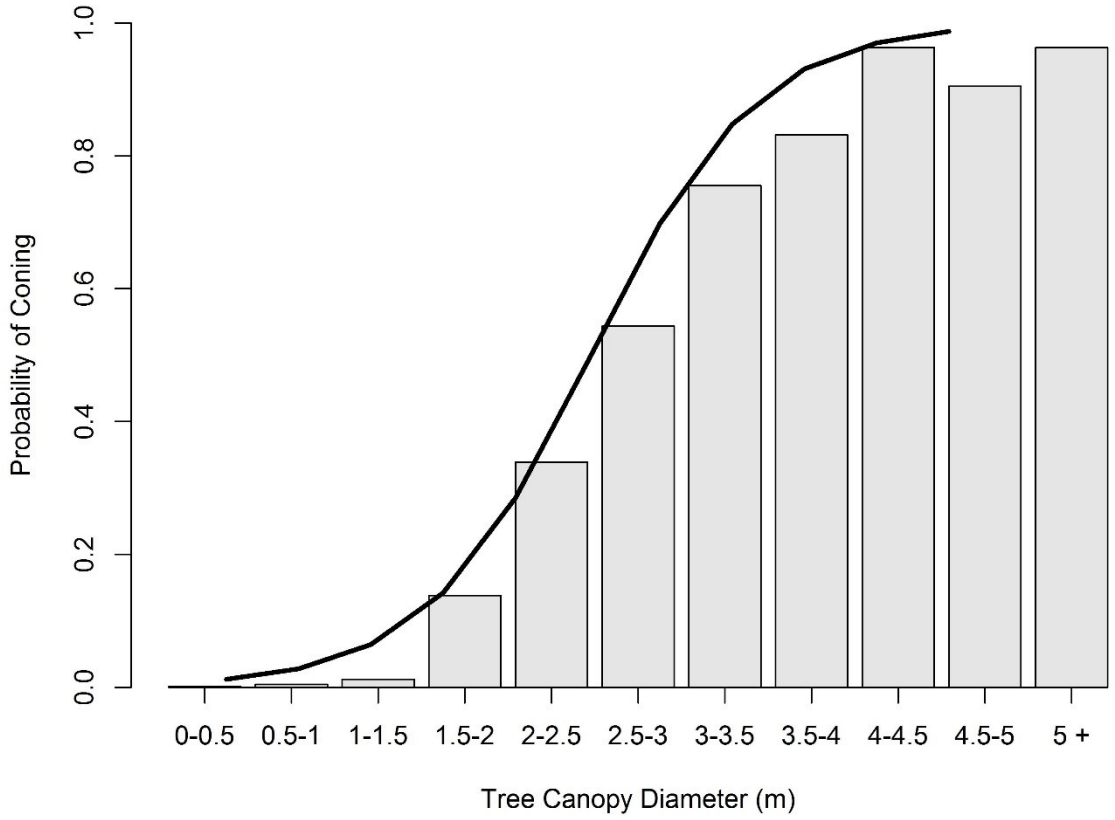

Figure 2.2 Proportion of coning trees versus canopy diameter. The black logistic curve represents a fitted generalised linear regression. A Hoslem test for goodness of fit on the regression found that it was a good fit (p-value > 0.05), meaning that the observed and expected values were not significantly different from each other.

When I examined the presence/absence of trees coning as a function of their canopy diameter and the surrounding tree density, I found that density did not have a strong effect on the likelihood of a tree coning, compared to canopy diameter (Table 2.1). Without the interaction term, the model found that canopy was the only significant variable; density was still not significant. Using a simple goodness of fit test by comparing the model's predicted response to the fitted data, I calculated an R^2 value of 0.71, indicating a good model fit. As expected, there was a relatively high amount of variation between the tree densities of the plots as detected by significant random effects in a Likelihood Ratio Test comparing a generalised linear mixed effects model and a generalised linear model (p-value = 1.4×10^{-9}).

Table 2.1 Results of the generalised linear mixed effects model examining coning as a function of canopy diameter and surrounding density.

Variable	Odds Ratio Estimate	Standard Error	p-value
Canopy diameter (m)	2.52	0.23	$2x10^{-16}$
Density (trees/m^2)	0.30	1.5	0.84
Interaction effects	-0.60	0.50	0.23

2.3.2 Detection of tree sizes across densities

For the small tree sizes there were high commission errors (false positives) at low densities and high omission errors (false negatives) at high densities (Fig. 2.3a). The aerial imagery and imagery classification technique under-estimated the number of small trees at high densities. The lowest total classification error rates were found for trees with canopy diameter > 2m and > 2.5m (total error rates = 21% and 23% respectively). For these largest size classes, high errors of commission were found at low tree densities while errors of omission were consistently low across densities (Fig 2.3). This suggests that the number of large trees (canopy diameter > 2.5m) was over-estimated at low tree density.

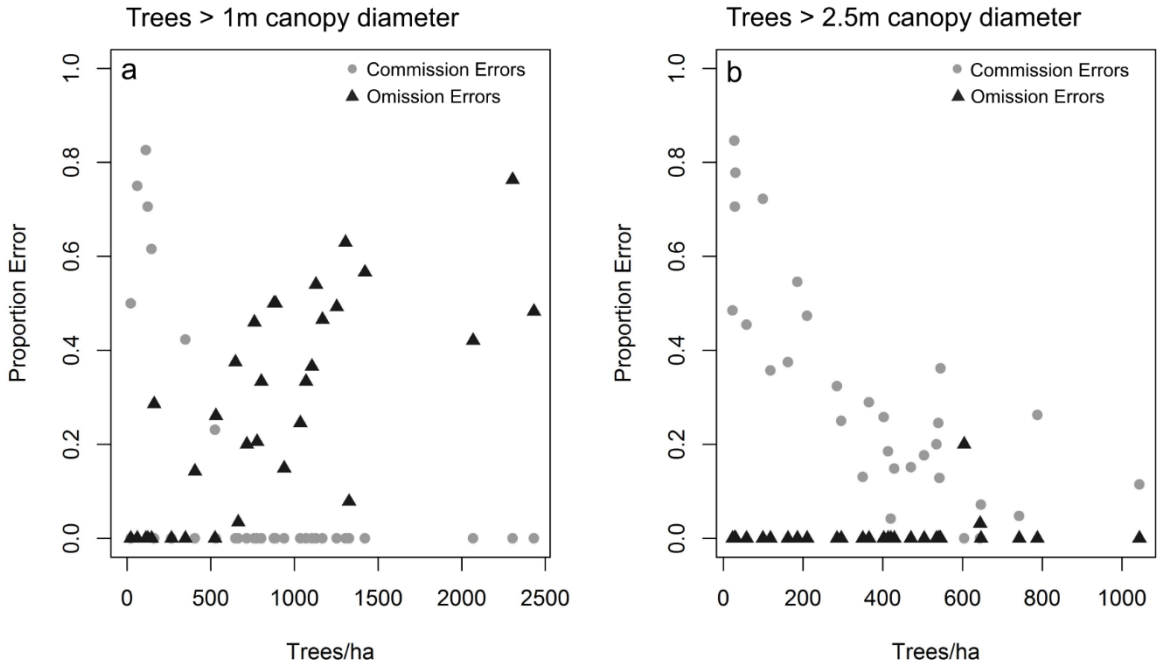

Figure 2.3 Error rates for trees over 1m in canopy diameter (a) and trees over 2.5m in canopy diameter (b). Commission errors are high at low densities for both size groups of trees. Omission errors increase with density for the small size class of trees (a) and are low across densities for the large size class of trees (b).

There were significant biases irrespective of tree canopy diameter in estimates of tree density (Fig. 2.4). I was not able to detect small trees well at mid or high densities, although I was able to potentially detect these trees at low densities (Fig 2.4a, b). In these cases, both the intercept and slope were significantly different than the null expectation such that aerial imagery over-estimated tree density at low densities but produced underestimates at higher densities. Most trees with a canopy diameter over 2m were detected, although these trees were still under-estimated at high densities (Fig 2.4c, regression line below the red 1:1 line). I can detect trees with a canopy diameter over 2.5m with high confidence since slopes were not significantly different from one. However, all intercepts of the size classes departed from zero which indicated a consistent over-estimate of tree density irrespective of actual tree density. Because the canopy diameter >2.5m represented the best fit to the 1:1 line and had a low error rate, I focused on using this size threshold for spatial analyses. The results of the significance tests comparing the slope and intercept values to the null expectation are in Appendix A.

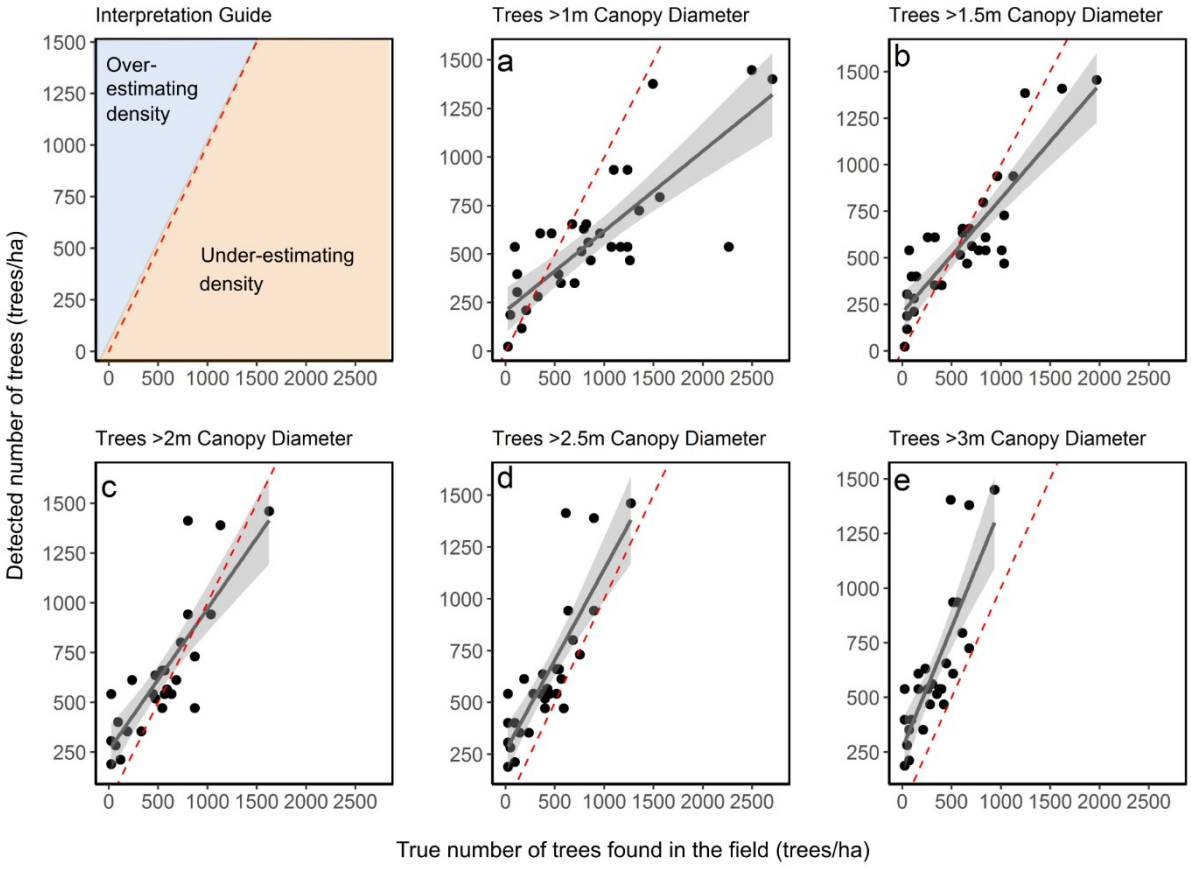

Figure 2.4 Detection of trees across densities. The top left panel shows a guide for interpreting the meaning of the regression lines in relation to the 1:1 null line. The other five panels show a different size group of trees, starting from the more inclusive group of canopy diameter of >1m in the upper middle panel (a) to the trees with the largest canopy diameter of >3m in the lower right corner (e). The dashed red line represents a 1:1 line.

2.3.3 Spatial patterns

Across all densities, the spatial patterns of the trees detected by aerial imagery data were not significantly different from the patterns of trees >2.5m in canopy measured in the field (p-value = 0.105, mean difference between indices = 0.12, 95% CI = 0.15). Plotting the spatial indices data against density (Fig. 2.5), the polynomial term for both of these groups was significant (p-value = 0.02 for trees over 2.5m; p-value = 0.009 for trees detected). As tree density increased, the spatial distribution of trees became more clustered as might be expected. This trend was found whether the aerial imagery data or ground-truthed observations were used, and in general, aerial imagery data presented evidence towards greater clustering than the ground-truthed field observations.

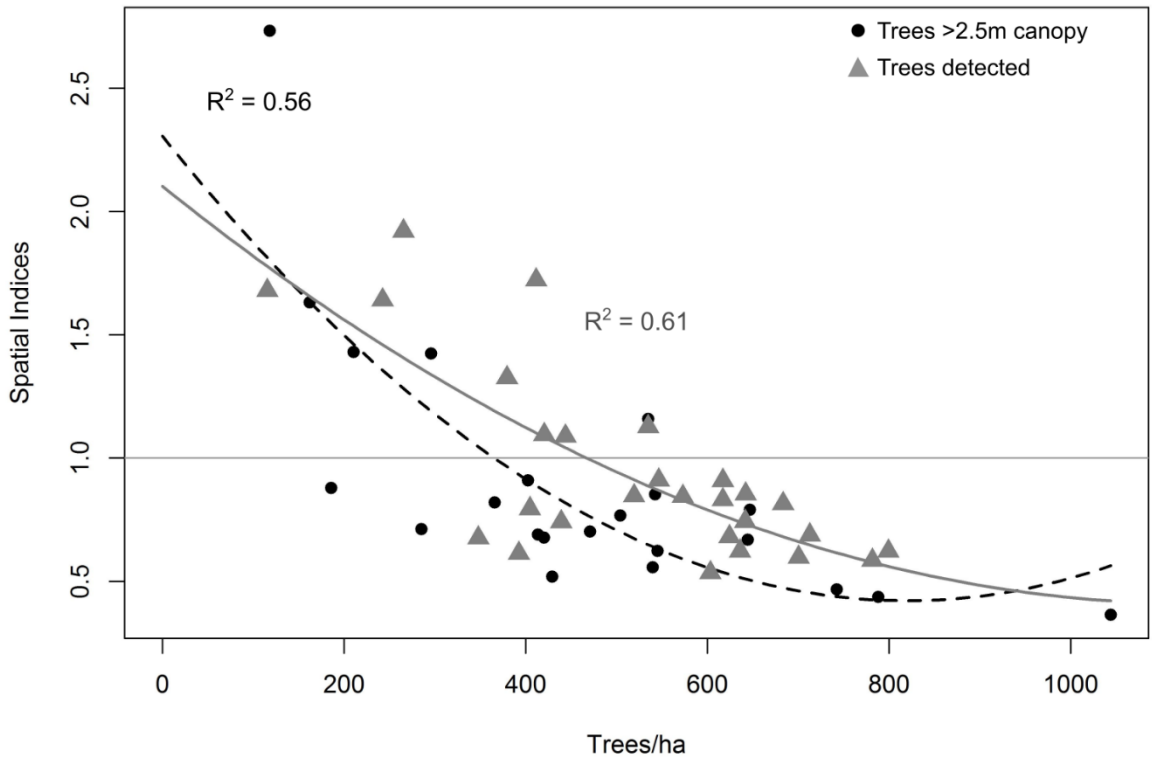

Figure 2.5 Spatial indices of each plot graphed against density of the plot. The black points represent the data for the trees with a canopy diameter of >2.5m, and the grey triangles represent the data for the trees detected by aerial imagery. The light grey horizontal line at 1 represents an index of random spatial pattern. The points above the light grey line at 1 represent plots that are over-dispersed and the points below the light grey line represent plots that are clustered.

2.4 Discussion

I examined how tree density influenced the ability to detect alien conifers using freely available aerial imagery. When I assessed the detection of age structure, I found that while I was not able to detect

whether or not a tree was coning, canopy size was the strongest predictor of reproductive stage. I found that particularly for small-sized trees, density has a large effect on the ability to detect alien conifers when using watershedding classification techniques. For small-sized trees, the results suggest that I could detect smaller conifers at lower densities, although at high densities I could not detect these small trees with great accuracy. While density seems to heavily influence the detection of small trees, the ability to detect large-sized trees does not depend on density as much and I can likely detect them across all densities.

While I found that I could detect smaller trees at low densities, I could detect trees larger than 2.5m in canopy diameter across all densities. Additionally, I found that I could reliably measure the spatial patterns for trees at this size threshold, but not below. This finding signifies that aerial imagery can be used to detect and summarise the spatial patterns of reproductive individuals behind and beyond an invasion front.

While these results were promising, I have identified several limitations in the methodology. First, I found that I could not map the exact locations of individual trees accurately at high densities. This was due to both the inability to detect all trees at high densities using aerial imagery and also GPS errors at high densities. Under dense canopy cover, the GPS had average precision errors of around 1.6m which made it difficult to match up tree locations recorded in the field with those detected in the imagery. However, as I am able to detect and determine the locations of individual trees at low densities, I am more confident in the ability of aerial imagery to map large, sparse trees. The study site also had particularly high density areas compared to other studies (Delmas, Delzon, & Lortie, 2011). For example, Tomiolo et al. (2016) found densities at around 300 trees/ha for a *Pinus contorta* invasion in New Zealand, and Taylor et al. (2016) predicted densities of conifer invasions to be between 0-2000 trees/ha for most sites worldwide compared to the upwards of 2500 trees/ha that I measured in the field plots. Potentially sites with lower densities could expect to have less detection bias than I found. Thus most conifer invasions are likely to reflect densities that I classed as low and would be suitable for the application of aerial imagery.

I also brought to light limitations to using aerial imagery for detecting trees across densities. I could not detect all tree size classes equally, and the types of classification errors changed with size class as well. Also, detection was sensitive to density, implying that density needs to be accounted for when using aerial imagery for detection. I recommend expanding upon the methodologies of Bradley (2014) and Congalton (1991) to include sampling across a range of tree densities in an invasion and testing for the effect of density on detection. Furthermore, in this study I could not distinguish between different species, and if this is important, hyperspectral imagery would be a better alternative (Andrew & Ustin, 2009; He, Rocchini, Neteler, & Nagendra, 2011; Huang & Asner, 2009). If cost is not an issue for the study, higher specification imagery could also be used to detect individual trees and densities. Airborne Laser Scanning (ALS) and hyperspectral sensors have been proven to accurately

detect individual tree canopies, although these types of imagery come at a relatively high cost (Dalponte, Ørka, Ene, Gobakken, & Næsset, 2014; Dash, Pearse, Watt, & Paul, 2017; Lawrence, Wood, & Sheley, 2006).

Despite these limitations, this study identified several benefits of using aerial imagery data. The imagery was able to detect small trees in low density areas, a capability which managers currently need to prevent the spread of an invading population (Yokomizo, Possingham, Thomas, & Buckley, 2009). Although the imagery is sensitive to tree density, I can still detect high density areas, which managers also need to do in order to identify areas of certain control types (i.e., boom spraying by helicopter or plane) (Department of Conservation 2018). Large trees can also be detected, and even though not all of these large trees are coning, this study's estimates probably over-estimated the number of coning trees.

Another benefit of aerial imagery is that it could detect the spatial patterns of the mid-to-large sized trees. Thus, I would suggest that low-cost aerial imagery could also be used to gain insights into the spatial spread patterns of tree invasions, similar to Dovčiak, Hrivnák, Ujházy, & Gömöry (2014). Especially since these images are available over large areas and sometimes over multiple time steps, examining the spatial patterns over time can assist assessments of invasion risk as well as identifying landscape and land use features which facilitate spread (Bradley & Mustard, 2006; He et al., 2011; Müllerová, Pyšek, Jarošík, & Pergl, 2005). Low-cost aerial imagery thus enables the study of spatial patterns within invasions, with the caveat that only the spread patterns of the mid-to-large sized trees can be quantified.

In addition to these benefits I identified in this study, another bonus of aerial imagery is its widespread availability in countries where invasive conifers are a problem. For example, South Africa offers free, sub-meter resolution aerial imagery through their National Geo-spatial Information Services (Department of Rural Development and Land Reform, 2018). Several states in Australia offer free or low-cost historic and recent aerial photography (e.g., Department of Finance, Service and Innovation: Spatial Services, 2018; Landgate, 2018). Furthermore, online services such as OpenAerialMap supply free, open-license high-resolution imagery acquired from satellites, airplanes, and Unmanned Aerial Vehicles (OpenAerialMap, 2018). More generally, many countries such as the United States and Canada have free, high-resolution aerial imagery through programmes such as the National Agriculture Imagery Program (Mauck, Brown, & Carswell Jr, 2016) and the National Air Photo Library (Natural Resources Canada, 2016), and these data could be used to study other tree and woody shrub invasions.

2.4.1 Conclusion

This study was important both from a management and a methodological perspective. I found that the ability to detect conifers changes with density and therefore future studies need to account for density

when assessing detection accuracy. In general, the aerial imagery could most accurately detect trees over 2.5m in canopy diameter across densities, but it could detect smaller trees at low densities. Aerial imagery could also detect the spatial patterns of the mid-to-large sized trees, which suggests that it could be a useful tool for studying spread patterns. While I found that low-cost aerial imagery could have important uses, scientists and managers must account for the detection bias across densities when assessing the accuracy of aerial imagery.

2.5 References

Andrew, M. E., & Ustin, S. L. (2009). Habitat suitability modelling of an invasive plant with advanced remote sensing data. *Diversity and Distributions*, 15(4), 627–640. https://doi.org/10.1111/j.1472-4642.2009.00568.x

Asner, G. P., Jones, M. O., Martin, R. E., Knapp, D. E., & Hughes, R. F. (2008). Remote sensing of native and invasive species in Hawaiian forests. *Remote Sensing of Environment*, 112(5), 1912–1926. https://doi.org/10.1016/j.rse.2007.02.043

Bivand, R., Keitt, T., & Rowlingson, B. (2017). rgdal: Bindings for the Geospatial Data Abstraction Library. R package version 1.2-8. Retrieved from https://cran.r-project.org/package=rgdal

Bolker, B. M., & Pacala, S. W. (1997). Using moment equations to understand stochastically driven spatial pattern formation in ecological systems. *Theoretical Population Biology*, 52(3), 179–197. https://doi.org/10.1006/tpbi.1997.1331

Bradley, B. A. (2014). Remote detection of invasive plants: A review of spectral, textural and phenological approaches. *Biological Invasions*, 16(7), 1411–1425. https://doi.org/10.1007/s10530-013-0578-9

Bradley, B. A., & Mustard, J. F. (2006). Characterizing the landscape dynamics of an invasive plant and risk of invasion using remote sensing. *Ecological Applications*, 16(3), 1132–1147. https://doi.org/10.1890/1051-0761(2006)016[1132:CTLDOA]2.0.CO;2

Buckley, Y. M., Brockerhoff, E., Langer, L., Ledgard, N. J., North, H., & Rees, M. (2005). Slowing down a pine invasion despite uncertainty in demography and dispersal. *Journal of Applied Ecology*, 42(6), 1020–1030. https://doi.org/10.1111/j.1365-2664.2005.01100.x

Caplat, P., Coutts, S., & Buckley, Y. M. (2012). Modeling population dynamics, landscape structure, and management decisions for controlling the spread of invasive plants. *Annals of the New York Academy of Sciences*, 1249(1), 72–83. https://doi.org/10.1111/j.1749-6632.2011.06313.x

Carreiras, J. M. B., Pereira, J. M. C., & Pereira, J. S. (2006). Estimation of tree canopy cover in evergreen oak woodlands using remote sensing. *Forest Ecology and Management*, 223(1–3), 45–53. https://doi.org/10.1016/j.foreco.2005.10.056

Clark, J. S., Lewis, M., & Horvath, L. (2001). Invasion by extremes: Population spread with variation in dispersal and reproduction. *The American Naturalist*, 157(5), 537–554. https://doi.org/10.1086/319934

Clark, P. J., & Evans, F. C. (1954). Distance to nearest neighbor as a measure of spatial relationships in populations. *Ecology*, 35(4), 445–453. https://doi.org/10.2307/1931034

Congalton, R. G. (1991). A review of assessing the accuracy of classifications of remotely sensed data. *Remote Sensing of Environment*, 37(1), 35–46. https://doi.org/10.1016/0034-4257(91)90048-B

Dalponte, M., Ørka, H. O., Ene, L. T., Gobakken, T., & Næsset, E. (2014). Tree crown delineation and tree species classification in boreal forests using hyperspectral and ALS data. *Remote Sensing of Environment*, 140, 306–317. https://doi.org/10.1016/j.rse.2013.09.006

Dash, J. P., Pearse, G. D., Watt, M. S., & Paul, T. (2017). Combining airborne laser scanning and aerial imagery enhances echo classification for invasive conifer detection. *Remote Sensing*, 9(2), 156. https://doi.org/10.3390/rs9020156

Delmas, C., Delzon, S., & Lortie, C. (2011). A meta-analysis of the ecological significance of density in tree invasions. *Community Ecology*, 12(2), 171–178. https://doi.org/10.1556/ComEc.12.2011.2.4

Deng, S., Katoh, M., Yu, X., Hyyppä, J., & Gao, T. (2016). Comparison of tree species classifications at the individual tree level by combining ALS data and RGB images using different algorithms. *Remote Sensing*, 8(12), 1034. https://doi.org/10.3390/rs8121034

Department of Conservation. (2018). Methods of control for wilding conifers. Retrieved July 23, 2018, from https://www.doc.govt.nz/nature/pests-and-threats/common-weeds/wilding-conifers/methods-of-control/

Department of Finance, Service and Innovation: Spatial Services, N. S. W. (2018). Mapping and Spatial Services: Information Sheet. Retrieved July 23, 2018, from http://spatialservices.finance.nsw.gov.au/mapping_and_imagery

Department of Rural Development and Land Reform. (2018). National Aerial Photography and Imagery Programme. Retrieved July 23, 2018, from http://www.ngi.gov.za/index.php/what-we-do/aerial-photography-and-imagery

Dieckmann, U., Law, R., & Metz, J. A. J. (2000). The Geometry of Ecological Interactions. Cambridge Studies in Adaptive Dynamics (Vol. 1). Cambridge, United Kingdom: Cambridge University Press. https://doi.org/10.1017/CBO9780511525537

Dovčiak, M., Hrivnák, R., Ujházy, K., & Gömöry, D. (2014). Patterns of grassland invasions by trees: Insights from demographic and genetic spatial analyses. *Journal of Plant Ecology*, 8(5), 468–479. https://doi.org/10.1093/jpe/rtu038

Falkowski, M. J., Smith, A. M. S., Gessler, P. E., Hudak, A. T., Vierling, L. A., & Evans, J. S. (2008). The influence of conifer forest canopy cover on the accuracy of two individual tree measurement algorithms using LiDAR data. *Canadian Journal of Remote Sensing*, 34(Supplement 2), 338–350. https://doi.org/10.5589/m08-055

Froude, V. A. (2011). Wilding conifers in New Zealand: Status report. Bay of Islands. https://doi.org/978-0-478-40010-6

Gougeon, F. A. (1995). A crown-following approach to the automatic delineation of individual tree crowns in high spatial resolution aerial images. *Canadian Journal of Remote Sensing*, 21(3), 274–284. https://doi.org/10.1080/07038992.1995.10874622

Haby, N., Tunn, Y., & Cameron, J. (2010). Application of QuickBird and aerial imagery to detect *Pinus radiata* in remnant vegetation. *Austral Ecology*, 35(6), 624–635. https://doi.org/10.1111/j.1442-9993.2009.02070.x

He, K. S., Rocchini, D., Neteler, M., & Nagendra, H. (2011). Benefits of hyperspectral remote sensing for tracking plant invasions. *Diversity and Distributions*, 17(3), 381–392. https://doi.org/10.1111/j.1472-4642.2011.00761.x

Higgins, S. I., & Richardson, D. M. (1998). Pine invasions in the Southern Hemisphere: Modelling interactions between organism, environment and disturbance. *Plant Ecology*, 135(1), 79–93. https://doi.org/10.1023/A:1009760512895

Hijmans, R. J. (2016). raster: Geographic Data Analysis and Modeling. R package version 2.5-8. Retrieved from https://cran.r-project.org/package=raster

Huang, C.-Y., & Asner, G. P. (2009). Applications of remote sensing to alien invasive plant studies. *Sensors*, 9(6), 4869–89. https://doi.org/10.3390/s90604869

Hulet, A., Roundy, B. A., Petersen, S. L., Jensen, R. R., & Bunting, S. C. (2013). Assessing the relationship between ground measurements and object-based image analysis of land cover classes in pinyon and juniper woodlands. *Photogrammetric Engineering & Remote Sensing*, 79(9), 799–808. https://doi.org/10.14358/PERS.79.9.799

Illian, J., Penttinen, A., Stoyan, H., & Stoyan, D. (2008). Statistical Analysis and Modelling of Spatial Point Patterns. International Statistical Review (Vol. 76). Chichester, England: John Wiley & Sons. https://doi.org/10.1002/9780470725160

Ke, Y., & Quackenbush, L. J. (2011). A review of methods for automatic individual tree-crown detection and delineation from passive remote sensing. *International Journal of Remote Sensing*, 32(17), 4725–4747. https://doi.org/10.1080/01431161.2010.494184

Kelcey, J., & Lucieer, A. (2012). Sensor correction of a 6-band multispectral imaging sensor for UAV remote sensing. *Remote Sensing*, 4(5), 1462–1493. https://doi.org/10.3390/rs4051462

Komura, R., Kubo, M., & Muramoto, K. (2004). Delineation of tree crown in high resolution satellite image using circle expression and watershed algorithm. In Geoscience and Remote Sensing Symposium, 2004. IGARSS '04 (pp. 1577–1580). IEEE. https://doi.org/10.1109/IGARSS.2004.1370616

Lamar, W. R., McGraw, J. B., & Warner, T. A. (2005). Multitemporal censusing of a population of eastern hemlock (*Tsuga canadensis* L.) from remotely sensed imagery using an automated segmentation and reconciliation procedure. *Remote Sensing of Environment*, 94(1), 133–143. https://doi.org/10.1016/j.rse.2004.09.003

Landgate, G. of W. A. (2018). Online Aerial Photography. Retrieved July 23, 2018, from https://www0.landgate.wa.gov.au/maps-and-imagery/imagery/aerial-photography/aerial

Law, R., & Dieckmann, U. (2000). A dynamical system for neighborhoods in plant communities. *Ecology*, 81(8), 2137–2148. https://doi.org/10.1890/0012-9658(2000)081{[}2137:ADSFNI]2.0.CO;2

Lawrence, R. L., Wood, S. D., & Sheley, R. L. (2006). Mapping invasive plants using hyperspectral imagery and Breiman Cutler classifications (Random Forest). *Remote Sensing of Environment*, 100(3), 356–362. https://doi.org/10.1016/j.rse.2005.10.014

Ledgard, N. J. (2001). The spread of lodgepole pine (*Pinus contorta*, Dougl.) in New Zealand. *Forest Ecology and Management*, 141(1–2), 43–57. https://doi.org/10.1016/S0378-1127(00)00488-6

Madsen, M. D., Zvirzdin, D. L., Davis, B. D., Petersen, S. L., & Roundy, B. A. (2011). Feature extraction techniques for measuring piñon and juniper tree cover and density, and comparison with field-based management surveys. *Environmental Management*, 47(5), 766–776. https://doi.org/10.1007/s00267-011-9634-3

Mast, J. N., Veblen, T. T., & Hodgson, M. E. (1997). Tree invasion within a pine/grassland ecotone: An approach with historic aerial photography and GIS modeling. *Forest Ecology and Management*, 93(3), 181–194. https://doi.org/10.1016/S0378-1127(96)03954-0

Mauck, J., Brown, K., & Carswell Jr, W. J. (2016). The National Map - Orthoimagery. Retrieved July 23, 2018, from https://pubs.usgs.gov/fs/2009/3055/

Ministry of Primary Industries. (2014). The right tree in the right place: New Zealand wilding conifer

management strategy 2015-2030. Retrieved from http://www.wildingconifers.org.nz/about-us/programme-2/the-national-wilding/

Mirik, M., Chaudhuri, S., Surber, B., Ale, S., & Ansley, R. J. (2013). Evaluating biomass of juniper trees (*Juniperus pinchotii*) from imagery-derived canopy area using the Support Vector Machine classifier. *Advances in Remote Sensing*, 2, 181–192. https://doi.org/10.4236/ars.2013.22021

Müllerová, J., Pyšek, P., Jarošík, V., & Pergl, J. (2005). Aerial photographs as a tool for assessing the regional dynamics of the invasive plant species *Heracleum mantegazzianum*. *Journal of Applied Ecology*, 42(6), 1042–1053. https://doi.org/10.1111/j.1365-2664.2005.01092.x

Natural Resources Canada. (2016). National Air Photo Library. Retrieved July 23, 2018, from http://www.nrcan.gc.ca/earth-sciences/geomatics/satellite-imagery-air-photos/9265

Nuñez, M. A., Chiuffo, M. C., Torres, A., Paul, T., Dimarco, R. D., Raal, P., Policelli, N., Moyano, J., García, R. A., van Wilgen, B. W., Pauchard, A., & Richardson, D. M. (2017). Ecology and management of invasive Pinaceae around the world: Progress and challenges. *Biological Invasions*, 19(11), 3099–3120. https://doi.org/10.1007/s10530-017-1483-4

OpenAerialMap. (2018). The Open Collection of Aerial Imagery. Retrieved July 23, 2018, from https://openaerialmap.org/

Pau, G., Fuchs, F., Sklyar, O., Boutros, M., & Huber, W. (2010). EBImage - an R package for image processing with applications to cellular phenotypes. *Bioinformatics*, 26(7), 979–981.

Pebesma, E. J., & Bivand, R. S. (2005). Classes and methods for spatial data in R. R News, 5(2), 1–21. Retrieved from https://cran.r-project.org/doc/Rnews/

Peters, H. A. (2003). Neighbour-regulated mortality: The influence of positive and negative density dependence on tree populations in species-rich tropical forests. *Ecology Letters*, 6(8), 757–765. https://doi.org/10.1046/j.1461-0248.2003.00492.x

Poznanovic, A. J., Falkowski, M. J., Maclean, A. L., Smith, A. M. S., & Evans, J. S. (2014). An accuracy assessment of tree detection algorithms in juniper woodlands. *Photogrammetric Engineering & Remote Sensing,* 80(5), 627–637. https://doi.org/10.14358/PERS.80.7.627

R Core Team. (2017). R: A language and environment for statistical computing. Vienna, Austria: R Foundation for Statistical Computing. Retrieved from https://www.r-project.org/

Richardson, D. M., Van Wilgen, B. W., & Nuñez, M. A. (2008). Alien conifer invasions in South America: Short fuse burning? *Biological Invasions*, 10(4), 573–577. https://doi.org/10.1007/s10530-007-9140-y

Richardson, D. M., Williams, P. A., & Hobbs, R. J. (1994). Pine invasions in the Southern Hemisphere: Determinants of spread and invadability. *Journal of Biogeography*, 21(5), 511–527. https://doi.org/10.2307/2845655

Sahara, E. A., Sarr, D. A., Van Kirk, R. W., & Jules, E. S. (2015). Quantifying habitat loss: Assessing tree encroachment into a serpentine savanna using dendroecology and remote sensing. *Forest Ecology and Management*, 340, 9–21. https://doi.org/10.1016/j.foreco.2014.12.019

Shigesada, N., Kawasaki, K., & Takeda, Y. (1995). Modeling stratified diffusion in biological invasions. *The American Naturalist*, 146(2), 229–251. https://doi.org/10.1086/285796

Simberloff, D., Nuñez, M. A., Ledgard, N. J., Pauchard, A., Richardson, D. M., Sarasola, M., Van

Wilgen, B. W., Zalba, S. M., Zenni, R. D., Bustamante, R., Peña, E. & Ziller, S. R. (2010). Spread and impact of introduced conifers in South America: Lessons from other Southern Hemisphere regions. *Austral Ecology*, 35(5), 489–504. https://doi.org/10.1111/j.1442-9993.2009.02058.x

Strand, E. K., Robinson, A. P., & Bunting, S. C. (2007). Spatial patterns on the sagebrush steppe/Western juniper ecotone. *Plant Ecology*, 190(2), 159–173. https://doi.org/10.1007/s11258-006-9198-0

Sykes, M. T. (2001). Modelling the potential distribution and community dynamics of lodgepole pine (*Pinus contorta* Dougl. ex. Loud.) in Scandinavia. *Forest Ecology and Management*, 141(1–2), 69–84. https://doi.org/10.1016/S0378-1127(00)00490-4

Taylor, K. T., Maxwell, B. D., Pauchard, A., Nuñez, M. A., Peltzer, D. A., Terwei, A., & Rew, L. J. (2016). Drivers of plant invasion vary globally: Evidence from pine invasions within six ecoregions. *Global Ecology and Biogeography*, 25(1), 96–106. https://doi.org/10.1111/geb.12391

Tomiolo, S., Harsch, M. A., Duncan, R. P., & Hulme, P. E. (2016). Influence of climate and regeneration microsites on *Pinus contorta* invasion into an alpine ecosystem in New Zealand. *AIMS Environmental Science*, 3(3), 525–540. https://doi.org/10.3934/environsci.2016.3.525

Tomljenovic, I., Tiede, D., & Blaschke, T. (2016). A building extraction approach for Airborne Laser Scanner data utilizing the Object Based Image Analysis paradigm. *International Journal of Applied Earth Observation and Geoinformation*, 52, 137–148. https://doi.org/10.1016/j.jag.2016.06.007

Visser, V., Langdon, B., Pauchard, A., & Richardson, D. M. (2014). Unlocking the potential of Google Earth as a tool in invasion science. *Biological Invasions*, 16(3), 513–534. https://doi.org/10.1007/s10530-013-0604-y

Wang, L., Gong, P., & Biging, G. S. (2004). Individual tree-crown delineation and treetop detection in high-spatial-resolution aerial imagery. *Photogrammetric Engineering & Remote Sensing*, 70(3), 351–357.

Yokomizo, H., Possingham, H. P., Thomas, M. B., & Buckley, Y. M. (2009). Managing the impact of invasive species: The value of knowing the density-impact curve. *Ecological Applications*, 19(2), 376–386. https://doi.org/10.1890/08-0442.1

Yu, X., Hyyppä, J., Vastaranta, M., Holopainen, M., & Viitala, R. (2011). Predicting individual tree attributes from airborne laser point clouds based on the random forests technique. *ISPRS Journal of Photogrammetry and Remote Sensing,* 66(1), 28–37. https://doi.org/10.1016/j.isprsjprs.2010.08.003

Zhu, K., Woodall, C. W., Monteiro, J. V. D., & Clark, J. S. (2015). Prevalence and strength of density-dependent tree recruitment. *Ecology*, 96(9), 2319–2327. https://doi.org/10.1890/14-1780.1

Chapter 3

Detection bias affects estimates of the difference between local and regional population growth

3.1 Introduction

For many species, it is crucial to measure population dynamics at broad spatial scales (Gurevitch, Fox, Fowler, & Graham, 2016; Leibold et al., 2004; Levin, 1992; Levin, Grenfell, Hastings, & Perelson, 1997). This will enable us to respond to large scale challenges such as climate change, biological invasions and the spread of pathogens (Gamelon et al., 2017; Hui, Fox, & Gurevitch, 2017; Salguero-Gómez et al., 2015). Unfortunately, large scale population dynamics are difficult to measure directly and must often be extrapolated from observations at small spatial scales usually less than one ha (Salguero-Gómez et al., 2015; Sandel & Smith, 2009; Wheatley & Johnson, 2009). Here, I will define a population as the individuals of a species of interest in a single location, and population growth (per unit area) as the change in density of a population in an area between one time step and the next (Gurevitch et al., 2016).

It is difficult to scale up measurements of population growth because many key ecological factors can vary depending on the scale at which they are observed (Allen & Hoekstra, 2015; Huston, 2002; Sandel & Smith, 2009; Turner & Gardner, 2015). Examples of these ecological factors include abiotic variables, interactions with other species, dispersal, stochastic extinction and environmental heterogeneity (Allen and Hoekstra, 2015; Cottenie, 2005; Hanski, 2001). Indeed, the consequences of these factors on population growth can also be correlated at large spatial scales, making them difficult to distinguish empirically (Gurevitch et al., 2016). Additionally, as a result of these factors and their cross-scale correlations, populations can have variable local densities, making the average regional density of a population unrepresentative of the individual local scale densities (Murrell, Purves, & Law, 2001; Tilman, Lehman, & Kareiva, 1997). What is needed are reliable estimates of how population growth depends on scale, and at present it is not clear how much sampling is necessary to accomplish this.

Instead of parameterizing large scale models of population growth, we often settle on using what is known as the mean field approximation of population growth (Law & Dieckmann, 2000; Law, Murrell, & Dieckmann, 2003). The mean field approximation averages the density of individuals across the area a population occupies and then estimates population growth from the average density (Morozov & Poggiale, 2012). By doing so, the mean field approximation effectively ignores spatial variation such as environmental heterogeneity (Bocedi, Pe'er, Heikkinen, Matsinos, & Travis, 2012; Purves & Law, 2002; Stoll & Weiner, 2000).

The mean field assumption is unlikely to hold in natural systems. For example Hovanes et al. (2018) found that the spatial arrangement of bunchgrasses are likely due to scale-dependent processes. Because the bunchgrasses exhibited an over-dispersed pattern rather than a random one, processes such as competition likely discouraged grasses from growing close to each other. This finding contradicts the mean field assumption that plants care only about density averaged over a broad region (Murrell et al., 2001; Ying et al., 2014). While interactions between individuals occur at small spatial scales, scaling up these dynamics proves to be difficult because the interactions are not the same at broad spatial scales (Murrell et al., 2001; Zenner & Peck, 2018).

A more realistic understanding of broad scale population dynamics will require us to quantify the difference between actual population dynamics and simplified mean field models (Melbourne & Chesson, 2006). Chesson pointed out that the spatial processes ignored by the mean field can be boiled down into two factors: the effects of local ecological interactions, including intra- and interspecific competition and mutualism, and the spatial variation of density (Chesson, 2012; Chesson, Donahue, Melbourne, & Sears, 2005). By quantifying these two factors, we can quantify the difference between the mean field population growth and the true regional population growth (Chesson et al., 2005).

Quantifying both the local density dependence and the spatial variation of a population requires a repeated observations over space and time (Benedetti-Cecchi et al., 2012; Melbourne & Chesson, 2006). Local density dependence of a population can be quantified by measuring how population growth changes with density (Lewis & Kareiva, 1993; Peters, 2003), and spatial variation of density can be quantified by calculating the variance in densities of a population (i.e., from densities measured in field plots) (Turner & Gardner, 2015). However, the large datasets required for these methods are susceptible a great deal of uncertainty (Kellner & Swihart, 2014).

Uncertainty in population density can take two forms: one is observation error, which are errors due to random or sampling errors from the method used to measure population density (Ahrestani, Hebblewhite, & Post, 2013); the other form is detection bias, which is a systematic flaw in the way that population density or abundance is observed. Observation errors are well-studied and have been documented for a wide range of sampling techniques (Chen, Kéry, Plattner, Ma, & Gardner, 2013; Kéry & Schmidt, 2008): spotlighting mammals (Lindenmayer et al., 2001), counting amphibians in ponds (Schmidt, 2005), and surveying plants (Chen et al., 2013; Chen, Kéry, Zhang, & Ma, 2009). Additionally studies have already examined the effect of observation error on the components of the difference between the mean field approximation and regional population growth. Failure to account for observation error can lead to an over-estimation of the prevalence of density dependence (Lebreton & Gimenez, 2013; Santin-Janin et al., 2014) and biased estimates of the spatial variance of density (Royle, Nichols, & Kéry, 2005).

While observation errors are well-studied, detection bias is not often quantified or documented, nor are its effects on scaling up population growth well understood. There are a few studies which have

recorded a detection bias due to landscape or environmental heterogeneity. For example, in a survey of plants, a flowering herbaceous annual was more difficult to detect in low elevation habitats where it was rare (Chen et al., 2013). Additionally, we know that estimates of density dependence can be biased by environmental heterogeneity (Gamelon et al., 2017; Zhu, Mi, Ren, & Ma, 2010). In this study, while I recognise that detection bias can be due to environmental heterogeneity, I am most concerned about detection which is biased because of density. The density of a population affects not only the growth of individuals through density dependence, but density is also a key factor in how we scale up population growth between the local and regional scales. From previous work in Chapter 2 and the literature (Yu et al. 2011), I know that density affects the ability to detect individuals and population abundance in an area. However, I do not know how this systematic bias in detection affects the estimates of the difference between the local and regional population growth.

The purpose of this study is to determine how detection bias affects the estimates of the difference between the local and regional population growth and whether we can still reliably estimate this difference when we have systematic detection biases in the data. I will study this question using three objectives:

1. First I will determine analytically the effect of detection bias on the difference between local and regional population growth. I will examine its effect without any observation error in order to understand the effect of detection bias on its own. I will show that modest detection bias does little to interfere with the estimates of the difference between local and regional growth rates.

2. I will use simulations to test the combined effects of detection bias and observation error on the ability to detect the difference between local and regional population growth. I will show that observation error leads to substantial uncertainty on its own. Additionally, I will demonstrate that under some circumstances observation error acts synergistically with detection bias to impede reliable estimates of the difference between local and regional population growth.

3. Finally, I will look at an empirical case study in which the detection of individuals was biased due to density. I will use this case study to illustrate the effect of detection bias and observation error on the difference between local and regional population growth estimates for empirical studies. I show that for the mid- to large-sized individuals, detection bias did not affect this study's estimates and therefore did not have a large effect on the study.

3.2 Methods and Results

3.2.1 Estimating the difference between local and regional population growth

First I need to establish how to calculate the difference between local and regional population growth. To do this, I will examine how to calculate local population growth and then examine how to scale up this estimate by accounting for large-scale spatial processes.

Estimating local population growth

For my model of population growth, I am assuming that for a population at a given site, I can measure the density of individuals, for example by setting up field plots across a landscape. I focus this study on one of the simplest models of population growth, the Verhulst parameterization of the logistic model:

$$\Delta N_{t,i} = rN_{t,i} + aN_{t,i}^2 \qquad \text{(Equation 3.1)}$$

$N_{t,i}$ represents initial densities of individuals, and $\Delta N_{t,i}$ represents the change in densities between time t and time $t+1$ ($\Delta N_{t,i} = N_{t+1,i} - N_{t,i}$). For the sake of visualisation of these equations, I will think of $N_{t,i}$ as representing the initial densities of individuals in many plots i across a site. r represents the intrinsic growth rate (i.e., birth rate – death rate when the species is rare), and a represents density dependence. A value of a close to 0 implies that density dependence is weak and only has a small effect on growth rate. A negative value of a implies that density dependence negatively affects growth (i.e., higher densities lead to slower growth rates), and a positive value of a implies that density dependence positively affects growth. I chose the Verhulst parameterization because it behaves more realistically at range margins (Gabriel, Saucy, & Bersier, 2005), unlike the textbook "r-K" parametrization (Morin, 1999). This phenomena, called the Ginzburg paradox, results in populations with high densities having a positive growth rate even when intrinsic growth (r) is negative (Gabriel et al., 2005; Mallet, 2012). In the Verhulst parameterization, carrying capacity is not fixed but instead depends on the balance between density dependent and density independent growth $K=r/a$.

Although Equation 3.1 will give an estimate of the local population growth, I cannot assume this growth is the same at the regional scale because the equation fails to account for spatial processes. Therefore I need a way to scale up local population growth to regional population growth.

Scaling of population growth

To estimate the difference between local and regional population growth, I need to determine the difference between the mean field estimate and regional population growth.

The regional population growth rate is the difference between the average number of individuals in one time step (t) and the average number of individuals in the following time step ($t+1$). The average regional population growth can be represented mathematically as:

$$\overline{f(N_{t,\mathrm{i}})}$$

In the equation above, $f(N_{t,i})$ represents the function to approximate the population growth between N_t and N_{t+1} across an area comprised of many plots or locations i in which the density of individuals was recorded. If a study had recorded the population density across many plots, the value of N_{t+1} means that the population growth would be approximated for each plot i and then averaged. However, because a population can occur at large spatial scales and it is very time-consuming and expensive to measure population densities of an entire population, the mean field approximation is often implicitly used to estimate population growth. The mean field approximation, which represents when population growth depends only on average population density, can be written mathematically as:

$$mean\ field\ approximation\ of\ population\ growth = f(\overline{\mathrm{N}_t})$$

Here, the average density is taken first of N_t (the initial densities of plots across a landscape; i.e., the mean field) and then this average is applied to the population growth function $f(N_t)$.

The difference between the mean field approximation for population growth and the regional population growth represents the difference between local and regional growth. This difference can be expressed mathematically as (Chesson et al., 2005):

$$Difference\ between\ regional\ and\ meanfield\ population\ growth =$$

$$\underbrace{\overline{f(N_t)}}_{Regional} - \underbrace{f(\overline{N_t})}_{Mean\ field\ approximation} \approx \frac{1}{2}\ \underbrace{f''(\overline{N_t})}_{\substack{Density \\ Dependence}}\ \underbrace{var(N_t)}_{\substack{Spatial \\ variance}} \qquad \text{(Equation 3.2)}$$

In Equation 3.2, $var(N_t)$ represents the variance of densities across plots in the landscape. $f''(N_t)$ is an extremely general way to represent density dependence as the second derivative of population growth with respect to population density. For the Verhulst logistic model this is:

$$f''(N_{t,i}) = \frac{d^2(\Delta N_{t,i})}{dN_{t,i}{}^2} = 2a$$

When population density can be measured with certainty, I can estimate a empirically by measuring the relationship between N_{t+1} and N_t using a polynomial regression. The quadratic term in this regression is an estimate of a, and this is because Equation 3.1 can be re-arranged into the same form as polynomial regression:

$$N_{t+1,i} = (1 + r)N_{t,i} + aN_{t,i}^2 \qquad \text{(Equation 3.3)}$$

Thus in the regression, the linear coefficient equals $(1+r)$ and the polynomial coefficient equals a.

Thus far I have assumed that the estimates of $N_{t,i}$ and $N_{t+1,i}$ are unbiased and do not have error. However, I know from Chapter 2 and previous studies that there is detection bias due to density in studies using population density data (Falkowski et al., 2008; Yu, Hyyppä, Vastaranta, Holopainen, & Viitala, 2011). Therefore I will explore how to quantify detection bias due to density in the next section.

Quantifying detection bias

To account for detection bias in the data and determine how it propagates through the estimates of population growth, I must first determine how detection bias affects the observations of the true field data. To do this, I can think of detection bias across densities as a linear function relating the true density of individuals to the observed density of individuals which was detected. For N_t:

$$N_{bias,t,i} = (slope)N_{t,i} + intercept + \varepsilon_i \qquad \text{(Equation 3.4)}$$

Slope and *intercept* describe how the value of densities measured in the field ($N_{t,i}$) can vary from the observed, biased estimate ($N_{bias,\,t,\,i}$). The slope term is dependent on density and therefore indicates how detection changes with density. For example, often if the slope is below zero, this represents an under-estimation of the density of individuals in the field plot. The intercept term is not dependent on density and therefore represents how well I can detect individuals regardless of the surrounding density. For example, an intercept greater than zero indicates that when the density is very low (i.e., there are few or no individuals in a plot), individuals are still detected. The interpretation of the slope term depends on the magnitude of the intercept term as well. If the intercept term is significantly greater than zero, then even if the slope is less than one, the number of individuals at low densities will still be over-estimated. This scenario is depicted in the red line in Figure 3.1. This diagram illustrates the meaning of Equation 3.4 when estimating detection bias in which the blue line represents a perfect 1:1 detection and the red line represents imperfect detection (Fig. 3.1).

Along with a bias due to density, we also can have observation error (ε) in the data. This error term is not dependent on density and is not systematic in the way that detection bias is. This error can be due to the sampling method used as well as random effects such as environment and observational conditions (Ahrestani et al., 2013; Chen et al., 2013).When the observed densities of individuals are modelled against the field-measured densities as in Equation 3.4, I can estimate the observation error using the residual uncertainty in the regression (James, Witten, Hastie, & Tibshirani, 2013).

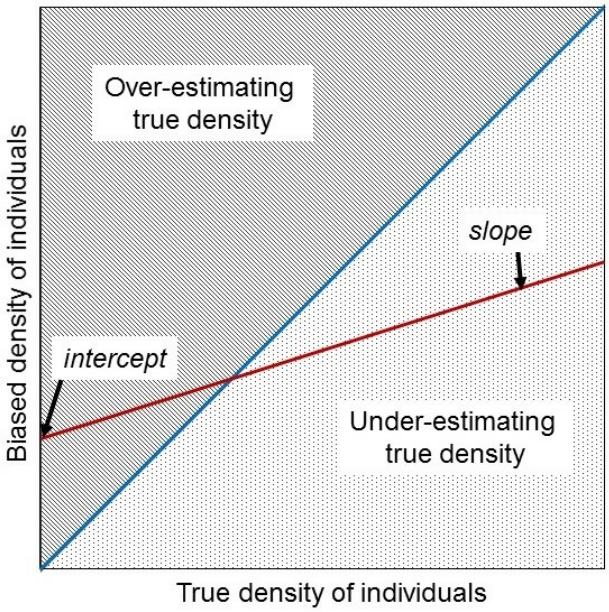

Figure 3.1 Schematic of an example of detection bias in a linear regression. The blue line represents a perfect detection with a slope of one and intercept of zero. The red line has a slope less than one, meaning that the biased density tends to under-estimate the true density particularly at high densities. The red line also has an intercept greater than zero, meaning that the biased density over-estimates the true density at low densities.

With these general definitions in place, I can proceed to analyse how detection bias affects inferences of population growth, particularly the difference between local and regional population growth.

3.2.2 Determining the effect of detection bias without observation error

To understand the effect of detection bias on the difference between local and regional population growth, I first solved for the analytic solution in which I substituted the observed (biased) densities into the equations of population growth.

It turns out that there is a simple expression for the effect of bias on the estimate of the difference between local and regional growth when I ignore observation error (ε). To find this I substituted the expression for biased densities (N_{bias}) into the equation for population growth (Equation 3.1). I calculated the effect of detection bias on density dependence using a polynomial regression of Equation 3.3 in which I modelled the biased estimate of population densities at time $t+1$ as a function of the biased estimate of the population densities at time t. I calculated the effect of detection bias on the variance of the initial densities by using common identities of variance (Ross, 2010). Once I determined the effect of detection bias on the two components of the difference between local and regional population growth, I next multiplied these effects to obtain the total effect on this difference.

First, to find expected value for density dependence ($f''(N_{t,i,bias})$), I substituted the equation for detection bias (Equation 3.4) into the equation for population growth (Equation 3.1). I found that:

$$N_{t+1,true} = \overbrace{(1 + r + 2a_{biased}(intercept))}^{biased\ estimate\ of\ (1+r)} N_{t,true} + \overbrace{a_{biased}(slope)}^{biased\ estiamte\ of\ a} {N_{t,true}}^2 + \underbrace{r\left(\frac{intercept}{slope}\right) + a_{biased}(intercept^2)/slope}_{biased\ estimate\ of\ intercept} \qquad \text{(Equation 3.5)}$$

This means that when I use a polynomial regression with biased estimates of N_t and N_{t+1} to estimate a the estimate will be equal to:

$$a_{biased} = a_{true}/slope$$

This is because the biased estimate of a equalled a_{biased} multiplied by a factor of the slope of detection bias. Again, the intercept term of detection bias did not affect the estimate of a. I should note though that as slope approaches zero, a_{biased} approaches negative infinity. Therefore if the slope is close to zero, the values of a_{biased} will be incorrect. If the slope is close to zero though, then detection would be so poor that the observed densities of a population would be highly unreliable.

Appendix B.1 has the complete steps to the above solutions and Equation 3.5.

Next, I determined that the expected value for $var(N_{bias})$ is $var(slope N_{ti}+intercept)$. From identities of the variance (Ross, 2010), this can be simplified to:

$$Var(N_{t,i,bias}) = slope^2 * Var(N_{t,i})$$

Thus, the variance of the biased initial densities differs from the variance of the true initial densities by a factor of the slope squared. The bias in variance does not depend on the intercept of the detection bias.

To find the effect of detection bias on the estimate of the difference between local and regional population growth, I substituted the solutions for the effect of bias on $var(N_{bias})$ and $f''(N_{bias})$ into Equation 3.2. The complete steps to this substitution and the below results are in Appendix B3.

$$Biased\ Difference\ between\ local\ and\ regional\ population\ growth =$$

$$-(slope)\ \underbrace{(a_{true} Var(N_{t,true}))}_{Unbiased\ estimate} \qquad \text{(Equation 3.6)}$$

When I used biased estimates for N_t and N_{t+1}, the estimate for the difference between local and regional growth rates is equal to the true value multiplied by the slope (Equation 3.6). Note that this solution does not depend on the intercept term of detection bias from Equation 3.4.

Equation 3.6 is surprisingly simple as it depends linearly on slope, while the variance and density dependence components both depend non-linearly on slope. These analytic results provide a useful starting point for how the slope and intercept interact to affect the estimates. In the next section, I look at what happens when I add in observation error (ε) into the detection bias.

3.2.3 Simulations

While the above section is useful for determining what the effect of detection bias has on its own, datasets of observed densities with detection bias will likely have observation error as well. Since both detection bias and observation error occur simultaneously, I will next examine the synergies between bias and error using simulations. Additionally, I will determine whether there is a threshold of observation error above which I cannot estimate the difference between local and regional growth reliably.

The simulations were set up to systematically change the values of density dependence, initial densities of individuals, and the slope and intercept in the detection bias equation (Equation 3.4). The following flowchart (Fig. 3.2) illustrates the setup and procedure of the simulations.

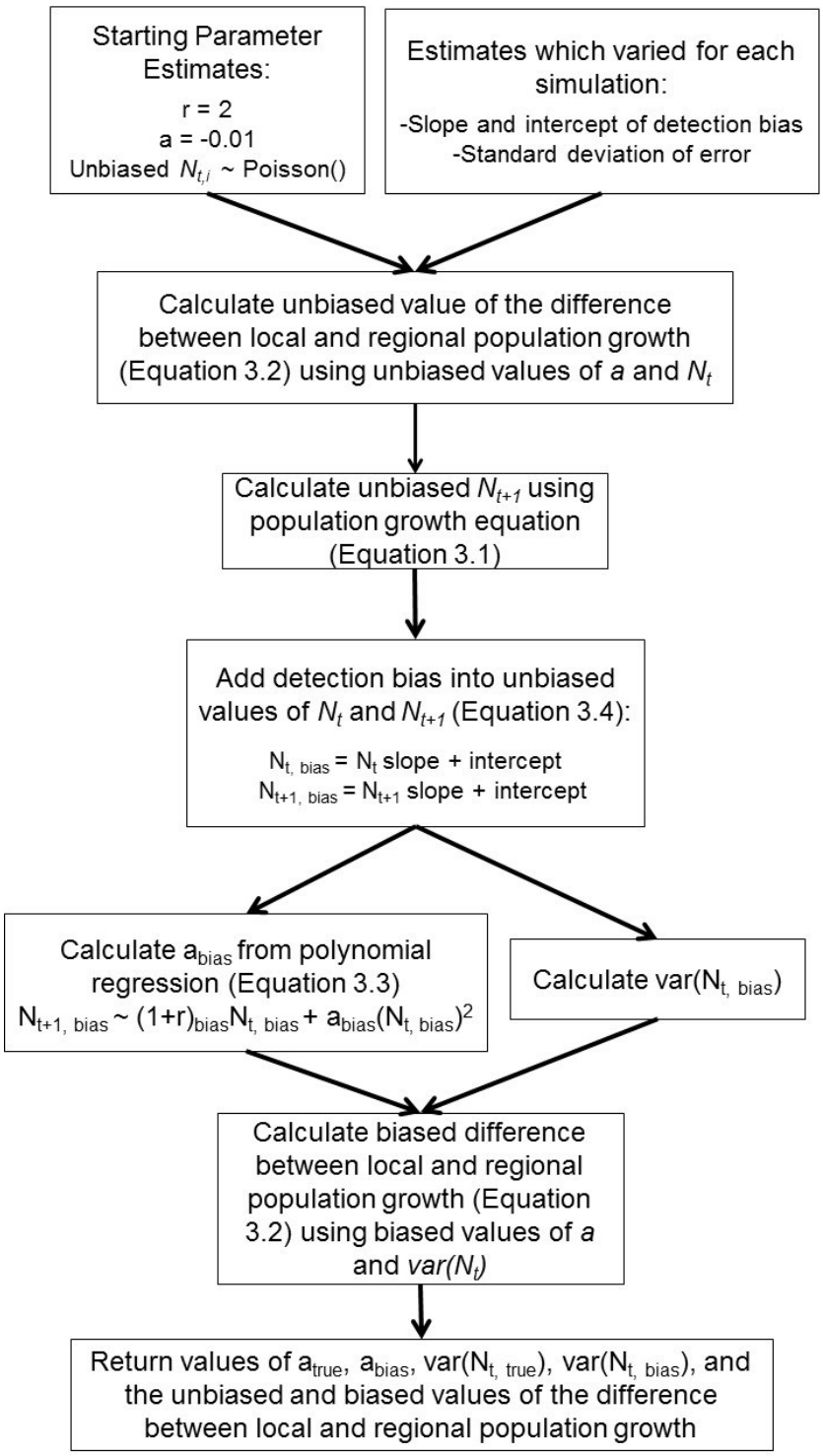

Figure 3.2 Flow chart of simulation setup.

Using this general setup, I ran 100 simulations while systematically changing each component of detection bias individually (slope and intercept). For both sets of simulations, I kept the following elements constant: density dependence, spatial variance of densities, initial densities as they would be measured in the field, and the intrinsic growth rate *r*. I used values similar to what is found in the literature (Bahn et al., 2008; Ross, 2009). Additionally I kept the standard deviation of the observation error constant and used a normal distribution with a mean of zero to generate error ($\varepsilon \sim N(0, 3)$) (Freckleton, Watkinson, Green, & Sutherland, 2006; Knape, 2008).

Several assumptions were made in these simulations. I assumed that the detection bias present in the data was from density and not from other sources such as the environment. Furthermore, I also assumed that the detection bias was defined by a linear regression (Eqn. 3.4). I modelled the population growth of adult individuals and did not include younger life history stages as I wanted to keep these results as generalisable as possible.

I wanted to determine how bias would affect the difference between the local and regional growth rates and also the components of this difference (density dependence and spatial variance of densities). To do this, first I examined how varying the slope values would affect the components of and the difference between the local and regional population growth while keeping the intercept term constant. Next I examined how varying the intercept values would affect the components of and the difference between local and regional population growth while keeping the slope value constant. I tested slope values from 0.4 – 1.3 at intervals of 0.1 and intercept values from -4 – 12 at intervals of four. These values represented typical detection biases due to density (Falkowski et al., 2008; Yu et al., 2011). Because it was possible to generate negative values of density when the intercept term of detection bias was negative, I removed these negative density values as they would not represent a possible value of the density in a field plot. I tested for a difference between the expected analytic solutions and the estimated values of density dependence, variance of initial densities, and the difference between the local and regional population growth using one sample t-tests. Due to the number of comparisons, I adjusted the p-values using the Holm method (Holm, 1979).

Next I examined the effect of the observation error (ε) on values of the difference between local and regional population growth to determine the threshold above which the estimates become inaccurate. This observation error is from the detection bias regression (Equation 3.4), and it accounts for the random uncertainty in the observed data. To vary the observation error, I increased standard deviation values of error from one to ten while keeping the mean of the error term constant at zero. I kept the slope and intercept values of the detection bias equation constant at 0.5 and 4 respectively, and I kept the true value of density dependence constant at -0.01 and the standard deviation of initial densities constant as well using values similar to the literature (Bahn et al., 2008; Ross, 2009). I ran each of the ten simulations with a different error term 100 times. I compared the simulation results to the analytic solutions using one sample t-tests, and adjusted the p-values using the Holm method (Holm, 1979).

Finally, I investigated how the estimates of the difference between local and regional population growth varied when I changed the number of plots examined. I wanted to determine whether there was a minimum number of plots that needed to be sampled in order to calculate the correct value of the difference between local and regional population growth. I systematically changed the number of plots from 20 to 10,000 and ran 100 simulations for each different sample size. While having 10,000 plots is unrealistic, I used this high upper limit to check for convergence as sample size increased. Other parameters in this simulation were: density dependence = -0.01, standard deviation of initial densities

= 5, slope = 0.5, and intercept = 4. From the simulations, I calculated the mean estimates of the difference between local and regional population growth when the data had detection bias and observation error and when the data was unbiased.

3.2.4 Simulation results

As expected by the analytic solutions, the values of density dependence, variance in initial densities, and the difference between local and regional population growth varied as the slope values changed but not as the intercept values changed (Fig. 3.3a, b, d, e, g, h). When observation error was small (i.e., a standard deviation below 3), the simulated results agreed with the analytic results.

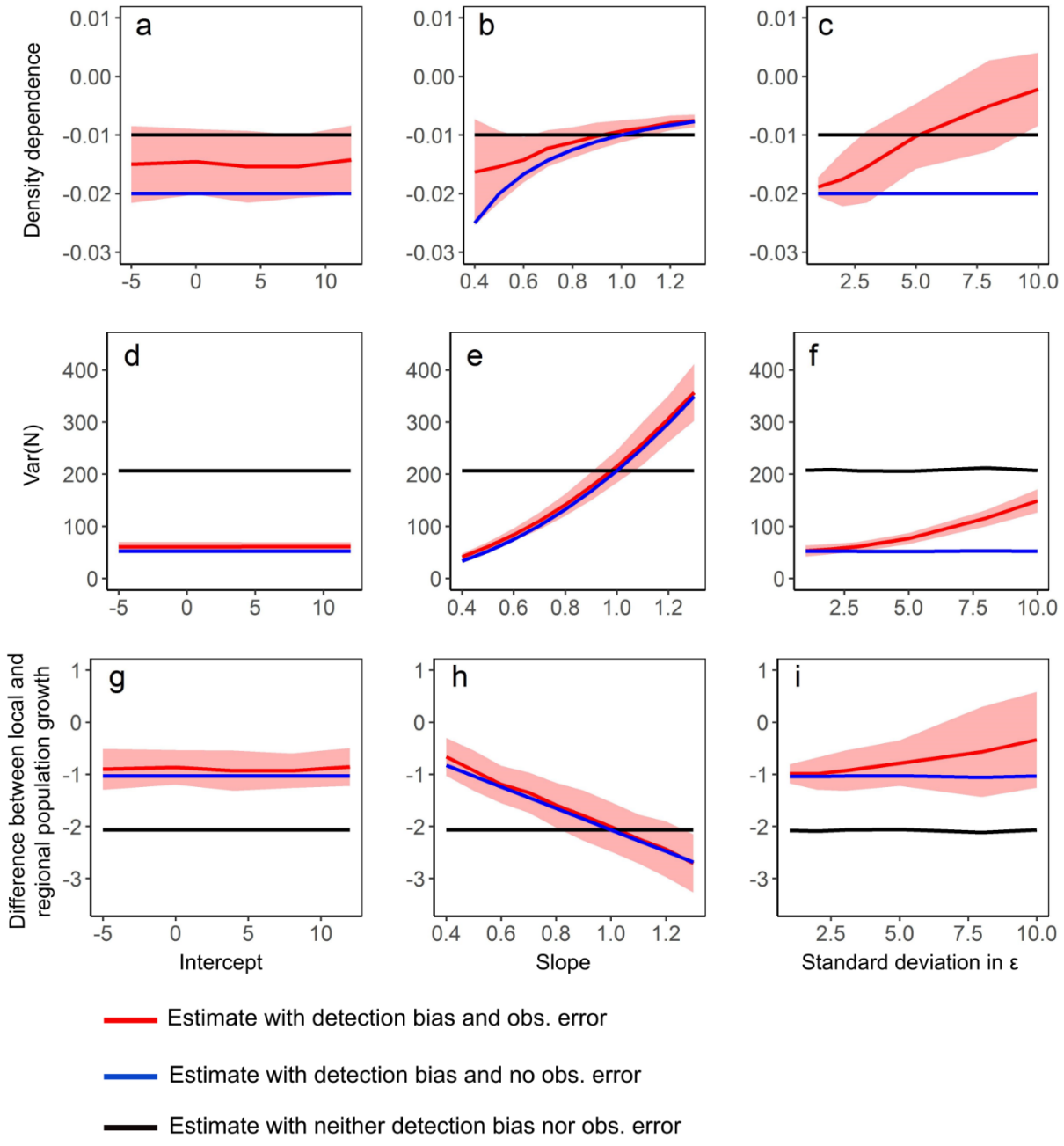

Figure 3.3 The slope of the detection bias equation strongly affected the components of and the difference between local and regional population growth itself. The left three panels (a, d, and g) show how the values of density dependence, variance of the initial densities, and the difference between local and regional population growth change with increasing intercept values. The centre three panels (b, e, and h) show how the values of density dependence, variance, and difference between local and regional population growth change with increasing slope values. The right three panels (c, f, and i) show how the values change with increasing the standard deviation of epsilon (observation error). The black line on each panel indicates the unbiased estimate when there was neither detection bias nor observation error, the blue line indicates the analytic value when there was detection bias but not observation error, and the red line indicates the biased estimate when there was detection bias and observation error in the data. The red areas indicate the standard deviation around the biased estimates. This figure shows the results when the true density dependence (black line) was set to -0.01, representing a relatively strong negative density dependence.

Because the estimates did not change with the intercept values of the detection equation (Fig. 3.3a, d, and g), this means that changing the number of false positives (or false negatives) at very low densities does not affect the difference between local and regional population growth estimates. However, these values all varied with the slope of the detection equation (Fig. 3.3a, e, and h). It is interesting to note as well that even though the estimates of the components of the difference between local and regional population growth vary non-linearly with slope (Fig. 3.3b and e), the estimates of the difference between local and regional population growth did vary linearly with slope (Fig. 3.3h).

When the standard deviation of the observation error is small, the parameter estimates did not appear to differ from what I would expect when observation error is zero (Fig. 3.3c, f, and i). However, as the standard deviation of error increases, I found that the simulation parameter values differed dramatically from what I would expect when error is zero. In fact, the simulated values of density dependence and variance of initial densities with large error (i.e., standard deviation = 10) had very different values and trends compared to the analytic results. However, as error increased and the deviations of the difference between local and regional population growth components from the expected analytic result also increased, these deviations seemed to cancel each other out somewhat as the estimated difference between local and regional population growth (Fig. 3.3i) still followed the same trend as the expected analytic solution.

Even when the observation error was small, many of the results were significantly different from what was expected when observation error equalled zero (Table 3.1). Therefore, even a relatively small amount of uncertainty in detection (here, standard deviation in observation error = 3) can cause values of the difference between local and regional population growth to be significantly different from the expected estimates. Tables of the simulation values of density dependence and the variance of initial densities with changing slope and intercept values are in Appendix C.

Table 3.1 Values of the difference between local and regional population growth with changing slope and intercept values from the analytic results and the simulated estimates. Asterisks indicate significance from one-sample t-tests. Observation error for these tests was $\varepsilon \sim N(0, 3)$.

Slope values	Analytic :: Simulation values of the difference between local and regional growth (± standard deviation)	Intercept value	Analytic :: Simulation values of the difference between local and regional growth (± standard deviation)
0.4	-0.83 :: -0.67 ± 0.36 ***	-4	-1.03 :: -0.90 ± 0.39 ***
0.6	-1.24 :: -1.19 ± 0.36 ***	0	-1.03 :: -0.87 ± 0.33 ***
0.8	-1.65 :: -1.59 ± 0.43 ***	4	-1.03 :: -0.93 ± 0.38 ***
1.0	-2.07 :: -2.01 ± 0.48 ***	8	-1.03 :: -0.93 ± 0.33 ***
1.2	-2.48 :: -2.44 ± 0.54 ***	12	-1.03 :: -0.86 ± 0.36 ***

These values of the difference between local and regional population growth in Table 3.1 are mostly around -1 to -2 individuals per time-step per plot. To interpret these values biologically, this means that there were one to two less individuals per plot than what was expected from the mean field population growth estimate.

As the number of plots examined increased estimate of the difference between local and regional population growth converged (Fig. 3.4). Interestingly, the estimate derived from simulations converged to a value slightly closer to 0 than the analytic solution (red line vs blue line in Fig. 3.4).

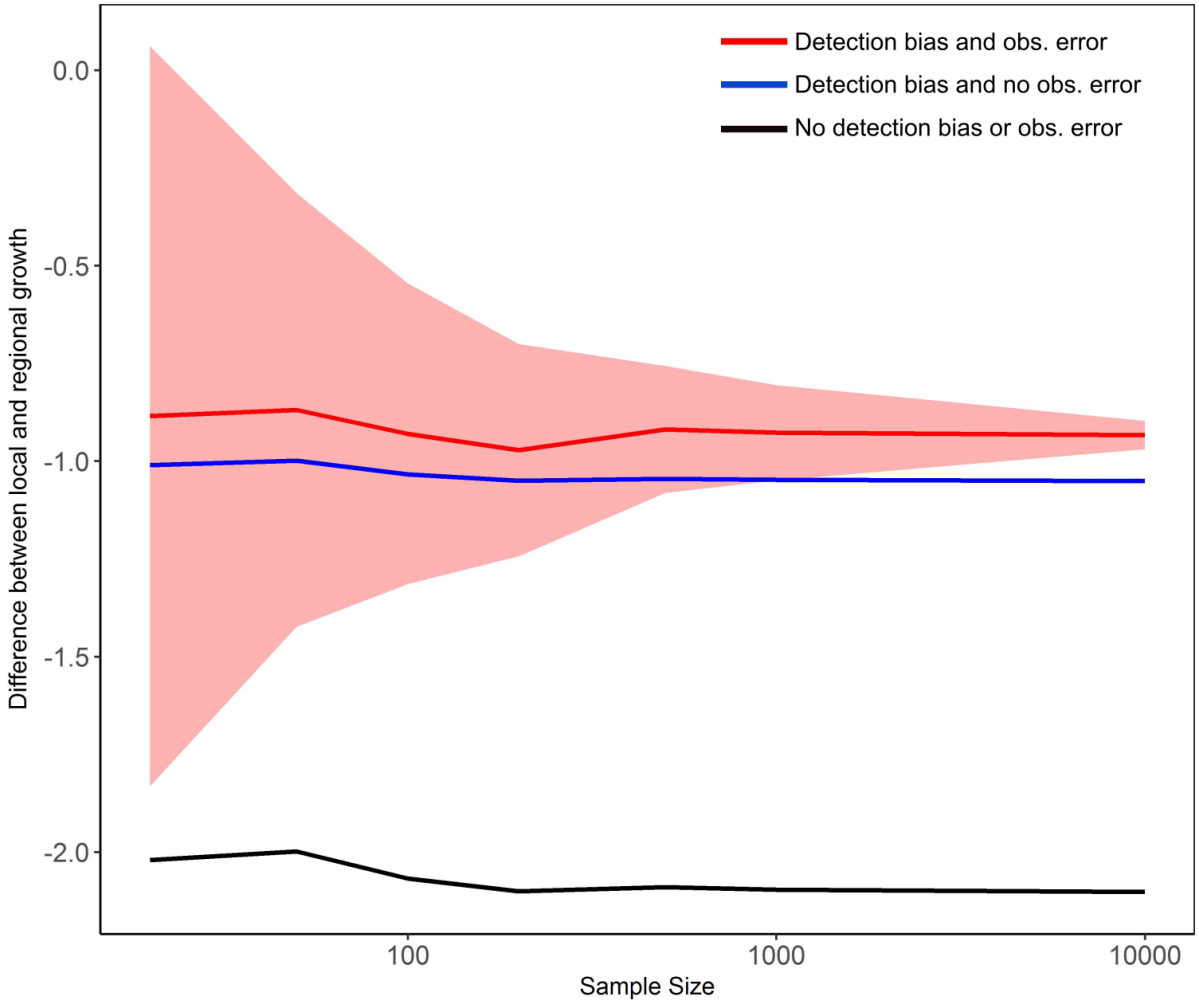

Figure 3.4 As the sample size increases, the uncertainty around the estimated difference between local and regional population growth decreases. The red line represents the biased estimate of the difference between local and regional population growth, and the red area around the red line represents the standard deviation. The blue line represents the expected analytic estimate of the difference between local and regional population growth, and the black line represents the unbiased estimate of the difference between local and regional population growth.

3.2.5 Case study

Case study methods

This case study comes from Chapter 2, which used aerial imagery data to detect invasive conifer trees. In Chapter 2, the number of trees estimated per plot by aerial imagery was often a biased estimate of the true number of trees per plot counted and measured in the field. The methods to collect aerial imagery and field data are summarised below; more details can be found in Chapter 2.

The aerial imagery and field measurements were taken at Mt Barker (171°35′15″ E, 43°21′30″ S) on the South Island of New Zealand. Mt Barker has been invaded by conifer trees comprised mostly of *Pinus nigra*. For this case study, the population only included the adult conifer trees in this area; I did not include saplings or seedlings in the definition of the population as I found that the aerial imagery data could not reliably detect these trees in Chapter 2.

The imagery data was retrieved from the Land Information New Zealand (LINZ) archives. The data was taken in 2016 and had a 0.3m pixel resolution and 3 spectral brands (RGB). An automated imagery classification procedure was then used to detect and identify point locations of individual trees. Using methods similar to Deng et al., (2016); Gougeon, (1995); Komura et al., (2004); Lamar et al., (2005); and Wang et al., (2004), the image classification separated the dark-coloured conifer tree vegetation from the light-coloured background tussock vegetation. Then a watershedding procedure delineated individual tree canopies, resulting in a final output of point locations of individual trees. All image classification procedures were done in R using the following packages: EBImage (Pau, Fuchs, Sklyar, Boutros, & Huber, 2010), raster (Hijmans, 2016), rgdal (Bivand, Keitt, & Rowlingson, 2017), and sp (Pebesma & Bivand, 2005) (R Core Team, 2017).

Forty 20x20m plots were set up in a random stratified design across densities. Within the plots, all trees over 50cm in height were measured. For each tree, the maximum canopy diameter and GPS location were recorded.

To assess the accuracy and potential bias of the aerial imagery, I compared the number of trees detected in the imagery to the number of trees measured in the field within each plot. While perhaps not measured perfectly, I took the trees measured in the field to represent the true, unbiased density of trees and examined the detected number of trees for observation error and detection bias. To do this, I modelled the relationship between the trees detected and the trees measured as a linear regression. The slope and intercept of the regression were compared to one and zero, respectively, as a slope of one and intercept of zero would indicate perfect detection (see Fig. 3.1). If the ability of aerial imagery data to detect trees varied with density of trees (i.e., detection was not consistent across densities), then the detection was biased.

I also examined how the detection of trees of different diameter sizes changed across densities to determine which sizes of trees could be detected across all densities. To do this, I varied the size

thresholds of trees modelled using a linear regression. I first modelled the most inclusive size threshold of trees greater than 1m in canopy diameter and then systematically increased the size threshold to include only the mid- to large-sized trees. The size thresholds of tree canopies I tested were as follows: canopies > 1m, canopies > 1.5m, canopies > 2m, canopies > 2.5m, and canopies > 3m.

In the analytic and simulations sections, I found that the effect of detection bias on the estimates of the difference between local and regional population growth depended on the slope of the detection bias regression. Because of this, I tested how the estimates varied with the size thresholds of trees. I first calculated the difference between the local and regional population growth from my field data, which I assumed to be unbiased. I next calculated the difference between local and regional population growth using the aerial imagery data, which I tested for detection biases depending on the size threshold of trees examined.

To determine the uncertainty in the estimates of the difference between local and regional population growth, I ran simulations. I kept the values of intrinsic growth rate (r), density dependence (a), and initial densities of N_t constant. For growth rate, I used a value of approximately one, as reported in the literature for invasive pine trees (Buckley et al., 2005). For density dependence, I used a moderately strong, negative value at -0.01, and I used the density of trees detected using aerial imagery as the N_t values. I used the slopes and intercepts found for each size threshold; these values are reported in Table 3.2. For generating uncertainty in the estimates, I simulated a normal distribution of the error term with a mean of zero and a variance from the residual variance reported in the linear regressions of each size threshold. Finally, I examined how the estimates from the field data and from the aerial imagery data differed from each other for different slopes/size thresholds.

Case study results

The aerial imagery detection data was found to be biased due to density. Additionally, the detection bias changed with varying size thresholds of trees' canopy diameters. Table 3.2 below shows the results of the linear regressions for each of the size thresholds.

Table 3.2 Results of linear regressions from Chapter 2. The slope and intercept values of the regressions show how the detection bias changes with size threshold of trees.

Size threshold	Detection bias
Trees >1m	$N_{t,bias} = 0.41 * N_{t,true} + 8.8 + \varepsilon_1$
Trees >1.5m	$N_{t,bias} = 0.61 * N_{t,true} + 8.8 + \varepsilon_2$
Trees >2m	$N_{t,bias} = 0.71 * N_{t,true} + 11 + \varepsilon_3$
Trees >2.5m	$N_{t,bias} = 0.88 * N_{t,true} + 11.2 + \varepsilon_4$
Trees >3m	$N_{t,bias} = 1.1 * N_{t,true} + 11.4 + \varepsilon_5$

As shown in Table 3.2, the smaller threshold sizes, for example trees with a canopy diameter of 1m and more, were more likely to over-estimate the density of trees at very low densities and under-estimate the density of trees at high densities. However, the detection bias of mid- to large-sized trees was found to be small since the detection was relatively consistent across densities.

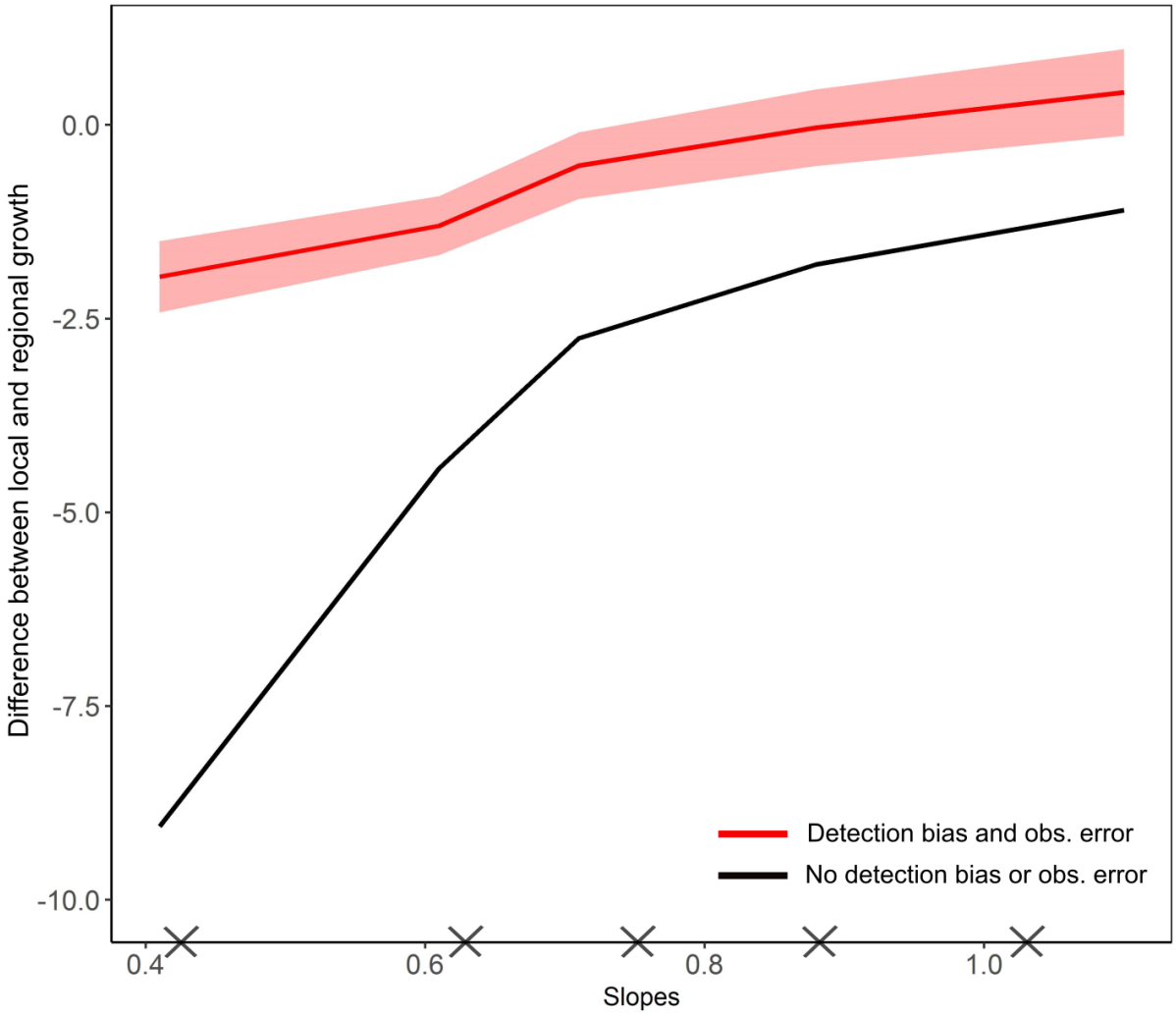

Figure 3.5 Estimates of the difference between local and regional growth when detection bias and observation error (red line, aerial imagery data) were present in the data were lower in magnitude than when detection bias and observation error were not present in the data (black line, fieldwork data). The red error areas around the estimates with detection bias and observation error are standard deviations. The black X's on the x axis represent where the slope values are for each diameter size threshold (trees > 1m, trees > 1.5m, trees > 2m, trees 2.5m, and trees > 3m).

When I compared the values of the difference between local and regional population growth as estimated from fieldwork data and from aerial imagery data, I found that these values were indeed different (Fig. 3.5). As expected, as the size threshold increased, the slope values increased as well. Additionally, as the slope values increased the difference between the fieldwork (unbiased) and aerial imagery (biased) estimates became smaller. However, the estimates from the aerial imagery data were always smaller in magnitude than the estimates from the fieldwork data. Therefore, a detection bias

from aerial imagery data may be more likely for this study to have more conservative estimates of the difference between local and regional population growth than what they actually might be.

The uncertainty in the values estimated from aerial imagery data was not large. Therefore the observation error in the detection bias regressions was not large enough to cause the estimated values of the difference between local and regional population growth to be very inaccurate.

3.3 Discussion

This study sought to elucidate the effects of detection bias on scaling up population growth from a local to regional scale. Using analytic solutions, simulations, and a case study, I found that detection bias does affect estimates of the difference between local and regional population growth. In particular, I found that the degree to which detection depended on the density of trees had a large effect on this study's estimates. This degree, represented by the slope of the detection bias regression, linearly affected the estimates of the difference between local and regional population growth. The closer the slope of the regression was to one, the less influence it had on the estimates. The other insight gained from this study was that observation error, represented by the residual variance term in the detection bias regression, also greatly affected the estimates. If the observation error was large, the estimates of the difference between local and regional population growth became very unreliable. Because there is a strong synergy between observation error and the slope of the detection bias relationship, I would recommend that readers need a strong understanding of detection bias since observation error is inherent in many population density studies.

The most obvious way to remedy the problem of observation error is to increase the sample of plots examined. Based on my results from studying the effect of sample size on estimates of the difference between local and regional growth, I found that sample sizes above 100 plots started to converge. However, I realise that 100 field plots may be unreasonable to survey; therefore, I would recommend having at least 40-50 plots as estimates started to converge and have lower standard deviations after this sample size. If observation error is low, then 40-50 plots should be sufficient.

The case study supported the insights gained about the synergies between detection bias and observation error. I found that as long as the slope and observation error were close to one and were small, respectively, then the estimates of the difference between the local and regional population growth were reliable. Since the use of remote sensing data is becoming more prevalent in studies of population density and abundance (Pettorelli et al., 2014; Rocchini et al., 2015), these findings will be incredibly useful. As long as studies examine the accuracy of their detection data against field data, they can determine how reliable their population estimates are.

For interpreting the magnitude of the difference between local and regional population growth in the case study, a value of -1 represents a value of one less individual per plot than what was expected from the mean field population growth estimate. Thus, if the difference between local and regional growth

is small, then the mean field approximation of population growth is adequate. When the size threshold is small (i.e., for detecting trees > 1m canopy diameter), the biased estimate of the difference between local and regional population growth is different from the unbiased estimate by over 6 trees/plot/time step (Fig. 3.5). While the biased estimate of the difference between local and regional population growth implies that the mean field approximation is relatively accurate, the unbiased estimate implies that there is a larger difference between the regional and mean field estimates of growth. Therefore the smaller size thresholds may result in misleading interpretations of the difference between local and regional population growth when using biased observational data.

While this study is the first of its kind to examine detection bias and scaling up population growth, other studies have examined the effects of observation error on estimates of local density dependence and spatial variation (such as Chen et al., 2013; Gamelon et al., 2017). For example, Lebreton and Gimenez (2013) found that observation error tends to cause the uncertainty in these estimates to increase more than might be expected. I found similar results in that as the observation errors increased, this study's estimates of the local density dependence also became very large and thus unreliable. Even though observation error may be unavoidable in a dataset, accounting for it in population growth estimates is crucial to avoid incorrect estimates (Santin-Janin et al., 2014).

This study focused on detection bias due to density; however there are other factors which could lead to a systematic detection bias in studies of population density. Environmental heterogeneity has been shown to influence components of population growth (Gamelon et al., 2017; Zhu et al., 2010). In the future, these effects should be studied as well. Similarly, I only focused on the effect of detection bias on scaling up population growth. Since I found that detection bias can affect this aspect of growth, future work could examine the effects of detection bias on aspects such as demographic traits and spread rates of invasive species.

3.3.1 Conclusion

As we continue to study large-scale phenomena such as biological invasions, we need reliable estimates of how to calculate and scale up population growth between local and regional scales (Chave, 2013; Gurevitch et al., 2016). Chesson et al. (2005) suggest a method to do this using estimates of local density dependence and spatial variation. As more studies use remote sensing data and other large scale datasets to estimate population density, understanding the effect of detection bias is needed. In this study, I proved that I could estimate a way to scale up population growth rates despite having detection bias in the data. Not only did this study demonstrate a way to calculate the difference between local and regional estimates of population growth, but this study also showed when these estimates can be trusted and when they cannot. In the future, I would like to see more studies examining a way to scale between local and regional scales. I also would like to assess whether there are certain environmental factors which affect these estimates.

3.4 References

Ahrestani, F. S., Hebblewhite, M., & Post, E. (2013). The importance of observation versus process error in analyses of global ungulate populations. *Scientific Reports*, 3. https://doi.org/10.1038/srep03125

Allen, T. F. H., & Hoekstra, T. W. (2015). *Toward a Unified Ecology* (Second Ed.). New York: Columbia University Press.

Bahn, V., Krohn, W. B., & O'Connor, R. J. (2008). Dispersal leads to spatial autocorrelation in species distributions: A simulation model. *Ecological Modelling*, 213(3–4), 285–292. https://doi.org/10.1016/j.ecolmodel.2007.12.005

Benedetti-Cecchi, L., Tamburello, L., Bulleri, F., Maggi, E., Gennusa, V., & Miller, M. (2012). Linking patterns and processes across scales: The application of scale-transition theory to algal dynamics on rocky shores. *Journal of Experimental Biology*, 215(6), 977–985. https://doi.org/10.1242/jeb.058826

Bivand, R., Keitt, T., & Rowlingson, B. (2017). rgdal: Bindings for the Geospatial Data Abstraction Library. R package version 1.2-8. Retrieved from https://cran.r-project.org/package=rgdal

Bocedi, G., Pe'er, G., Heikkinen, R. K., Matsinos, Y., & Travis, J. M. J. (2012). Projecting species' range expansion dynamics: Sources of systematic biases when scaling up patterns and processes. *Methods in Ecology and Evolution*, 3(6), 1008–1018. https://doi.org/10.1111/j.2041-210X.2012.00235.x

Buckley, Y. M., Brockerhoff, E., Langer, L., Ledgard, N. J., North, H., & Rees, M. (2005). Slowing down a pine invasion despite uncertainty in demography and dispersal. *Journal of Applied Ecology*, 42(6), 1020–1030. https://doi.org/10.1111/j.1365-2664.2005.01100.x

Chave, J. (2013). The problem of pattern and scale in ecology: What have we learned in 20 years? *Ecology Letters*, 16(SUPPL.1), 4–16. https://doi.org/10.1111/ele.12048

Chen, G., Kéry, M., Plattner, M., Ma, K., & Gardner, B. (2013). Imperfect detection is the rule rather than the exception in plant distribution studies. *Journal of Ecology*, 101(1), 183–191. https://doi.org/10.1111/1365-2745.12021

Chen, G., Kéry, M., Zhang, J., & Ma, K. (2009). Factors affecting detection probability in plant distribution studies. *Journal of Ecology*, 97(6), 1383–1389. https://doi.org/10.1111/j.1365-2745.2009.01560.x

Chesson, P. (2012). Scale transition theory: Its aims, motivations and predictions. *Ecological Complexity*, 10, 52–68. https://doi.org/10.1016/j.ecocom.2011.11.002

Chesson, P., Donahue, M. J., Melbourne, B. A., & Sears, A. L. W. (2005). Scale transition theory for understanding mechanisms in metacommunities. In M. Holyoak, M. A. Leibold, & R. D. Holt (Eds.), *Metacommunities: Spatial Dynamics and Ecological Communities* (pp. 279–306). Chicago: University of Chicago Press.

Cottenie, K. (2005). Integrating environmental and spatial processes in ecological community dynamics. *Ecology Letters*, 8(11), 1175–1182. https://doi.org/10.1111/j.1461-0248.2005.00820.x

Deng, S., Katoh, M., Yu, X., Hyyppä, J., & Gao, T. (2016). Comparison of tree species classifications at the individual tree level by combining ALS data and RGB images using different algorithms. *Remote Sensing*, 8(12), 1034. https://doi.org/10.3390/rs8121034

Falkowski, M. J., Smith, A. M. S., Gessler, P. E., Hudak, A. T., Vierling, L. A., & Evans, J. S. (2008). The influence of conifer forest canopy cover on the accuracy of two individual tree measurement algorithms using LiDAR data. *Canadian Journal of Remote Sensing*, 34(Supplement 2), 338–350. https://doi.org/10.5589/m08-055

Freckleton, R. P., Watkinson, A. R., Green, R. E., & Sutherland, W. J. (2006). Census error and the detection of density dependence. *Journal of Animal Ecology*, 75(4), 837-851. https://doi.org/10.1111/j.1365-2656.2006.01121.x

Gabriel, J. P., Saucy, F., & Bersier, L. F. (2005). Paradoxes in the logistic equation? *Ecological Modelling*, 185(1), 147–151. https://doi.org/10.1016/j.ecolmodel.2004.10.009

Gamelon, M., Grøtan, V., Nilsson, A. L. K., Engen, S., Hurrell, J. W., Jerstad, K., Phillips, A. S., Røstad, O. W., Slagsvold, T. ,Walseng, B., Stenseth, N. C., & Sæther, B.-E. (2017). Interactions between demography and environmental effects are important determinants of population dynamics. *Science Advances*, 3(2), e1602298. https://doi.org/10.1126/sciadv.1602298

Gougeon, F. A. (1995). A crown-following approach to the automatic delineation of individual tree crowns in high spatial resolution aerial images. *Canadian Journal of Remote Sensing*, 21(3), 274–284. https://doi.org/10.1080/07038992.1995.10874622

Gurevitch, J., Fox, G. A., Fowler, N. L., & Graham, C. H. (2016). Landscape demography: Population change and its drivers across spatial scales. *The Quarterly Review of Biology*, 91(4), 459–485. https://doi.org/10.1086/689560

Hanski, I. (2001). Spatially realistic theory of metapopulation ecology. *Naturwissenschaften*, 88(9), 372-381. https://doi.org/10.1007/s001140100246

Hijmans, R. J. (2016). raster: Geographic Data Analysis and Modeling. R package version 2.5-8. Retrieved from https://cran.r-project.org/package=raster

Holm, S. (1979). A simple sequentially rejective multiple test procedure. *Scandinavian Journal of Statistics*, 6(2), 65–70. https://doi.org/10.2307/4615733

Hovanes, K. A., Harms, K. E., Gagnon, P. R., Myers, J. A., & Elderd, B. D. (2018). Overdispersed spatial patterning of dominant bunchgrasses in Southeastern pine savannas. *The American Naturalist*, 191(5), 658-667. https://doi.org/10.1086/696834

Hui, C., Fox, G. A., & Gurevitch, J. (2017). Scale-dependent portfolio effects explain growth inflation and volatility reduction in landscape demography. *Proceedings of the National Academy of Sciences*, 114(47), 12507-12511. https://doi.org/10.1073/pnas.1704213114

Huston, M. A. (2002). Introductory essay: Critical issues for improving predictions. In J. M. Scott, P. J. Heglund, M. L. Morrison, J. Haufler, M. G. Raphael, W. A. Wall, & F. B. Samson (Eds.), *Predicting Species Occurrences: Issues of Accuracy and Scale* (pp. 7–22). Washington: Island Press.

James, G., Witten, D., Hastie, T., & Tibshirani, R. (2013). *An Introduction to Statistical Learning with Applications in R*. Springer New York.

Kellner, K. F., & Swihart, R. K. (2014). Accounting for imperfect detection in ecology: A quantitative review. *PLoS ONE*, 9(10), e111436. https://doi.org/10.1371/journal.pone.0111436

Kéry, M., & Schmidt, B. (2008). Imperfect detection and its consequences for monitoring for conservation. *Community Ecology*, 9(2), 207–216. https://doi.org/10.1556/ComEc.9.2008.2.10

Knape, J. (2008). Estimability of density dependence in models of time series data. *Ecology*, 89(11), 2994–3000. https://doi.org/10.1890/08-0071.1

Komura, R., Kubo, M., & Muramoto, K. (2004). Delineation of tree crown in high resolution satellite image using circle expression and watershed algorithm. In Geoscience and Remote Sensing Symposium, 2004. IGARSS '04 (pp. 1577–1580). IEEE. https://doi.org/10.1109/IGARSS.2004.1370616

Lamar, W. R., McGraw, J. B., & Warner, T. A. (2005). Multitemporal censusing of a population of eastern hemlock (*Tsuga canadensis* L.) from remotely sensed imagery using an automated segmentation and reconciliation procedure. *Remote Sensing of Environment*, 94(1), 133–143. https://doi.org/10.1016/j.rse.2004.09.003

Law, R., & Dieckmann, U. (2000). A dynamical system for neighborhoods in plant communities. *Ecology*, 81(8), 2137–2148. https://doi.org/10.1890/0012-9658(2000)081{[}2137:ADSFNI]2.0.CO;2

Law, R., Murrell, D. J., & Dieckmann, U. (2003). Population growth in space and time: Spatial logistic equations. *Ecology*, 84(1), 252–262. https://doi.org/10.1890/0012-9658(2003)084[0252:PGISAT]2.0.CO;2

Lebreton, J.-D., & Gimenez, O. (2013). Detecting and estimating density dependence in wildlife populations. *Journal of Wildlife Management*, 77(1), 12–23. https://doi.org/10.1002/jwmg.425

Leibold, M. A., Holyoak, M., Mouquet, N., Amarasekare, P., Chase, J. M., Hoopes, M. F., Holt, R. D., Shurin, J. B., Law, R., Tilman, D., Loreau, M., & Gonzalez, A. (2004). The metacommunity concept: A framework for multi-scale community ecology. *Ecology Letters*, 7(7), 601-613. https://doi.org/10.1111/j.1461-0248.2004.00608.x

Levin, S. A. (1992). The problem of pattern and scale in ecology: The Robert H. MacArthur Award Lecture. *Ecology*, 73(6), 1943–1967. https://doi.org/doi:10.2307/1941447

Levin, S. A., Grenfell, B., Hastings, A., & Perelson, A. S. (1997). Mathematical and computational challenges in population biology and ecosystems science. *Science*, 275(5298), 334–343. https://doi.org/10.1126/science.275.5298.334

Lewis, M. A., & Kareiva, P. (1993). Allee dynamics and the spread of invading organisms. *Theoretical Population Biology*, 43(2), 141–158. https://doi.org/10.1006/tpbi.1993.1007

Lindenmayer, D. B., Cunningham, R. B., Donnelly, C. F., Incoll, R. D., Pope, M. L., Tribolet, C. R., Viggers, K., & Welsh, A. H. (2001). How effective is spotlighting for detecting the greater glider (*Petauroides volans*)? *Wildlife Research*, 28(1), 105–109. https://doi.org/10.1071/WR00002

Mallet, J. (2012). The struggle for existence: How the notion of carrying capacity, K, obscures the links between demography, Darwinian evolution, and speciation. *Evolutionary Ecology Research*, 14(5), 627–665.

Melbourne, B. A., & Chesson, P. (2006). The scale transition: Scaling up population dynamics with field data. *Ecology*, 87(6), 1478–1488. https://doi.org/10.1890/0012-9658(2006)87[1478:TSTSUP]2.0.CO;2

Morin, P. J. (1999). *Community Ecology*. New Brunswick, New Jersey: Blackwell Science.

Morozov, A., & Poggiale, J. C. (2012). From spatially explicit ecological models to mean-field dynamics: The state of the art and perspectives. *Ecological Complexity*, 10, 1–11. https://doi.org/10.1016/j.ecocom.2012.04.001

Murrell, D. J., Purves, D. W., & Law, R. (2001). Uniting pattern and process in plant ecology. *Trends in Ecology and Evolution*, 16(10), 529–530. https://doi.org/10.1016/S0169-5347(01)02292-3

Pau, G., Fuchs, F., Sklyar, O., Boutros, M., & Huber, W. (2010). EBImage - an R package for image processing with applications to cellular phenotypes. *Bioinformatics*, 26(7), 979–981.

Pebesma, E. J., & Bivand, R. S. (2005). Classes and methods for spatial data in R. *R News*, 5(2), 1–21. Retrieved from https://cran.r-project.org/doc/Rnews/

Peters, H. A. (2003). Neighbour-regulated mortality: The influence of positive and negative density dependence on tree populations in species-rich tropical forests. *Ecology Letters*, 6(8), 757–7 65. https://doi.org/10.1046/j.1461-0248.2003.00492.x

Pettorelli, N., Laurance, W. F., O'Brien, T. G., Wegmann, M., Nagendra, H., & Turner, W. (2014). Satellite remote sensing for applied ecologists: Opportunities and challenges. *Journal of Applied Ecology*, 51(4), 839-848. https://doi.org/10.1111/1365-2664.12261

Purves, D. W., & Law, R. (2002). Fine-scale spatial structure in a grassland community: Quantifying the plant's-eye view. *Journal of Ecology*, 90(1), 121–129. https://doi.org/10.1046/j.0022-0477.2001.00652.x

R Core Team. (2017). R: A language and environment for statistical computing. Vienna, Austria: R Foundation for Statistical Computing. Retrieved from https://www.r-project.org/

Rocchini, D., Boyd, D. S., Féret, J.-B., Foody, G. M., He, K. S., Lausch, A., Nagendra, H., Wegmann, M., & Pettorelli, N. (2015). Satellite remote sensing to monitor species diversity: Potential and pitfalls. *Remote Sensing in Ecology and Conservation*, 2(1), 25-36. https://doi.org/10.1002/rse2.9

Ross, S. (2010). *A First Course in Probability* (8th ed.). Upper Saddle River, New Jersey: Pearson Prentice Hall.

Ross, J. V. (2009). A note on density dependence in population models. *Ecological Modelling*, 220(23), 3472–3474. https://doi.org/10.1016/j.ecolmodel.2009.08.024

Royle, J. A., Nichols, J. D., & Kéry, M. (2005). Modelling occurrence and abundance of species when detection is imperfect. *Oikos*, 110(2), 353–359. https://doi.org/10.1111/j.0030-1299.2005.13534.x

Salguero-Gómez, R., Jones, O. R., Archer, C. R., Buckley, Y. M., Che-Castaldo, J., Caswell, H., Hodgson, D., Scheuerlein, A., Conde, D.A., Brinks, E., de Buhr, H., Farack, C., Gottschalk, F., Hartmann, A., Henning A., Hoppe, G., Römer, G., Runge, J., Ruoff, T., Wille, J., Zeh, S., Davison, R., Vieregg, D., Baudisch, A., Altwegg, R., Colchero, F., Dong, M., de Kroon, H., Lebreton, J.-D., Metcalf, C. J. E., Neel, M. M., Parker, I. M., Takada, T., Valverde, T., Vélez-Espino, L. A., Wardle, G. M., Franco, M., & Vaupel, J. W. (2015). The Compadre Plant Matrix Database: An open online repository for plant demography. *Journal of Ecology*, 103(1), 202–218. https://doi.org/10.1111/1365-2745.12334

Sandel, B., & Smith, A. B. (2009). Scale as a lurking factor: Incorporating scale-dependence in experimental ecology. *Oikos*, 118(9), 1284–1291. https://doi.org/10.1111/j.1600-0706.2009.17421.x

Santin-Janin, H., Hugueny, B., Aubry, P., Fouchet, D., Gimenez, O., & Pontier, D. (2014). Accounting for sampling error when inferring population synchrony from time-series data: A Bayesian state-space modelling approach with applications. *PLoS ONE*, 9(1). https://doi.org/10.1371/journal.pone.0087084

Schmidt, B. R. (2005). Monitoring the distribution of pond-breeding amphibians when species are detected imperfectly. *Aquatic Conservation: Marine and Freshwater Ecosystems,* 15, 681–692. https://doi.org/10.1002/aqc.740

Stoll, P., & Weiner, J. (2000). A neighborhood view of interactions among individual plants. In U. Dieckmann, R. Law, & J. A. J. Metz (Eds.), *The Geometry of Ecological Interactions: Simplifying Spatial Complexity* (pp. 11–27). Cambridge, United Kingdom: Cambridge University Press.

Tilman, D., Lehman, C. L., & Kareiva, P. (1997). Population dynamics in spatial habitats. In D. Tilman & P. Kareiva (Eds.), *Spatial Ecology: The Role of Space in Population Dynamics and Interspecific Interactions* (pp. 3–20). Princeton, New Jersey: Princeton University Press.

Turner, M. G., & Gardner, R. H. (2015). *Landscape Ecology Theory and Practice: Pattern and Process* (2nd ed.). New York: Springer-Verlag.

Wang, L., Gong, P., & Biging, G. S. (2004). Individual tree-crown delineation and treetop detection in high-spatial-resolution aerial imagery. *Photogrammetric Engineering & Remote Sensing*, 70(3), 351–357.

Wheatley, M., & Johnson, C. (2009). Factors limiting our understanding of ecological scale. *Ecological Complexity*, 6(2), 150-159. https://doi.org/10.1016/j.ecocom.2008.10.011

Ying, Z., Liao, J., Wang, S., Lu, H., Liu, Y., Ma, L., & Li, Z. (2014). Species coexistence in a lattice-structured habitat: Effects of species dispersal and interactions. *Journal of Theoretical Biology*, 359, 184–191. https://doi.org/10.1016/j.jtbi.2014.05.048

Yu, X., Hyyppä, J., Vastaranta, M., Holopainen, M., & Viitala, R. (2011). Predicting individual tree attributes from airborne laser point clouds based on the random forests technique. *ISPRS Journal of Photogrammetry and Remote Sensing*, 66(1), 28–37. https://doi.org/10.1016/j.isprsjprs.2010.08.003

Zenner, E. K., & Peck, J. L. E. (2018). Floating neighborhoods reveal contribution of individual trees to high sub-stand scale heterogeneity. *Forest Ecology and Management*, 412, 29–40. https://doi.org/10.1016/j.foreco.2018.01.054

Zhu, Y., Mi, X., Ren, H., & Ma, K. (2010). Density dependence is prevalent in a heterogeneous subtropical forest. *Oikos*, 119(1), 109–119. https://doi.org/10.1111/j.1600-0706.2009.17758.x

Chapter 4
Conifer invasions are constrained by the interaction between density dependence and spatial variation of density

4.1 Introduction

Ecologists need to understand the processes which shape population dynamics at broad spatial scales (Gurevitch, Fox, Fowler, & Graham, 2016; Leibold et al., 2004; Levin, Grenfell, Hastings, & Perelson, 1997). However the vast majority of studies on population dynamics collect data at a smaller scale. In studies of plant ecology for example we often gather data on individual plots, often less than one hectare in size (Estes et al., 2018; Salguero-Gómez et al., 2015). We lack a general understanding of when plot-scale estimates of population growth lead to errors when we extrapolate to broader scales (Miller, Turner, Smithwick, Dent, & Stanley, 2004; Scholes, 2017). Because plot-level estimates may be misleading it will be difficult to anticipate the broad scale effects issues such as climate change and species invasions (Chave, 2013; Estes et al., 2018; Hui, Fox, & Gurevitch, 2017; Miller et al., 2004).

As a way around this issue, ecologists need reliable methods scale up population dynamics (Scholes, 2017). However, scaling up population growth is difficult because population growth is scale dependent (Levin, 1992; Sandel, 2015; Steen & Haydon, 2000). This scale dependence is brought about by environmental heterogeneity, dispersal, and the effects of density. Environmental heterogeneity causes the growth rates of a population to vary across a landscape, and furthermore, the amount of environmental heterogeneity can change depending on the observational scale (Allen & Hoekstra, 2015; Gurevitch et al., 2016; Tilman, 1994). Dispersal affects the future spatial structure of a population through determining the recruitment area, thereby changing its affects with scale (Cousens, Dytham, & Law, 2008; Nathan & Muller-Landau, 2000). The effects of density on ecological processes such as competition and survival can depend on scale (Gunton & Kunin, 2007). Density dependent growth, or the process by which the growth rate of individuals responds differently depending on the density of the local neighbourhood, varies with distance and will thus cause the observed population growth to change with scale (Condit, Hubbell, & Foster, 1994; Y. Zhu, Mi, Ren, & Ma, 2010). Furthermore, density dependent growth is particularly important for plants because they cannot move to change their local neighbourhood density (Law et al., 2009; Peters, 2003; Stoll & Weiner, 2000). For connecting small to regional spatial scales, local density dependence and its variability affect population dynamics at a broad scale but it is difficult to capture this variation when simply observing processes at a small scale (Belmaker et al., 2015; Sandel, 2015; Wisz et al., 2013).

In practice, the most common approach is to ignore scale dependent processes by averaging population dynamics over the landscape. When we do so, we revert to what is known as the mean field

population growth estimate (Melbourne & Chesson, 2005). The mean field is calculated by averaging density and therefore density-dependent effects on population growth across an entire region (Dieckmann, Law, & Metz, 2000; Morozov & Poggiale, 2012). This estimate is accurate when density and individual growth responses to density do not affect population growth. Since the density of individuals varies across a landscape (Turner & Gardner, 2015), we cannot assume that an individual has the same local neighbourhood density and therefore grows the same across a landscape in response to its neighbourhood effects (Murrell, Purves, & Law, 2001; Ying et al., 2014). As such, many studies (ex. (Stoll & Weiner, 2000; Zenner & Peck, 2018)) have not found support for the assumption that the effects of density are the same across a region.

One way to estimate the severity of this scaling problem is to use a Scale Transition Term (STT) to scale up population growth (Chesson, 2012; Chesson, Donahue, Melbourne, & Sears, 2005). This approach approximates the difference between local and regional population growth rates using information on variation in density among plots and density dependence of a population growth within plots (Chesson et al., 2005; Melbourne, Sears, Donahue, & Chesson, 2005). In doing so, the STT quantifies the effect of spatial processes on population growth, represented by the difference between the mean field and the regional estimate of population growth (Melbourne & Chesson, 2006). Because this method focuses on population dynamics at the plot level, it requires far less data than other scaling approaches that focus on the dynamics of individuals (Adams, Holland, Law, Plank, & Raghib, 2013; Cipriotti, Wiegand, Pütz, Bartoloni, & Paruelo, 2016).

Several studies have empirically estimated the STT (Table 4.1) and all have found that the STT is large and negative. This indicates that when we do not account for spatial variation and the effect of local neighbourhoods on growth, we over-estimate the ability of a population to grow. However, most of these studies examined only small-scale, single site systems to estimate the STT (Benedetti-Cecchi et al., 2012; Melbourne & Chesson, 2005, 2006). For example, Melbourne & Chesson (2006) examined a stream ecosystem with freshwater organisms at a local scale of individual rocks (100-300 cm^2) and a regional scale of a 5km long stream. Without knowing whether the spatial processes quantified in the STT are important for population growth at a broad-scale and for multiple sites, we do not know the broad relevance of the STT. While all of the studies estimated the density dependence of their study systems, all of the estimates of STT have been made for systems which are stable and have a non-varying long-term average growth (Benedetti-Cecchi et al., 2012; Englund & Leonardsson, 2008; Holt & Chesson, 2016; Melbourne & Chesson, 2006). As such, none of these studies accounted for dispersal or recruitment at the regional scale as well, instead assuming that dispersal disappeared at a large scale (Melbourne & Chesson, 2006). Therefore, none of these studies statistically accounted for dispersal in their models and thus did not capture the spatial effects of dispersal. We still do not know whether the mean field estimates hold true for broad-scale dynamic systems where climate change and species invasions are most concerning (Gurevitch et al., 2016).

Table 4.1 Summary of studies which have empirically estimated the STT

Study System	Scale (Local and Regional)	Number of sites and time	Data Collection Approach	Examined a dynamic system (Y/N)	Findings	STT as Percentage of Mean field Estimate	Reference
Caddisfly larvae and adult lifecycle	Local: riffles Regional: stream (dimensions were not specified)	1 simulated site (stream)	Used simulated field data based on expected densities of larvae and the lifecycle of caddisflies	No	Total simulated STT was negative and moderately sized	STT was 13-17% of mean field estimate	(Melbourne & Chesson, 2005)
Freshwater organisms in a stream in NSW Australia	Local: individual rocks (100-300cm^2 sized patches) Regional: stream (5km long stream)	1 stream, 2-3 weeks of monitoring	Measured periphyton initial and final densities with and without predators; to estimate spatial variance in densities, used a hierarchical sampling design	No	Total STT was large and negative	STT reduced the mean field estimate by 98%	(Melbourne & Chesson, 2006)
Turf-forming algae on a Mediterranean Island (Capraia Island)	Local: patches on the shore line (400cm^2 plots) Regional: island-wide shore (island is approximately 19 km^2)	1 island, 2 years of monitoring	Measured algae cover and estimated competition using competitive exclusion experiments; used hierarchical sampling design to estimate spatial variation of algae cover	No	Total STT was large and negative	STT reduced the mean field estimated by 73%	(Benedetti-Cecchi et al., 2012)

To broaden our understanding of the relationship between plot level and regional population growth, I will examine tree invasions as a dynamic study system. Tree invasions are a massive problem worldwide (Rejmánek & Richardson, 2013; Richardson & Rejmánek, 2011). Individual invasions can cover tens of kilometres, but often population parameters and growth of these invasions are measured at a small scale (i.e., plot scale (Carrillo-Gavilán & Vilà, 2010) or small area of transects (Langdon, Pauchard, & Aguayo, 2010; Nuñez & Paritsis, 2018)). Therefore, these systems are extremely suitable for studying for the difference between local and regional scale population growth. Furthermore, since tree invasions are both expanding and occur at broad regional scales, I will be able to address the gap in the literature on the effect of spatial processes on population growth.

I focus more specifically on invasions of conifers, as they are rapidly spreading species and an issue for many countries in the Southern Hemisphere (Higgins and Richardson, 1998; Richardson and Rejmanek, 2004). There is evidence that density affects the spread of conifer invasions through both facilitation and competition (Dovčiak, Hrivnák, Ujházy, & Gömöry, 2014; Hayward, Horton, Pauchard, & Nuñez, 2015; Nuñez, Horton, & Simberloff, 2009; Richardson & Bond, 1991); therefore I would expect that spatial processes have a large influence on population growth. However, so far, the estimates of the population growth of these invasions have largely ignored spatial processes from density (but see Higgins & Richardson (1998) and Higgins, Richardson, & Cowling (2001)). Thus I want to test whether we are over-simplifying and over-estimating the population growth of these invasions.

As demonstrated in Chapter 2, remote sensing data provide a means to estimate the populations of trees over large areas and several years (Pettorelli et al., 2014; Rocchini et al., 2015). Many of the studies which have estimated the STT before have been for small sites or have only been for one site (Table 4.1). Using these remote sensing data for multiple sites and over long periods of time, I am maximising an underexploited approach to calculate the STT. These data will enable me to expand the knowledge of the STT by examining broad-scale and temporal trends in the STT estimates.

By combining remote sensing imagery data with population dynamic models, I am able estimate the STT for a dynamic system at broad spatial scales for the first time. The questions of this study are as follows:

1. How strong are the components of the STT (spatial variation of density and density dependence)?

2. How large is the STT? In other words, when we ignore the spatial effects of density on population growth, how incorrect are the estimates of population growth?

3. Is the STT consistent across multiple sites and years?

4.2 Methods

To scale up population growth estimates and determine the effect of spatial processes on estimates of population growth, I gathered data from eight large-scale invasion sites over several time steps. Time steps were dictated by the availability of aerial and satellite images for each of the sites. These imagery data have been collected every 2-3 years for the past decade, giving me 1-2 time intervals per site. With these data, I divided the sites into one hectare-sized plots and then used these data to estimate the difference between the local and regional estimates of population growth. I will first provide details of the data collection and then I will show our population growth model. Finally, I will describe my methods for calculating the STT.

4.2.1 Remote Sensing Imagery and Data Processing

To acquire population density data of conifer invasions to run the population models, I used high resolution remote sensing data. I gathered imagery from eight invasion sites across the South Island of New Zealand for multiple time steps (2-4 points in time) using a combination of high resolution aerial imagery gathered from the Land Information New Zealand (LINZ) archives and high resolution satellite imagery downloaded from Google Earth. Sites had to be located in grasslands in order to easily detect the invading trees using remote sensing data. Imagery had to be available from multiple time steps, separated by at least 2 years and have sub-meter spatial resolution to accurately detect trees. To avoid confounding factors, I considered only sites where it was possible to distinguish intentionally planted areas of trees and any managed areas where trees were cut down or sprayed with herbicide. This way I could determine where the invasion source was, which trees were invading and which were intentionally planted, and whether the invasion had been modified.

The spatial resolution for each site was approximately 0.5m and the spectral resolution was 3 bands (Red, Green, and Blue) for a natural colour image. Imagery from LINZ was georeferenced but imagery from Google Earth had to be manually geo-referenced. Appendix E summarises the complete specifications of the imagery gathered and shows photos of the imagery for each site and time step. Figure 4.1 shows the locations of the eight sites.

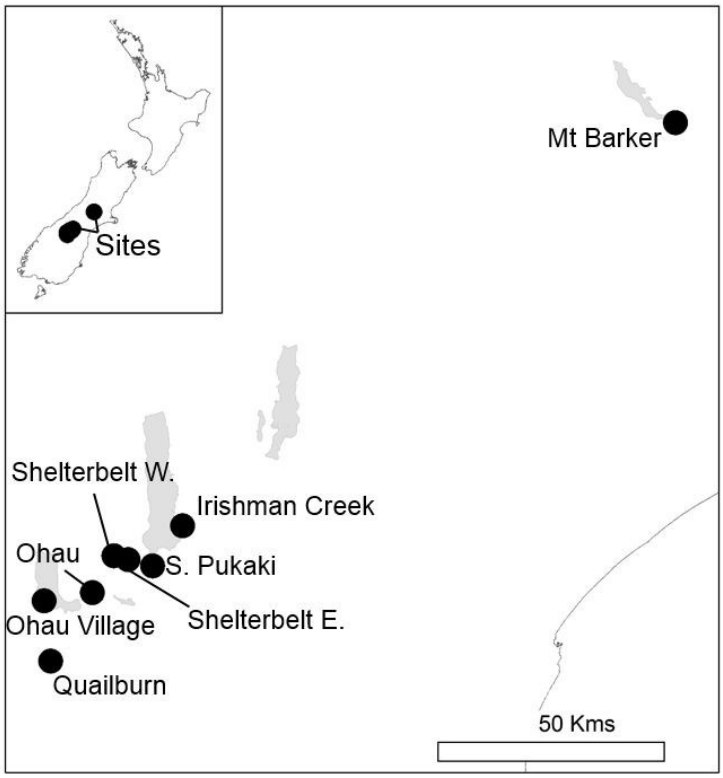

Figure 4.1 Locations of the eight invasion sites are indicated by the black points. All of the sites were located in the Canterbury province on the South Island of New Zealand. Prominent lakes in the region (shown in light grey) were added to the map as areas of reference.

To detect conifers, I used an unsupervised, pixel-based classification method. First I thresholded the imagery to separate out the dark-coloured trees against the light-coloured background vegetation (Ke & Quackenbush, 2011). Then I segmented the pixels identified as trees using a process called watershedding in order to delineate the trees' canopies (Deng, Katoh, Yu, Hyyppä, & Gao, 2016; Komura, Kubo, & Muramoto, 2004; Wang, Gong, & Biging, 2004). I extracted the centre point of each polygon identified as a tree, and for each site and time step, I generated a file of the point locations of every tree detected. More details of this image classification procedure and ground truthing can be found in Chapter 2.

All image classification was conducted in R using the following packages: EBImage (Pau, Fuchs, Sklyar, Boutros, & Huber, 2010), rgdal (Bivand, Keitt, & Rowlingson, 2017), raster (Hijmans, 2016), and sp (Pebesma & Bivand, 2005) (R Core Team, 2017).

To prepare the data derived from the image classification and detection methods to be used in the population growth models, I first divided each site into a grid of 100 x 100 m or one hectare grid-cells, and I counted the number of trees in each cell for each time step. I used one hectare as the cell size because this represents the area where most of tree seeds would disperse (Buckley et al., 2005; Caplat, Nathan, & Buckley, 2012). I removed the grid-cells with no trees in them in the first time step. This was because the population growth models did not account for long-distance dispersal and thus did not

account for dispersal into un-adjacent, empty cells between time steps. New trees appearing in empty cells would thus bias growth parameter estimates. I also removed any outlier cells in which the imagery was either misaligned slightly or the tree locations from the time steps did not precisely align.

4.2.2 Population Growth Models

I used the Gompertz population model to estimate the population growth parameters of density dependence and density independent growth. The Gompertz model is closely related to the familiar logistic model of population growth. Like the logistic, the Gompertz model contains two parameters one for density dependent growth and one for density independent growth. However, the parameters in the Gompertz model are easier to estimate empirically than those in the logistic (parameters). As a result the Gompertz model has been frequently used to estimate density dependence of populations (e.g., (Roy, McIntire, & Cumming, 2016; Thorson et al., 2015)).

The equation for population growth (*F(N)*) is expressed in the Gompertz form as:

$$F(N_t) = N_{t+1} = N_t e^{a+(b-1)\log(N_t)}$$

where N_t is population density at time *t*, *a* is density independent growth of the population, and *b* is the degree of density dependence.

I can simplify this equation to make it straightforward to model and interpret. Taking the natural log of both sides of this equation for *F(N)* results in the Gompertz model in the following form:

$$\log(N_{t+1}) = a + b\, log(N_t) + \epsilon_t \qquad \text{(Equation 4.1)}$$

A value of *b* greater than 1 represents exponential growth, a value of *b = 1* implies no density dependence, a value of *b* less than but close to 1 represents weak density dependence, and a value of *b* close to 0 represents strong density dependence. The model includes an error term too, ε_t, which represents environmental stochasticity. This model can be fit using linear regression of $log(N_t)$ against $log(N_{t+1})$, with the intercept serving as an estimate for *a* and the slope serving as an estimate for *b*. Since the estimates of both *a* and *b* were used to calculate the STT, I examined the strength of these values and how they varied between and across the invasion sites.

In the interests of simplifying the models and focusing the scope of this study, I decided to only examine the population growth process known as infilling. Infilling can be defined as when the spreading population colonises areas within its existing range, and it occurs because of local dispersal (L. A. V. Taylor, Hasenkopf, & Cruzan, 2015; Warren, Ursell, Keiser, & Bradford, 2013). Because most of the population growth of these tree invasions occurs at short distances (Buckley et al., 2005; Nuñez & Paritsis, 2018; K. T. Taylor et al., 2016), I will limit my scope to infilling.

To account for spatial autocorrelation due to dispersal at short to intermediate distances and correlated environmental conditions in adjacent areas, I added a spatial random effects term to the Gompertz equation. I used a Conditional Autoregressive (CAR) model for the spatial random effects term since this model was straight forward to set up and is known to perform well with spatial data (Duncan, White, & Mengersen, 2017). This auto-regressive model works by accounting for the local neighbourhood and effectively smooths over adjacent areas.

Equal weight (*w*) was given to each neighbouring plot, so that:

$$w_{i,j} = \begin{cases} 1\,; if\ areas\ i\ and\ i\ are\ neighbours \\ 0\,; if\ areas\ i\ and\ j\ are\ not\ neighbours \end{cases}$$

Since each neighbouring plot had the same weight, the CAR model assumed the datasets were isotropic. Therefore, this model must be interpreted with caution because the datasets were potentially anisotropic. For each site and set of time-steps examined, I defined a new neighbourhood matrix based on the occupied areas in the site.

I ran the models in a Bayesian framework. I used informative priors based on estimates of density dependence and density independent growth for similar Gompertz models in the literature (Dennis, Ponciano, Lele, Taper, & Staples, 2006; Thorson et al., 2015). The following prior distributions were used:

$$a \sim N(0, 0.2)$$

$$b \sim N(0, 1)$$

$$\tau \sim G(01., 0.1)$$

I used a CAR normal distribution for the prior of the CAR model, with a precision term τ_{sp} with a gamma distribution.

I set up and ran a model for each time interval and site. Time intervals were defined as the difference between one time step and another, and there were different lengths of time between time steps due to which imagery data was available. I ran the models with Markov Chain Monte Carlo (MCMC) sampling, implemented in the R package Nimble (de Valpine et al., 2017). I tested whether the spatial model improved fit over an aspatial model without the spatial random effects term. To compare the spatial and aspatial models, I calculated the Watanabe-Akaike Information Criterion (WAIC) values (Watanabe, 2010). WAIC values are recommended to be used instead of Deviance Information Criterion (DIC) values according to Vehtari et al. (2016). Each model used 3 chains and ran for 10,000 iterations with the first 5,000 samples discarded as the burn-in. The initial conditions of each chain were randomly generated within the expected parameter range. MCMC samples were not thinned as

thinning has been shown to decrease the precision of estimates from MCMC sampling (Link & Eaton, 2012).

To check for model convergence, I used the trace plots, posterior densities, and $\hat{R}$ values from the R package shinystan (Gabry, 2018), similar to methods by (Elderd & Miller, 2016). I also examined the goodness of fit of the models by plotting their predictive intervals with the observed data to determine whether the model could predict all of the observed values (Gelman, Meng, & Stern, 1996). All of the models were coded and run in R (R Core Team, 2017), and the model code is shown in Appendix G.1.

4.2.3 Estimating the Scale Transition Term

At the local scale, population growth can be described as the following equation:

$$N_{t+1} = F(N_t)$$

where N_{t+1} is the population density at time $t+1$ and $F(N_t)$ is the population growth function of the population density at time t (or N_t).

Chesson et al. (2005) shows that regional population growth rate can be approximated as the mean field growth rate plus a correction term representing $F(N)$ approximated by a second-order Taylor series expansion. This correction term (the STT) can be expressed as:

$$STT = \frac{1}{2} Var(N_t) F''(\overline{N_t}) \qquad \text{(Equation 4.2)}$$

Thus, at a regional scale, the population growth will be the function for population growth of the mean field plus a correction term (the STT):

$$\overline{N_{t+1}} = F(\overline{N_t}) + \frac{1}{2} Var(N_t) F''(\overline{N_t})$$

As seen in Equation 4.2 above, the STT depends on the variance in tree densities at the start of the observation period ($var(N)$) and the density dependence of the site's population ($F''(N)$). To calculate the variance in densities across a site, I used the population level formula for variance among all plots in a given site. In this calculation I excluded sites with a tree density of zero, since these were ignored in the population model.

To calculate the nonlinear growth component of the STT, $F''(N)$, I took the second derivative of the population growth equation with respect to population density. This derivation is solved and explained in more details in Appendix F. Because the nonlinear growth term needed the estimates of the density independent growth and density dependence, I used the distributions for these parameters estimated from the population growth model to calculate $F''(N)$ for each site and time interval.

To calculate the STT, I used the above Eqn 4.2 and my estimates of the components of the STT. I used the 95% credible intervals of the STT estimates to determine whether the estimates were significantly different from zero for each site examined.

To determine whether estimates of the STT were consistent across sites, I compared values of the STT, paying particular attention to those sites for which I had more than one time interval and therefore more than one estimate of the STT for the site.

I calculated the STT as a percentage of the estimated mean field population growth for each site and time interval to put the STT estimates in context. To estimate the mean field population growth, I substituted the mean density of the one hectare plots for each site and the estimated parameters values from the spatial models into the population growth model. Doing this allowed me to assess the magnitude of the STT estimates and in particular determine the overall importance of STT for estimating population growth.

4.3 Results

4.3.1 Sites and Models

The average size of the invasion sites was 3.0 km^2, with the smallest site being 0.24 km^2 and the largest being over 16 km^2. The number of trees detected at the sites ranged from approximately 3,500 for the small-sized sites to over 200,000 trees for the large sites. Table 4.2 summarises the mean number of trees per grid-cell and the variance of the number of trees per grid-cell for each site and time step.

Table 4.2 Mean density and variance of densities for each site and time-step.

Site	Imagery Source	Year Imagery Captured	Site Extent (km^2)	Mean Number of Trees per hectare	Variance in Number of Trees per hectare	Coefficient of Variation
Ohau	Google Earth	2011	5.15	17	541	1.37
Ohau	LINZ	2014	5.94	65	8554	1.42
Mt Barker	Google Earth	2010	4.84	212	13070	0.54
Mt Barker	LINZ	2016	6.02	412	58726	0.59
S. Pukaki	Google Earth	2006	2.33	64	5066	1.11
S. Pukaki	LINZ	2008	2.54	134	18411	1.01
S. Pukaki	LINZ	2014	2.89	235	58341	1.03
S. Pukaki	Google Earth	2016	3.30	319	121670	1.09
Shelterbelt W.	LINZ	2006	0.24	155	22269	0.96
Shelterbelt W.	Google Earth	2010	0.37	196	23463	0.78
Shelterbelt E.	LINZ	2008	0.42	141	25655	1.14
Shelterbelt E.	Google Earth	2010	0.60	264	73232	1.03
Shelterbelt E.	LINZ	2014	0.73	355	72678	0.76
Quailburn	LINZ	2008	1.41	211	53667	1.10
Quailburn	LINZ	2014	1.70	388	65350	0.66
Ohau Village	LINZ	2006	1.28	109	25152	1.45
Ohau Village	Google Earth	2011	1.43	298	66700	0.87
Irishman Creek	LINZ	2008	11.20	40	12209	2.76
Irishman Creek	LINZ	2014	16.60	105	21888	1.41

I ran models at eight sites, and in 3 sites it was possible to model two time intervals, leading to 11 models in total. In each case the spatial models better fit the data than the aspatial models which had omitted the spatial random effect (see Table G1 in Appendix G of WAIC values). Thus, the parameter estimates from the spatial models were used for every site and time interval. Appendix G shows the model code and diagnostics for the models.

4.3.2 Variation in Density and Estimates of Density Dependence

I found that density did vary greatly across an invasion landscape as shown by the coefficients of variation in Table 4.2. Most of the sites and time steps had coefficients of variation which were above one, indicating a high degree of variation in densities. The variation of density was not necessarily consistent for each site as well, with some sites having similar coefficients of variation between time steps (ex. Ohau, S. Pukaki, and Mt Barker) and others having very different coefficients of variation (ex. Quailburn, Ohau Village, and Irishman Creek). Figure 4.2 also illustrates the variation of density across one of the sites.

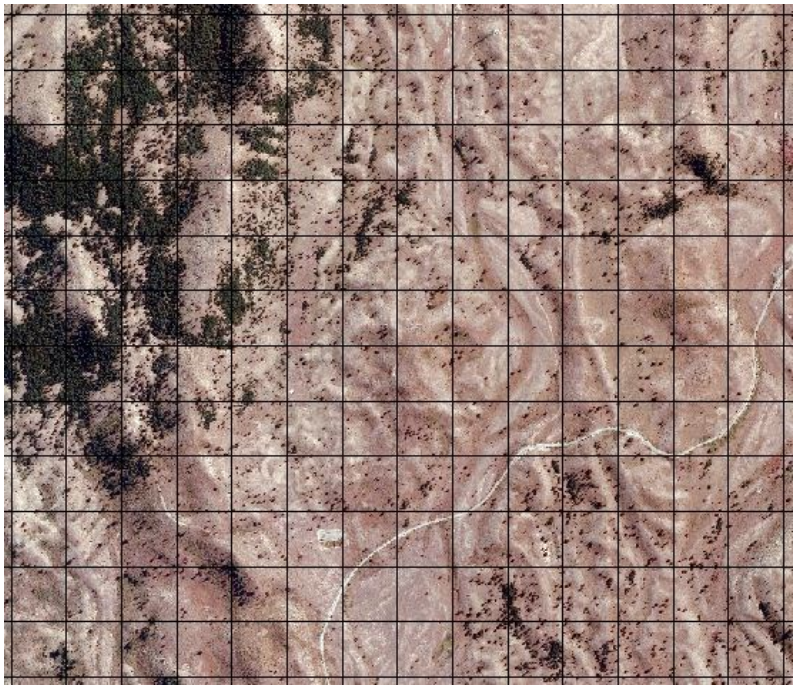

Figure 4.2 Example of the variation in tree densities at an invasion site. This imagery is of Irishman Creek site in 2014 with the grid of one hectare cells overlaid on it. Imagery courtesy of Land Information New Zealand.

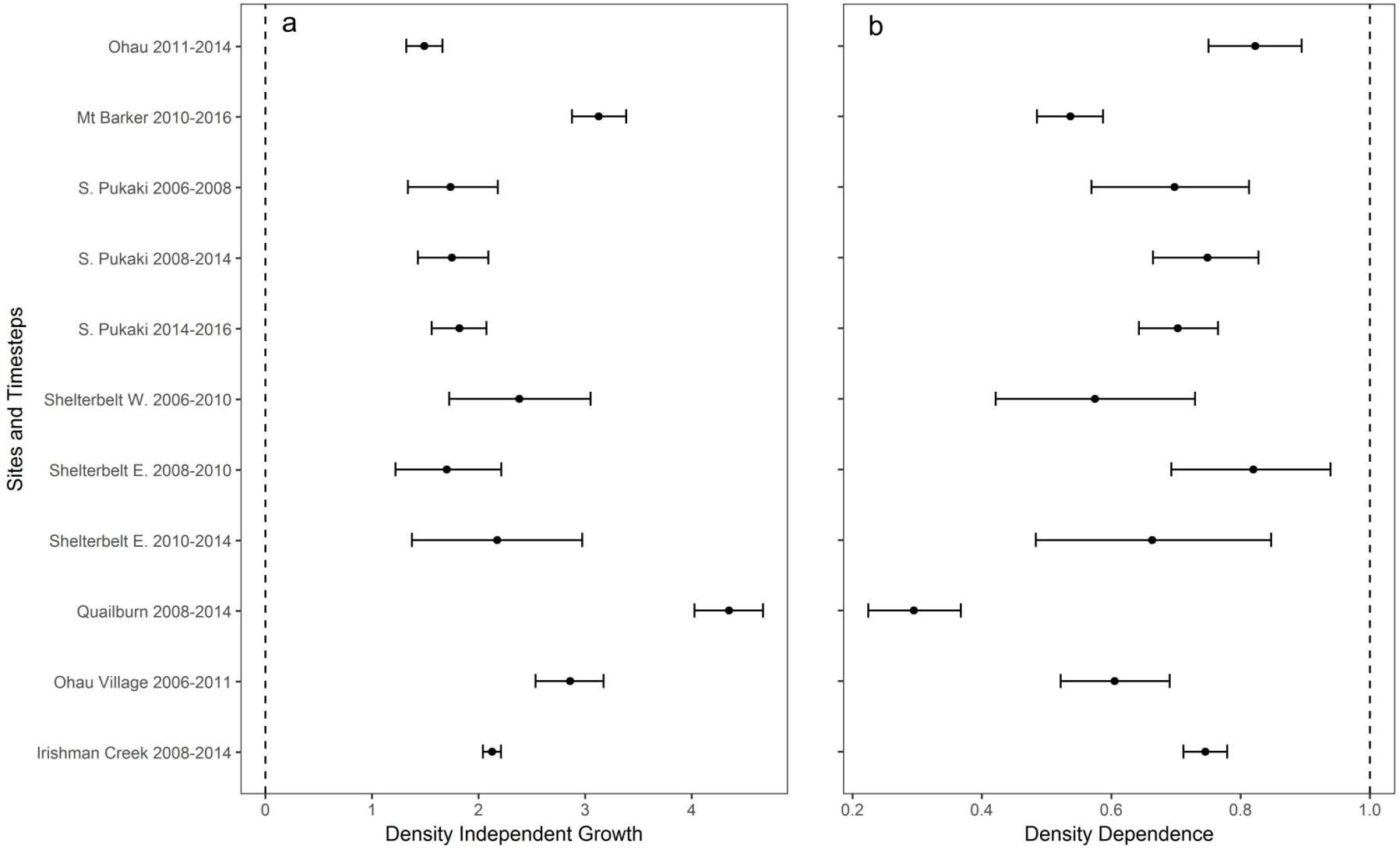

Figure 4.3 a) Estimates of density independent growth were high for all sites examined. These density independent growth values are the *a* parameter estimates from the model, and error bars are 95% credible intervals. b) Most site and time intervals had weak to moderate degrees of density dependence. These density dependence values are the *b* parameter estimates from the model, and error bars are 95% credible intervals. Dashed lines at zero in (a) and one in (b) represent when the respective terms equal zero.

Density independent growth was high, which was expected for these rapidly growing populations (Fig. 4.3a). There was some variation between sites, but most had a density independent growth of around 2. This implies that over that time interval, for every one tree in a plot in time *t*, there were around 6 more times as many trees in time *t+1* (this interpretation was obtained after back-transforming the parameter from a log scale).

Density dependence was negative and present at all sites and time intervals (Fig. 4.3b). For most sites, it was weak to moderate in strength, although for one site is was strong, as indicated by a value close to 0 for the Quailburn site.

When running the model diagnostics, I found that the estimates of density independent growth and density dependence were positively correlated (see Appendix G). Thus when the intrinsic growth rate was high, there was high density dependence as well. This correlation makes sense and did not affect the estimates of the STT.

4.3.3 Estimates of the Scale Transition Term

The estimates of the STT for all sites were negative, and all of the 95% credible intervals indicated that the estimates were significantly less than zero (Fig. 4.4a). For sites where I had multiple time intervals, the STT estimates became stronger (more negative) over time.

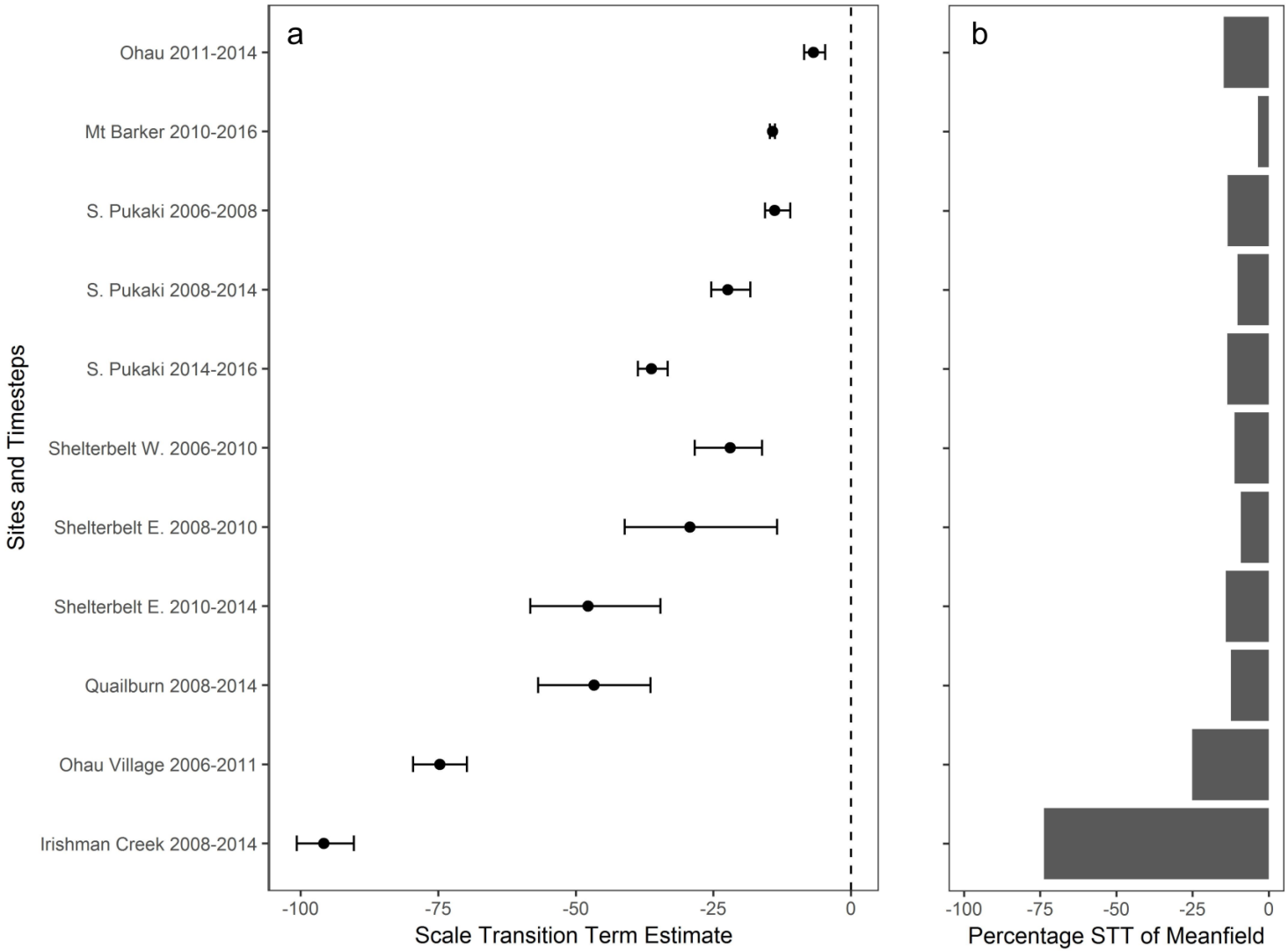

Figure 4.4 a) All estimates of the Scale Transition Term were negative and significantly different from 0. Error bars are 95% credible intervals. b) The magnitude of each STT expressed as the percentage of the mean field estimate of population growth.

To help with interpretation of Fig. 4.4a, a value of -7 (Ohau site) indicates of value of seven fewer trees per cell per time interval. Therefore a value of -95 (Irishman Creek site) would mean that there would be 95 fewer trees per cell per time interval than expected if population growth was estimated using the average density of trees across a landscape. Most sites are between -10 to -50 trees per cell per time interval. Since all of the estimates of the STT were significantly negative, this means that spatial processes slow population growth.

In Fig. 4.4b, when the STT estimates were expressed as a percentage of the mean field estimates, they were typically 10-25% of the mean-field estimates of population growth. This means that if the effects of spatial variation were ignored, estimates of population growth would be inflated by around 10-25% for most sites. Because the growth of these invasions can be on the order of magnitude of thousands of trees per site, this overestimate represents a large error in growth predictions. The only exception of these values was one site and time interval (Irishman Creek 2008-2014) when the STT estimate was almost 75% of the mean field estimate. This means that for this site, the expected population growth when spatial effects are ignored would be over-estimated by almost 75%.

4.4 Discussion

This study is the first to estimate the Scale Transition Term for multiple, large-scale sites and for a system which is rapidly changing. When I estimated the STT, I found that it was large and negative for most sites, and that for all sites, it was significantly different from zero. Both of the components of the STT, spatial variation of density and nonlinear growth, give insight into the spatial processes which cause population growth to differ between spatial scales, and they both contributed equally to the STT. I found that there was large spatial variation of density across the sites, and this variation contributed greatly to the STT. The nonlinear growth component of the STT was comprised of density independent and density dependence growth; therefore while both of these contributed to the STT estimates, they did not contribute as much as the spatial variation of density did.

Examining the estimates of density independence and density dependence more closely, I found that density independent growth was positive and high across all sites. These estimates were expected given that I already suspected that the growth of these conifer invasions was quite high (Buckley et al., 2005; Caplat, Coutts, & Buckley, 2012). I found that density dependence was negative and varied in magnitude between sites. These estimates were less expected because this is the first time that population-level density dependence has been estimated for multiple conifer populations at this scale. While I could not compare the density dependence results to studies examining expanding tree populations, this study's estimates of density dependence were consistent when comparing them to other forest systems (Brook & Bradshaw, 2006; D. J. Johnson, Beaulieu, Bever, & Clay, 2012; K. Zhu, Woodall, Monteiro, & Clark, 2015). This could be because the densities of some sites I examined were quite high, potentially similar to that of a natural forest.

When I examined the STT estimates across sites, there was some variation of the estimates. While I did not collect the data to discern why there was this variation, reasons could have been because there was large variation in the densities of grid-cells for some sites and some sites had either small or very large mean densities. Taken with previous estimates (Table 4.1) these results help to build an emerging picture of how population growth changes over scales. Across the board, estimates of STT were large and negative for stable systems (ex. Benedetti-Cecchi et al. (2012); Melbourne & Chesson (2006)) and the dynamic one I studied. This means that in general, the mean field estimates of population growth vastly over-estimate the regional population growth.

Thus, these results, taken together with the results of previous studies summarised in Table 4.1, prove that the mean field estimates of population growth for both stable and dynamic systems are often incorrect. When scaling up population growth data from a local to a regional scale, we must use the mean field approach with caution unless we can be certain that the individuals in a population are mobile and there is a strong degree of mixing of these individuals (Law, Dieckmann, & Metz, 2000). Instead, to properly scale up data, we will need to account for those spatial processes which occur because of the variance of density and individuals' growth response to density. The importance of these spatial processes for population growth has been acknowledged before (Chave, 2013; Dieckmann et al., 2000; Levin, 1992); however, accounting for these processes will now need to become part of the general practices of broad-scale ecology.

My methods provide a way forward for future studies and research on population growth. High resolution aerial imagery enabled me to capture population density data over time, for multiple sites, and at a broad spatial scale. The Bayesian population growth models allowed me to account for the spatial autocorrelation in the residuals as well as explain population parameters for multiple sites. Combining these methods with the methodology to estimate the STT (from Chesson (2012) and Chesson et al. (2005)), I was able to effectively scale up population growth estimates between small and broad spatial scales. Other studies seeking to study population growth at the broad scale should consider using these methods.

This study was not without its limitations. I only estimated density dependence at the scale of the grid-cells (100x100m). Other results may be possible using smaller grid cells because positive and negative density dependence in conifer invasions has been found to act at different scales (Dovčiak et al., 2014). This is an exciting possibility but one which will require a nuanced understanding of dispersal, which was outside the scope of this study. Additionally, I only looked at the adult life stage of the alien conifers. I determined in Chapter 2 that I could only reliably detect the mid-to-large sized trees (adults) when using aerial imagery; therefore for this Chapter, I have missed most of the younger sizes and life stages of conifer trees. From a management perspective however, this is likely sufficient as we mainly are interested in the reproductive individuals since they are responsible for the current spread. Furthermore, the adult reproductive life stage inherently captures the results of density dependent

growth from previous life stages (Harte, 2011). Another limitation of this study is that I only examined infilling population growth, which is when a population spreads into areas within its existing range (L. A. V. Taylor et al., 2015; Warren et al., 2013). Infilling is important and understudied (L. E. Johnson, Brawley, & Adey, 2012), but this approach offers fewer insights about another key stage in conifer invasions, long-distance dispersal.

For the management of these invasions, my findings mean that current predictions of population growth (Ministry of Primary Industries, 2014) are too high, and the outlook of growth due to infilling is perhaps not as bleak as predicted. Additionally, the population growth parameters estimated for each site can help with projections of population growth and spread, especially since a study of this kind has not been done before in New Zealand. For future research on introduced conifers, this study also illustrates an appropriate scale to study conifer invasions. By accounting for dispersal and environmental heterogeneity at one-hectare sized plots, I was able to estimate meaningful population growth parameters for these invasions.

In the future it would be interesting to explicitly account for dispersal, and in particular directional dispersal as we know that wind-dispersed conifers tend to spread in the direction of the prevailing winds. Other studies estimating the STT have accounted for dispersal at a local scale but because their systems are not expanding or shrinking, they have assumed that dispersal is not relevant at regional scales (Benedetti-Cecchi et al., 2012; Melbourne & Chesson, 2006). Because I am studying an expanding system and dispersal is the key process of that expansion, I suspect that dispersal is relevant at regional scales for dynamic systems (Loreau, Mouquet, & Holt, 2003; Meynard et al., 2013). The model offers a simple representation of dispersal, and in the future it would be desirable to include a more mechanistic model of dispersal. By explicitly including dispersal in the population growth model, I likely would include more low density cells, causing the spatial variation in densities to decrease. Including more low density cells would also cause density independent growth to increase and density dependence decrease potentially. Therefore, I would expect that including long distance dispersal would cause the STT estimates to decrease, although probably only by a slight amount unless there were many long-distance dispersal areas. However, this needs to be studied further to test this hypothesis.

4.4.1 Conclusion

This study demonstrates that population growth data can be scaled up for broad scale systems which are rapidly changing over time. These findings, taken collectively with the findings of previous studies on the STT, have proven that the regional scale dynamics are indeed different from the local scale dynamics. To move the field forward, my methods presented in this chapter provide the techniques to properly scale up population growth. By accounting for the effect of spatial processes on population growth, we now can seek to better understand and study broad-scale phenomena.

4.5 References

Adams, T. P., Holland, E. P., Law, R., Plank, M. J., & Raghib, M. (2013). On the growth of locally interacting plants: Differential equations for the dynamics of spatial moments. *Ecology*, 94(12), 2732–2743. https://doi.org/10.1890/13-0147.1

Allen, T. F. H., & Hoekstra, T. W. (2015). *Toward a Unified Ecology* (Second ed.). New York: Columbia University Press.

Belmaker, J., Zarnetske, P., Tuanmu, M.-N., Zonneveld, S., Record, S., Strecker, A., & Beaudrot, L. (2015). Empirical evidence for the scale dependence of biotic interactions. *Global Ecology and Biogeography*, 24(7), 750–761. https://doi.org/10.1111/geb.12311

Benedetti-Cecchi, L., Tamburello, L., Bulleri, F., Maggi, E., Gennusa, V., & Miller, M. (2012). Linking patterns and processes across scales: The application of scale-transition theory to algal dynamics on rocky shores. *Journal of Experimental Biology*, 215(6), 977–985. https://doi.org/10.1242/jeb.058826

Bivand, R., Keitt, T., & Rowlingson, B. (2017). rgdal: Bindings for the Geospatial Data Abstraction Library. R package version 1.2-8. Retrieved from https://cran.r-project.org/package=rgdal

Brook, B. W., & Bradshaw, C. J. A. (2006). Strength of evidence for density dependence in abundance time series of 1198 species. *Ecology*, 87(6), 1445–1451. https://doi.org/10.1890/0012-9658(2006)87[1445:SOEFDD]2.0.CO;2

Buckley, Y. M., Brockerhoff, E., Langer, L., Ledgard, N. J., North, H., & Rees, M. (2005). Slowing down a pine invasion despite uncertainty in demography and dispersal. *Journal of Applied Ecology*, 42(6), 1020–1030. https://doi.org/10.1111/j.1365-2664.2005.01100.x

Caplat, P., Coutts, S., & Buckley, Y. M. (2012). Modeling population dynamics, landscape structure, and management decisions for controlling the spread of invasive plants. *Annals of the New York Academy of Sciences*, 1249(1), 72–83. https://doi.org/10.1111/j.1749-6632.2011.06313.x

Caplat, P., Nathan, R., & Buckley, Y. M. (2012). Seed terminal velocity, wind turbulence, and demography drive the spread of an invasive tree in an analytical model. *Ecology*, 93(2), 368–377. https://doi.org/10.1890/11-0820.1

Carrillo-Gavilán, M. A., & Vilà, M. (2010). Little evidence of invasion by alien conifers in Europe. *Diversity and Distributions*, 16(2), 203-213. https://doi.org/10.1111/j.1472-4642.2010.00648.x

Chave, J. (2013). The problem of pattern and scale in ecology: What have we learned in 20 years? *Ecology Letters*, 16(SUPPL.1), 4–16. https://doi.org/10.1111/ele.12048

Chesson, P. (2012). Scale transition theory: Its aims, motivations and predictions. *Ecological Complexity*, 10, 52–68. https://doi.org/10.1016/j.ecocom.2011.11.002

Chesson, P., Donahue, M. J., Melbourne, B. A., & Sears, A. L. W. (2005). Scale transition theory for understanding mechanisms in metacommunities. In M. Holyoak, M. A. Leibold, & R. D. Holt (Eds.), *Metacommunities: Spatial Dynamics and Ecological Communities* (pp. 279–306). Chicago: University of Chicago Press.

Cipriotti, P. A., Wiegand, T., Pütz, S., Bartoloni, N. J., & Paruelo, J. M. (2016). Nonparametric upscaling of stochastic simulation models using transition matrices. *Methods in Ecology and Evolution*, 7(3), 313–322. https://doi.org/10.1111/2041-210X.12464

Condit, R., Hubbell, S. P., & Foster, R. B. (1994). Density dependence in two understory tree species in a neotropical forest. *Ecology*, 75(3), 671–680.

Cousens, R., Dytham, C., & Law, R. (2008). *Dispersal in Plants: A Population Perspective*. Oxford, UK: Oxford University Press. https://doi.org/10.1093/acprof:oso/9780199299126.001.0001

de Valpine, P., Turek, D., Paciorek, C. J., Anderson-Bergman, C., Temple Lang, D., & Bodik, R. (2017). Programming with models: Writing statistical algorithms for general model structures with NIMBLE. *Journal of Computational and Graphical Statistics*, 26, 403–413.

Deng, S., Katoh, M., Yu, X., Hyyppä, J., & Gao, T. (2016). Comparison of tree species classifications at the individual tree level by combining ALS data and RGB images using different algorithms. *Remote Sensing*, 8(12), 1034. https://doi.org/10.3390/rs8121034

Dennis, B., Ponciano, J. M., Lele, S. R., Taper, M. L., & Staples, D. F. (2006). Estimating density dependence, process noise, and observation error. *Ecological Monographs*, 76(3), 323–341. https://doi.org/10.1890/0012-9615(2006)76[323:EDDPNA]2.0.CO;2

Dieckmann, U., Law, R., & Metz, J. A. J. (2000). *The Geometry of Ecological Interactions*. Cambridge Studies in Adaptive Dynamics (Vol. 1). Cambridge, United Kingdom: Cambridge University Press. https://doi.org/10.1017/CBO9780511525537

Dovčiak, M., Hrivnák, R., Ujházy, K., & Gömöry, D. (2014). Patterns of grassland invasions by trees: Insights from demographic and genetic spatial analyses. *Journal of Plant Ecology*, 8(5), 468–479. https://doi.org/10.1093/jpe/rtu038

Duncan, E. W., White, N. M., & Mengersen, K. (2017). Spatial smoothing in Bayesian models: A comparison of weights matrix specifications and their impact on inference. *International Journal of Health Geographics*, 16(1). https://doi.org/10.1186/s12942-017-0120-x

Elderd, B. D., & Miller, T. E. X. (2016). Quantifying demographic uncertainty: Bayesian methods for integral projection models. *Ecological Monographs*, 86(1), 125–144. https://doi.org/10.1890/15-1526.1

Englund, G., & Leonardsson, K. (2008). Scaling up the functional response for spatially heterogeneous systems. *Ecology Letters*, 11(5), 440–449. https://doi.org/10.1111/j.1461-0248.2008.01159.x

Estes, L., Elsen, P. R., Treuer, T., Ahmed, L., Caylor, K., Chang, J., Choi, J. J., & Ellis, E. C. (2018). The spatial and temporal domains of modern ecology. *Nature Ecology and Evolution*, 2(5), 819–826. https://doi.org/10.1038/s41559-018-0524-4

Gabry, J. (2018). shinystan: Interactive Visual and Numerical Diagnostics and Posterior Analysis for Bayesian Models. R Package Version 2.5.0. Retrieved from https://cran.r-project.org/package=shinystan

Gelman, A., Meng, X.-L., & Stern, H. (1996). Posterior predictive assessment of model fitness via realized discrepancies. *Statistica Sinica*, 6, 733–807. Retrieved from http://citeseer.ist.psu.edu/viewdoc/summary?doi=10.1.1.142.9951

Gunton, R. M., & Kunin, W. E. (2007). Density effects at multiple scales in an experimental plant population. *Journal of Ecology*, 95(3), 435–445. https://doi.org/10.1111/j.1365-2745.2007.01226.x

Gurevitch, J., Fox, G. A., Fowler, N. L., & Graham, C. H. (2016). Landscape demography: Population change and its drivers across spatial scales. *The Quarterly Review of Biology*, 91(4), 459–485. https://doi.org/10.1086/689560

Harte, J. (2011). *Maximum entropy and ecology: A theory of abundance, distribution, and energetics* (Oxford Series). Oxford, UK: Oxford University Press.

Hayward, J., Horton, T. R., Pauchard, A., & Nuñez, M. A. (2015). A single ectomycorrhizal fungal species can enable a *Pinus* invasion. *Ecology*, 96(5), 1438–1444. https://doi.org/10.1890/14-1100.1

Higgins, S. I., & Richardson, D. M. (1998). Pine invasions in the Southern Hemisphere: Modelling interactions between organism, environment and disturbance. *Plant Ecology*, 135(1), 79–93. https://doi.org/10.1023/A:1009760512895

Higgins, S. I., Richardson, D. M., & Cowling, R. M. (2001). Validation of a spatial simulation model of a spreading alien plant population. *Journal of Applied Ecology*, 38(3), 571–584. https://doi.org/10.1046/j.1365-2664.2001.00616.x

Hijmans, R. J. (2016). raster: Geographic Data Analysis and Modeling. R package version 2.5-8. Retrieved from https://cran.r-project.org/package=raster

Holt, G., & Chesson, P. (2016). Scale-dependent community theory for streams and other linear habitats. *The American Naturalist*, 188(3), E59–E73. https://doi.org/10.1086/687525

Hui, C., Fox, G. A., & Gurevitch, J. (2017). Scale-dependent portfolio effects explain growth inflation and volatility reduction in landscape demography. *Proceedings of the National Academy of Sciences*, 114(47), 12507-12511. https://doi.org/10.1073/pnas.1704213114

Johnson, D. J., Beaulieu, W. T., Bever, J. D., & Clay, K. (2012). Conspecific negative density dependence and forest diversity. *Science*, 336(6083), 904–907. https://doi.org/10.1126/science.1220269

Johnson, L. E., Brawley, S. H., & Adey, W. H. (2012). Secondary spread of invasive species: Historic patterns and underlying mechanisms of the continuing invasion of the European rockweed *Fucus serratus* in eastern North America. *Biological Invasions*, 14(1), 79–97. https://doi.org/10.1007/s10530-011-9976-z

Ke, Y., & Quackenbush, L. J. (2011). A review of methods for automatic individual tree-crown detection and delineation from passive remote sensing. *International Journal of Remote Sensing*, 32(17), 4725–4747. https://doi.org/10.1080/01431161.2010.494184

Komura, R., Kubo, M., & Muramoto, K. (2004). Delineation of tree crown in high resolution satellite image using circle expression and watershed algorithm. In Geoscience and Remote Sensing Symposium, 2004. IGARSS '04 (pp. 1577–1580). IEEE. https://doi.org/10.1109/IGARSS.2004.1370616

Langdon, B., Pauchard, A., & Aguayo, M. (2010). *Pinus contorta* invasion in the Chilean Patagonia: Local patterns in a global context. *Biological Invasions,* 12(12), 3961–3971. https://doi.org/10.1007/s10530-010-9817-5

Law, R., Dieckmann, U., & Metz, J. A. J. (2000). Introduction. In U. Dieckmann, R. Law, & J. A. J. Metz (Eds.), *The Geometry of Ecological Interactions: Simplifying Spatial* Complexity (pp. 1–6). Cambridge, United Kingdom: Cambridge University Press.

Law, R., Illian, J., Burslem, D. F. R. P., Gratzer, G., Gunatilleke, C. V. S., & Gunatilleke, I. A. U. N. (2009). Ecological information from spatial patterns of plants: Insights from point process theory. *Journal of Ecology*, 97(4), 616–628. https://doi.org/10.1111/j.1365-2745.2009.01510.x

Leibold, M. A., Holyoak, M., Mouquet, N., Amarasekare, P., Chase, J. M., Hoopes, M. F., Holt, R. D., Shurin, J. B., Law, R., Tilman, D., Loreau, M., & Gonzalez, A. (2004). The metacommunity concept: A framework for multi-scale community ecology. *Ecology Letters*, 7(7), 601-613. https://doi.org/10.1111/j.1461-0248.2004.00608.x

Levin, S. A. (1992). The problem of pattern and scale in ecology: The Robert H. MacArthur Award Lecture. *Ecology*, 73(6), 1943–1967. https://doi.org/doi:10.2307/1941447

Levin, S. A., Grenfell, B., Hastings, A., & Perelson, A. S. (1997). Mathematical and computational challenges in population biology and ecosystems science. *Science*, 275(5298), 334–343. https://doi.org/10.1126/science.275.5298.334

Link, W. A., & Eaton, M. J. (2012). On thinning of chains in MCMC. *Methods in Ecology and Evolution*, 3(1), 112–115. https://doi.org/10.1111/j.2041-210X.2011.00131.x

Loreau, M., Mouquet, N., & Holt, R. D. (2003). Meta-ecosystems: A theoretical framework for a spatial ecosystem ecology. *Ecology Letters*, 6(8), 673-679. https://doi.org/10.1046/j.1461-0248.2003.00483.x

Melbourne, B. A., & Chesson, P. (2005). Scaling up population dynamics: Integrating theory and data. *Oecologia*, 145(2), 179–187. https://doi.org/10.1007/s00442-005-0058-8

Melbourne, B. A., & Chesson, P. (2006). The scale transition: Scaling up population dynamics with field data. *Ecology*, 87(6), 1478–1488. https://doi.org/10.1890/0012-9658(2006)87[1478:TSTSUP]2.0.CO;2

Melbourne, B. A., Sears, A. L. W., Donahue, M. J., & Chesson, P. (2005). Applying scale transition theory to metacommunities in the field. In M. Holyoak, M. A. Leibold, & R. D. Holt (Eds.), *Metacommunities: Spatial Dynamics and Ecological Communities* (pp. 307–330). Chicago: University of Chicago Press.

Meynard, C. N., Lavergne, S., Boulangeat, I., Garraud, L., Van Es, J., Mouquet, N., & Thuiller, W. (2013). Disentangling the drivers of metacommunity structure across spatial scales. *Journal of Biogeography*, 40(8), 1560–1571. https://doi.org/10.1111/jbi.12116

Miller, J. R., Turner, M. G., Smithwick, E. A. H., Dent, C. L., & Stanley, E. H. (2004). Spatial extrapolation: The science of predicting ecological patterns and processes. *BioScience*, 54(4), 310. https://doi.org/10.1641/0006-3568(2004)054[0310:SETSOP]2.0.CO;2

Ministry of Primary Industries. (2014). The right tree in the right place: New Zealand wilding conifer management strategy 2015-2030. Retrieved from http://www.wildingconifers.org.nz/about-us/programme-2/the-national-wilding/

Morozov, A., & Poggiale, J. C. (2012). From spatially explicit ecological models to mean-field dynamics: The state of the art and perspectives. *Ecological Complexity*, 10, 1–11. https://doi.org/10.1016/j.ecocom.2012.04.001

Murrell, D. J., Purves, D. W., & Law, R. (2001). Uniting pattern and process in plant ecology. *Trends in Ecology and Evolution*, 16(10), 529–530. https://doi.org/10.1016/S0169-5347(01)02292-3

Nathan, R., & Muller-Landau, H. C. (2000). Spatial patterns of seed dispersal, their determinants and consequences for recruitment. *Trends in Ecology & Evolution*, 15(7), 278–285. https://doi.org/10.1016/S0169-5347(00)01874-7

Nuñez, M. A., Horton, T. R., & Simberloff, D. (2009). Lack of belowground mutualisms hinders Pinaceae invasions. *Ecology*, 90(9), 2352–2359. https://doi.org/10.1890/08-2139.1

Nuñez, M. A., & Paritsis, J. (2018). How are monospecific stands of invasive trees formed? Spatio-temporal evidence from Douglas fir invasions. *Annals of Botany Plants*, 10(4). https://doi.org/10.1093/aobpla/ply041

Pau, G., Fuchs, F., Sklyar, O., Boutros, M., & Huber, W. (2010). EBImage - an R package for image processing with applications to cellular phenotypes. *Bioinformatics*, 26(7), 979–981.

Pebesma, E. J., & Bivand, R. S. (2005). Classes and methods for spatial data in R. *R News*, 5(2), 1–21. Retrieved from https://cran.r-project.org/doc/Rnews/

Peters, H. A. (2003). Neighbour-regulated mortality: The influence of positive and negative density dependence on tree populations in species-rich tropical forests. *Ecology Letters*, 6(8), 757–765. https://doi.org/10.1046/j.1461-0248.2003.00492.x

Pettorelli, N., Laurance, W. F., O'Brien, T. G., Wegmann, M., Nagendra, H., & Turner, W. (2014). Satellite remote sensing for applied ecologists: Opportunities and challenges. *Journal of Applied Ecology*, 51(4), 839-848. https://doi.org/10.1111/1365-2664.12261

R Core Team. (2017). R: A language and environment for statistical computing. Vienna, Austria: R Foundation for Statistical Computing. Retrieved from https://www.r-project.org/

Rejmánek, M., & Richardson, D. M. (2013). Trees and shrubs as invasive alien species - 2013 update of the global database. *Diversity and Distributions*, 19(8), 1093–1094. https://doi.org/10.1111/ddi.12075

Richardson, D. M., & Bond, W. J. (1991). Determinants of plant distribution: Evidence from pine invasions. *The American Naturalist*, 137(5), 639–668. https://doi.org/10.1086/285186

Richardson, D. M., & Rejmánek, M. (2004). Conifers as invasive aliens: A global survey and predictive framework. *Diversity and Distributions*, 10(5–6), 321–331. https://doi.org/10.1111/j.1366-9516.2004.00096.x

Richardson, D. M., & Rejmánek, M. (2011). Trees and shrubs as invasive alien species - a global review. *Diversity and Distributions*, 17(5), 788–809. https://doi.org/10.1111/j.1472-4642.2011.00782.x

Rocchini, D., Boyd, D. S., Féret, J.-B., Foody, G. M., He, K. S., Lausch, A., Nagendra, H., Wegmann, M., & Pettorelli, N. (2015). Satellite remote sensing to monitor species diversity: Potential and pitfalls. *Remote Sensing in Ecology and Conservation*, 2(1), 25-36. https://doi.org/10.1002/rse2.9

Roy, C., McIntire, E. J. B., & Cumming, S. G. (2016). Assessing the spatial variability of density dependence in waterfowl populations. *Ecography*, 39(10), 942–953. https://doi.org/10.1111/ecog.01534

Salguero-Gómez, R., Jones, O. R., Archer, C. R., Buckley, Y. M., Che-Castaldo, J., Caswell, H., Hodgson, D., Scheuerlein, A., Conde, D.A., Brinks, E., de Buhr, H., Farack, C., Gottschalk, F., Hartmann, A., Henning A., Hoppe, G., Römer, G., Runge, J., Ruoff, T., Wille, J., Zeh, S., Davison, R., Vieregg, D., Baudisch, A., Altwegg, R., Colchero, F., Dong, M., de Kroon, H., Lebreton, J.-D., Metcalf, C. J. E., Neel, M. M., Parker, I. M., Takada, T., Valverde, T., Vélez-Espino, L. A., Wardle, G. M., Franco, M., & Vaupel, J. W. (2015). The Compadre Plant Matrix Database: An open online repository for plant demography. *Journal of Ecology*, 103(1), 202–218. https://doi.org/10.1111/1365-2745.12334

Sandel, B. (2015). Towards a taxonomy of spatial scale-dependence. *Ecography*, 38(4), 358–369. https://doi.org/10.1111/ecog.01034

Scholes, R. J. (2017). Taking the mumbo out of the jumbo: Progress towards a robust basis for ecological scaling. *Ecosystems*, 20(1), 4–13. https://doi.org/10.1007/s10021-016-0047-2

Steen, H., & Haydon, D. (2000). Can population growth rates vary with the spatial scale at which they are measured? *Journal of Animal Ecology*, 69(4), 659–671. https://doi.org/10.1046/j.1365-2656.2000.00424.x

Stoll, P., & Weiner, J. (2000). A neighborhood view of interactions among individual plants. In U. Dieckmann, R. Law, & J. A. J. Metz (Eds.), *The Geometry of Ecological Interactions: Simplifying Spatial Complexity* (pp. 11–27). Cambridge, United Kingdom: Cambridge University Press.

Taylor, K. T., Maxwell, B. D., Pauchard, A., Nuñez, M. A., Peltzer, D. A., Terwei, A., & Rew, L. J. (2016). Drivers of plant invasion vary globally: Evidence from pine invasions within six ecoregions. *Global Ecology and Biogeography*, 25(1), 96–106. https://doi.org/10.1111/geb.12391

Taylor, L. A. V., Hasenkopf, E. A., & Cruzan, M. B. (2015). Barriers to invasive infilling by *Brachypodium sylvaticum* in Pacific Northwest forests. *Biological Invasions*, 17(8), 2247–2260. https://doi.org/10.1007/s10530-015-0871-x

Thorson, J. T., Skaug, H. J., Kristensen, K., Shelton, A. O., Ward, E. J., Harms, J. H., & Benante, J. A. (2015). The importance of spatial models for estimating the strength of density dependence. *Ecology*, 96(5), 1202–1212. https://doi.org/10.1890/14-0739.1.sm

Tilman, D. (1994). Competition and biodiversity in spatially structured habitats. *Ecology*, 75(1), 2–16. https://doi.org/10.2307/1939377

Turner, M. G., & Gardner, R. H. (2015). *Landscape Ecology Theory and Practice: Pattern and Process* (2nd ed.). New York: Springer-Verlag.

Vehtari, A., Gelman, A., & Gabry, J. (2016). Practical Bayesian model evaluation using leave-one-out cross-validation and WAIC. *Statistics and Computing*, 1–20. https://doi.org/10.1007/s11222-016-9696-4

Wang, L., Gong, P., & Biging, G. S. (2004). Individual tree-crown delineation and treetop detection in high-spatial-resolution aerial imagery. *Photogrammetric Engineering & Remote Sensing*, 70(3), 351–357.

Warren, R. J., Ursell, T., Keiser, A. D., & Bradford, M. A. (2013). Habitat, dispersal and propagule pressure control exotic plant infilling within an invaded range. *Ecosphere*, 4(2). https://doi.org/10.1890/ES12-00393.1

Watanabe, S. (2010). Asymptotic equivalence of Bayes cross validation and widely applicable information criterion in singular learning theory. *Journal of Machine Learning Research*, 11, 3571–3594.

Wisz, M. S., Pottier, J., Kissling, W. D., Pellissier, L., Lenoir, J., Damgaard, C. F., Dormann, C. F., Forchhammer, M. C., Grytnes, J. A., Guisan, A., Heikkinen, R. K., Høye, T. T., Kühn, I., Luoto, M., Maiorano, L., Nilsson, M. C., Normand, S., Öckinger, E., Schmidt, N. M., Termansen, M., Timmermann, A., Wardle, D. A., Aastrup, P., & Svenning, J. C. (2013). The role of biotic interactions in shaping distributions and realised assemblages of species: Implications for species distribution modelling. *Biological Reviews*, 88(1), 15–30. https://doi.org/10.1111/j.1469-185X.2012.00235.x

Ying, Z., Liao, J., Wang, S., Lu, H., Liu, Y., Ma, L., & Li, Z. (2014). Species coexistence in a lattice-structured habitat: Effects of species dispersal and interactions. *Journal of Theoretical Biology*, 359, 184–191. https://doi.org/10.1016/j.jtbi.2014.05.048

Zenner, E. K., & Peck, J. L. E. (2018). Floating neighborhoods reveal contribution of individual trees to high sub-stand scale heterogeneity. *Forest Ecology and Management*, 412, 29–40. https://doi.org/10.1016/j.foreco.2018.01.054

Zhu, K., Woodall, C. W., Monteiro, J. V. D., & Clark, J. S. (2015). Prevalence and strength of density-dependent tree recruitment. *Ecology*, 96(9), 2319–2327. https://doi.org/10.1890/14-1780.1

Zhu, Y., Mi, X., Ren, H., & Ma, K. (2010). Density dependence is prevalent in a heterogeneous subtropical forest. *Oikos*, 119(1), 109–119. https://doi.org/10.1111/j.1600-0706.2009.17758.x

Chapter 5
Discussion

This thesis estimated the scale dependence of population growth for a rapidly changing system. Although previous studies have explored the scaling of population growth, no studies have yet explored the scaling of dynamic and expanding systems and nor have they gathered enough data to properly tackle this issue. This thesis addressed these shortcomings by using big data to examine the scaling of population growth. I gathered large datasets of population growth data over time for many sites and examined the limitations for using these data to enhance the robustness of the scaling methodology. In doing so, I tested how the biases in the data would influence the estimates of scaling up population growth data. Finally, I extended existing scaling methodology to unstable, expanding systems and found that spatial processes slowed down the population growth of alien conifer trees. These findings will be important not only for future work predicting the growth of invasive species, but also for studies examining the scaling of broad-scale phenomena.

5.1 Major findings of the thesis

5.1.1 Detection using aerial imagery contains biases from density (Chapter 2)

To examine the scaling of population growth over broad extents and for many sites, I gathered population data from aerial imagery. Aerial imagery had been used before to study plant population changes over time (see Mast et al. (1997), Roques et al. (2001), and Müllerová et al. (2013) for examples). However, robust assessments of the utility and complexity of using aerial imagery source of big data have previously been lacking. It was unclear what the detection limitations were for assessing the density, age structure, and spatial pattern for invasions. I found that aerial imagery was able to detect both the spatial pattern and distribution of trees with canopy diameters greater than 2.5m. However, it could only detect smaller trees with certainty where they were found at low density, thereby introducing a detection bias in the size of trees it could reliably detect. Additionally, I found that because aerial imagery could detect the mid-to-large sized trees consistently, then it could likely detect the majority of the coning trees. Therefore, while assessments of the overall age-structure will under-estimate the number of small trees, the number and spatial pattern of larger reproductive individuals can still be adequately captured.

5.1.2 Detection biases do not have a large effect on the scaling of population growth data (Chapter 3)

Since I found detection biases in the data, my next step was then to test whether the detection bias and observation error in the data acquired from aerial imagery would affect my estimates of scaling population growth. While errors in estimates of plant abundance are well-documented (see Chen et al.

(2013) and Ng and Driscoll (2015)), it was not known how these errors could propagate and affect the inferences about the scaling of population growth. I found that with a detection bias that over-estimated the number of trees at sparse densities, I could still accurately estimate the difference between local and regional scale population growth. However, this finding only held true when the error was low; therefore the accurate scaling of population growth will rely on low error rates below 5%.

5.1.3 Spatial processes significantly influence the scaling of population growth (Chapter 4)

Having proven the sufficiency and robustness of using big data, the final step in my thesis was to evaluate the effect of spatial processes on growth. The scaling method I used had only been tested before on stable systems (i.e., Melbourne and Chesson (2006) and Benedetti-Cecchi et al. (2012)), and none of the previous studies had statistically accounted for dispersal. I extended the methodology to apply to dynamic systems with local dispersal. I found that when we ignore spatial processes, we drastically over-estimate the population growth of alien conifers. Because of spatial processes from density, dispersal, and environmental heterogeneity, the difference between local and regional population growth is significant and sometimes large.

5.2 Contributions to scaling methodology

By expanding upon and validating the methodology of the Scale Transition Term (STT) theory in this thesis, I have provided useful tools (methodology and statistical code) to scale up the dynamics of populations between a fine plot-level scale to a broad landscape-level scale. The STT theory offered an alternative to existing scaling methods. Rather than relying on detailed life history data or only working for particular metapopulation structures (Cipriotti et al., 2016; Purves et al., 2007; Vance et al., 2010), the STT approach allowed me to use large datasets over broad extents to examine the scaling of population growth (Denny & Benedetti-Cecchi, 2012).

I extended the relevance of the STT method to be applicable for systems which are expanding due to localised dispersal. The STT method has only been used before for stable systems (i.e., (Benedetti-Cecchi et al., 2012; Melbourne & Chesson, 2006; Melbourne, Sears, Donahue, & Chesson, 2005)). It has been difficult to move past analyses of static systems because of technical challenges due to dispersal and complexity in the data attributed to being from an uncontrolled real-world environment. Since I examined a system that was expanding, I needed to account for the population growth due to dispersal. To do that, I developed the method to statistically account for localised dispersal in the population growth models. In developing this method further, I also was able to maximise the utility of using a large, complicated dataset of population growth data rather than using data collected from a controlled experiment. This extension of the STT method will enable it to be applied to a broad range of real-world systems in the future.

I tested the STT method with two different population growth models: the logistic growth equation in Chapter 3 and the Gompertz growth equation in Chapter 4. My results showed that the Gompertz model was better than the Logistic model because the Logistic model presented challenges with properly accounting for error in both the x and y variables. Additionally, the Gompertz equation could deal with error propagation better than the Logistic equation and it was straightforward to use in a Bayesian framework. In this thesis I did not incorporate error propagation into the population growth models in Chapter 4. There are opportunities to explicitly account for error in a Bayesian framework by incorporating error propagation in the future using a Bayesian hierarchical model with detection bias as a hyper-prior (similar to methods by Knape et al. (2013); Zipkin et al. (2014)). This would be a significant further advance but time kept me from following up on this insight in Chapter 4. Additionally, the case study results in Chapter 3 suggested that the detection bias found in the population estimates using aerial imagery data should not dramatically influence estimates of the STT. Therefore, I would not expect a large difference in the scaling estimates if I had incorporated error propagation in the models.

This study is the first of its kind to apply the STT theory to big data. Using my extensive collection of conifer invasion data for eight different populations over time, I have provided strong evidence that the STT method works for dynamic, expanding systems. Therefore, because I have both extended the STT method's relevance to unstable, rapidly changing systems and tested this method using real population growth data, I have contributed greatly to the population ecology field. Scaling population dynamics between a plot-level to a region-level is not only possible but it is now achievable and accessible for a wide range of systems.

5.3 Contributions to studies of broad-scale population dynamics

This thesis has profound implications for studies on broad scale population dynamics because it extends our knowledge of the uses of aerial imagery, broadens our understanding of spatial processes for dynamic systems, and provides avenues to access and use plot-scale data at a broad scale. Other studies have found that aerial imagery can be used to study population dynamics (see Franklin et al. (1985); Higgins et al. (2001); Müllerová et al. (2005)), and this thesis adds to the knowledge on the optimum use of these methods. Additionally, this thesis is the first study to have examined the ability and limitations of using aerial imagery to validate the scaling of population growth. Since I found that detection bias from using aerial imagery did not affect the scaling estimates, I postulate that we can use aerial imagery for population dynamics studies and to test scaling estimates. Furthermore, I was able to estimate the components of the STT accurately using aerial imagery and therefore this tool can be used to estimate the STT.

Beyond expanding upon existing methods to scale up population growth estimates, this thesis also extends our understanding of spatial processes from stable systems to dynamic ones. We now know that spatial processes derived from the effects of density, dispersal, and environmental heterogeneity

affect population growth for rapidly expanding systems. Therefore, instead of using the mean field to estimate the difference between local and regional population growth, studies of broad scale population dynamics will need to take these processes into account.

By using aerial imagery and examining multiple sites over time, this thesis also offers a first look at the consistency of scaling across sites and time. Since I found that the STT estimates were not consistent across sites, this means that spatial processes will affect scaling differently depending on the site. For the few sites which I had multiple time periods for, the STT was also not consistent, meaning that spatial processes are variable across time as well. While these results need to be replicated further, the findings of this thesis point to spatial processes being both important and variable in broad-scale systems.

Overall, the findings and methodology developments of this thesis will open doors for using more ecological data to study broad-scale phenomena. Many studies collect population growth data at fine spatial scales (i.e., less than one hectare) (Estes et al., 2018; Wheatley & Johnson, 2009). Now, ecologists can potentially scale up these fine-scale data to be relevant at the scale at which these phenomena operate. Using the methods in this thesis, studies on the population growth of species invasions can scale up their data to be relevant at broad spatial scales, allowing us to explore questions such as the drivers of species success/failure at regional scales (i.e., Early et al. (2016) and Yokomizo et al. (2017)).

5.4 Contributions to the management of alien conifer invasions

5.4.1 Aerial imagery and remote sensing data

The findings of this thesis also have specific relevance for the management and future study of alien conifer invasions, particularly relating to studying the population dynamics of conifer invasions. Since I found that we can use aerial imagery to detect mid- to large- sized mature trees, free imagery will be a boon for future work because it could be used to identify new populations and examine invasions at the landscape scale. Additionally, other studies have found that high-specification remote sensing imagery can detect alien conifers in mixed shrub habitats, making it suitable for use in complex environments (Dash, Pearse, Watt, & Paul, 2017). Due to my finding that aerial imagery can detect adult, mature trees, aerial imagery can be used for management purposes to prioritise areas where there are mature individuals and determine which control strategy to use based on the estimated density of trees (Department of Conservation, 2018).

Given that there are many invasion sites in grasslands in New Zealand and there is available aerial imagery over time, future studies can make use of these data to study the growth and spread of alien conifers in further detail. Future research could examine spatial patterns over time to determine the importance of clusters for spread, similar to work by Nuñez and Paritsis (2018). More work could be done to study the change in spatial structure over time, as this knowledge will help better inform

management to determine management priority areas and how spatial structure changes with invasion stage (Fletcher & Westcott, 2013; Jafari, Phillips, & Pardalos, 2018).

5.4.2 Importance of spatial processes

The findings of this thesis pointed to the importance of spatial processes on population growth. Therefore, when studying alien conifer invasions, we cannot forget the effects of density as well as dispersal and environmental heterogeneity on population growth. To date, few studies have quantified density dependence in alien conifer invasions at a population level. Since I found in this thesis that density dependence was significantly different from zero at every site examined, I have strong evidence that density dependence exists at a population level. Therefore, when the population growth and spread is modelled in the future, the effects of density on growth should be taken into account.

As a thought exercise examining the importance of spatial processes and specifically density dependence, I used the population growth parameters to predict what the growth of an invasion might be in the future. When I predicted the average growth within a one hectare area without accounting for density dependence, the growth would be exponential, increasing from 100 trees/ha to over 10,000 trees/ha after 10 years, represented by the green dashed line in Figure 5.1. However, when density dependence is accounted for but spatial processes such as dispersal and environmental heterogeneity are not considered, the growth of a moderately dense hectare of trees (100 trees/ha) would increase to about 430 trees/ha, represented by the blue solid line in Figure 5.1. Based on the findings of this thesis, if all broad-scale spatial processes were accounted for, then predictions of population growth likely would be less than the solid blue line.

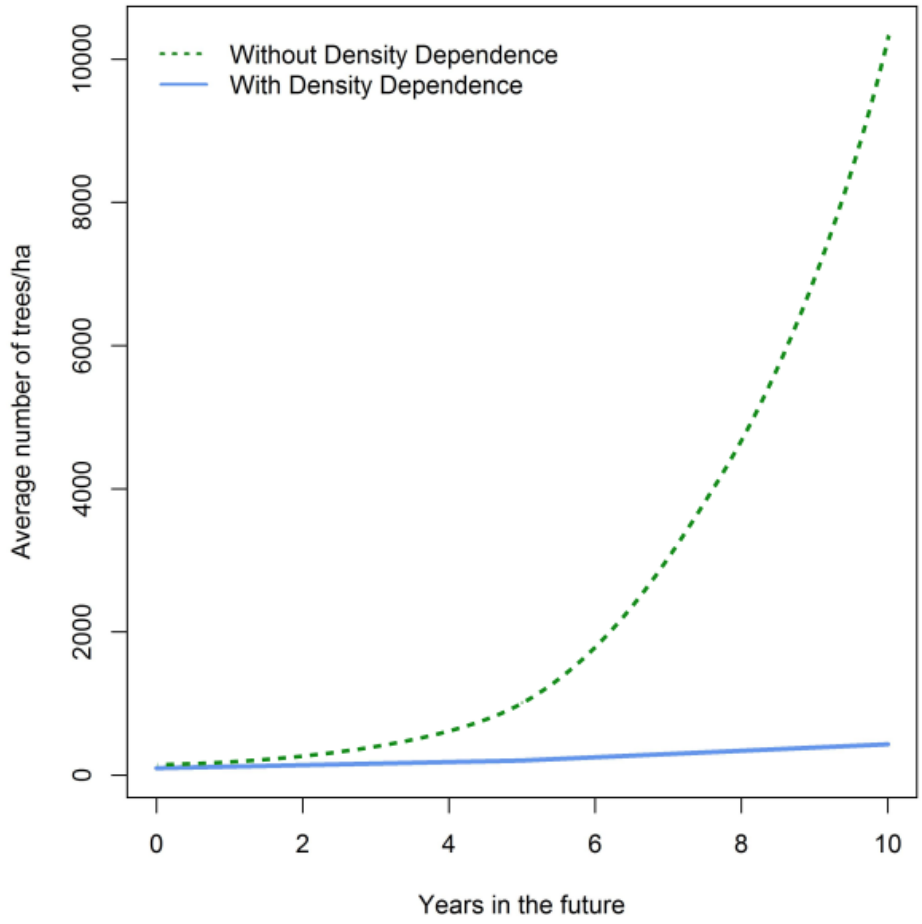

Figure 5.1 Approximate predictions of growth per hectare of moderately dense trees under two different modelling scenarios: one without accounting density dependence; and one accounting for density dependence (but not spatial processes such as dispersal).

Therefore, this thesis contributes greatly to our understanding of predicting the rate of population growth of conifer invasions. For management, these findings help strategize future areas of control because I found that density slows down growth. Using these findings, managers may decide to target sparse density areas before the dense areas because the growth of dense populations is slower.

Since I found that conifer populations are growing at a slower rate than expected due to density dependence and spatial processes, more work is needed to examine what this means for the areal spread of these populations. The Ministry of Primary Industries in New Zealand predicts that conifer invasions are expanding in area at a rate of 5% per year (Ministry of Primary Industries, 2014). Less area would be expected to be affected because the population growth is not as high as predicted, due to the findings of this thesis. More work is needed to connect the findings of the thesis on population growth with the predictions of areal spread to better inform where and how rapidly new areas will be invaded. Since I found that population growth depends on the surrounding density and environmental heterogeneity, future work could expand these findings to determine how management affects population growth. Would it be most effective to control an entire site rather than removing some

trees, lessening the density, and potentially increasing the growth rate? Extending the population growth models to examine what happens when some of the trees are removed would help to instruct how best to control an invading population.

For the management of conifer invasions, it would also be beneficial to examine how density dependence and intrinsic population growth vary across an invasion site and whether this variation changes with time. It has been hypothesised that density dependence is positive on the invasion front as evidence suggests that ectomycorrhizal fungi can facilitate the growth of individuals and even an invasion (Dickie, Bolstridge, Cooper, & Peltzer, 2010; Hayward, Horton, Pauchard, & Nuñez, 2015; Nuñez, Horton, & Simberloff, 2009). This would mean that the density of individuals on the edge of an invasion is enabling the spread and therefore should be targeted first for management. While I did not find evidence for positive density dependence, I did not estimate how density dependence varied spatially across the sites and therefore there could be strong density dependence overriding localised positive density dependence. Studying the variation in density dependence of an invasion would enable researchers to examine how this variation affects the spread patterns across a site (Walter, Johnson, & Haynes, 2017). Additionally, perhaps the intrinsic growth rate of conifers varies across a site depending on the suitability of habitats (Englert, Wells, & Norris, 2000; Thuiller et al., 2014). Again, this knowledge would assist management for identifying high priority areas for control since some areas could then spread faster than others. The work to address this suggested future research will build on the foundational findings of this thesis.

5.5 Limitations of this thesis

Although this thesis contributed greatly to methodologies for scaling up, studies on broad scale phenomena, and the management of wilding conifer invasions, it did have some limitations. The ground-truthing fieldwork in Chapter 2 was only done for one site even though in Chapter 4 I used aerial imagery for multiple sites without ground-truthing it. I therefore based my confidence in the detection ability of aerial and satellite imagery used for all sites on only one site. The surrounding vegetation was very similar across all sites (all sites had low-lying tussocks and grasses as the background vegetation), making it likely that my findings from the one site would be similar across all sites. However, if I repeated this study again, I would complete ground-truthing fieldwork at more than one site and at sites with different conifer species present. Additionally, another limitation is that I only used aerial imagery in this thesis, meaning that I used a low-specification type of remote sensing data. This limited my ability to detect smaller trees as well as differentiate between species. While this did not greatly detract from this thesis, in the future other types of imagery and remote sensing data should be explored for their relevance to population growth studies. Further on this point, using aerial and satellite imagery limited this thesis to only examining the population growth of adult trees. Using high specification imagery may allow for the detection and inclusion of saplings in future studies of conifer population growth. Finally, I only examined sites which were at a mid-to-late

invasion stage, making the findings potentially only valid for these stages. In the future, I would recommend expanding this study to include early invasion sites and compare my assessments of aerial imagery and estimates of STT across invasion stages.

5.6 Future directions

This research has opened many avenues of future invasion research as well as work in broad-scale systems. While this thesis examined how detection ability and detection bias/error could affect the scaling of population growth, in the future it would be interesting to examine how landscape factors such as topography or landscape connectivity could affect population growth across spatial scales (extending research such as Morel-Journel et al. (2018)). To examine the effect of topography, a detailed Digital Elevation Model (DEM) could be used and elevation over an invasion site could be added as a variable in the population growth models (Walter et al., 2015). Environmental factors such as land use could be added to the population growth model as well to determine how land use affects the growth of populations across an area (Brown, Spector, & Wu, 2008; Theoharides & Dukes, 2007). By explicitly accounting for environmental heterogeneity, these assessments would allow researchers to examine the varied effects of abiotic factors on localised growth while teasing apart the biotic factors of density dependence as well. Some of the next steps of invasion science are understanding the complexities of abiotic and biotic factors and how they affect spatial spread of invasions (Grayson & Johnson, 2018).

In the future, it would also be interesting to examine the scaling of systems with different dispersal methods such as bird or mammal dispersal of seeds (extending work such as Ramaswami et al. (2016) and García et al. (2017)). This would allow us to determine whether the assumption of the mean field growth holds for dynamic systems expanding via other dispersal types. I would hypothesize that systems which are expanding via bird or mammal dispersal could differ greatly from the mean field estimate, although in a different way than systems expanding via passive dispersal. It is likely that bird dispersal causes positive density dependence because dense areas attract more birds (Spiegel & Nathan, 2012). Therefore, when scaling up population growth of bird/mammal dispersed from a plot scale to a regional scale, the mean field growth may be less than what the regional growth rate truly is.

Additionally, the work in this thesis could be extended by connecting population growth at a regional scale to an individual plant scale, following methods suggested by Chesson et al. (2005). Related to this extension, it would be interesting to pursue the connection between the methodology of Chesson et al. (2005) used in this thesis and the spatial moment methods used by Bolker and Pacala (1997) and Law et al. (2003). Connecting these methods would enable researchers to examine how spatial processes affect population growth across time and at a finer scale than what was examined in this thesis. This would allow for further insights into demographic processes affecting growth across spatial and temporal scales and would likely improve the ability to predict population growth into the future.

5.7 Conclusions

In one of the seminal works in ecology, Levin noted that the scaling of population growth would be one of the largest issues facing ecologists (Levin, 1992). This paper led to many studies recognising the importance of spatial scale in ecology and changed the way ecologists interpret pattern and scale (Chave, 2013). My thesis accepts the challenge of spatial scale and pushes the boundaries of our knowledge of scaling population growth. Not only does this thesis improve existing methodology to scale up population growth data, but this thesis also explores the limitations and consequences of using large-scale data when scaling population parameter estimates. Furthermore, I found that spatial processes have a large effect on population growth in dynamic systems, thereby dramatically influencing estimates across spatial scales. These findings will thus alter the way that population growth is studied across scales.

5.8 References

Benedetti-Cecchi, L., Tamburello, L., Bulleri, F., Maggi, E., Gennusa, V., & Miller, M. (2012). Linking patterns and processes across scales: The application of scale-transition theory to algal dynamics on rocky shores. *Journal of Experimental Biology*, 215(6), 977–985. https://doi.org/10.1242/jeb.058826

Bolker, B. M., & Pacala, S. W. (1997). Using moment equations to understand stochastically driven spatial pattern formation in ecological systems. *Theoretical Population Biology*, 52(3), 179–197. https://doi.org/10.1006/tpbi.1997.1331

Brown, K. A., Spector, S., & Wu, W. (2008). Multi-scale analysis of species introductions: Combining landscape and demographic models to improve management decisions about non-native species. *Journal of Applied Ecology*, 45(6), 1639–1648. https://doi.org/10.1111/j.1365-2664.2008.01550.x

Chave, J. (2013). The problem of pattern and scale in ecology: What have we learned in 20 years? *Ecology Letters*, 16(SUPPL.1), 4–16. https://doi.org/10.1111/ele.12048

Chen, G., Kéry, M., Plattner, M., Ma, K., & Gardner, B. (2013). Imperfect detection is the rule rather than the exception in plant distribution studies. *Journal of Ecology*, 101(1), 183–191. https://doi.org/10.1111/1365-2745.12021

Chesson, P., Donahue, M. J., Melbourne, B. A., & Sears, A. L. W. (2005). Scale transition theory for understanding mechanisms in metacommunities. In M. Holyoak, M. A. Leibold, & R. D. Holt (Eds.), *Metacommunities: Spatial Dynamics and Ecological Communities* (pp. 279–306). Chicago: University of Chicago Press.

Cipriotti, P. A., Wiegand, T., Pütz, S., Bartoloni, N. J., & Paruelo, J. M. (2016). Nonparametric upscaling of stochastic simulation models using transition matrices. *Methods in Ecology and Evolution*, 7(3), 313–322. https://doi.org/10.1111/2041-210X.12464

Dash, J. P., Pearse, G. D., Watt, M. S., & Paul, T. (2017). Combining airborne laser scanning and aerial imagery enhances echo classification for invasive conifer detection. *Remote Sensing*, 9(2), 156. https://doi.org/10.3390/rs9020156

Denny, M., & Benedetti-Cecchi, L. (2012). Scaling up in ecology: Mechanistic approaches. *Annual Review of Ecology, Evolution, and Systematics*, 43(1), 1–22. https://doi.org/10.1146/annurev-ecolsys-102710-145103

Department of Conservation. (2018). Methods of control for wilding conifers. Retrieved July 23, 2018, from https://www.doc.govt.nz/nature/pests-and-threats/common-weeds/wilding-conifers/methods-of-control/

Dickie, I. A., Bolstridge, N., Cooper, J. A., & Peltzer, D. A. (2010). Co-invasion by *Pinus* and its mycorrhizal fungi. *New Phytologist*, 187(2), 475–484. https://doi.org/10.1111/j.1469-8137.2010.03277.x

Early, R., Bradley, B. A., Dukes, J. S., Lawler, J. J., Olden, J. D., Blumenthal, D. M., Gonzalez, P., Grosholz, E. D., Ibañez, I., Miller, L. P., Sorte, C. J. B., & Tatem, A. J. (2016). Global threats from invasive alien species in the twenty-first century and national response capacities. *Nature Communications,* 7(12485). https://doi.org/10.1038/ncomms12485

Englert, T. L., Wells, A. W., & Norris, R. A. (2000). Incorporation of changes in habitat quantity and quality into density-dependent population models. *Environmental Science & Policy*, 3(Supplement 1), 451–458. https://doi.org/10.1016/S1462-9011(00)00057-5

Estes, L., Elsen, P. R., Treuer, T., Ahmed, L., Caylor, K., Chang, J., Choi, J. J., & Ellis, E. C. (2018). The spatial and temporal domains of modern ecology. *Nature Ecology and Evolution*, 2(5), 819–826. https://doi.org/10.1038/s41559-018-0524-4

Fletcher, C. S., & Westcott, D. A. (2013). Dispersal and the design of effective management strategies for plant invasions: Matching scales for success. *Ecological Applications*, 23(8), 1881–1892. https://doi.org/10.1890/12-2059.1

Franklin, J., Michaelsen, J., Strahler, A. H., & Barbara, S. (1985). Spatial analysis of density dependent pattern in coniferous forest stands. *Vegetatio*, 64, 29–36. https://doi.org/10.1007/BF00033451

García, C., Klein, E. K., & Jordano, P. (2017). Dispersal processes driving plant movement: Challenges for understanding and predicting range shifts in a changing world. *Journal of Ecology*, 105(1), 1–5. https://doi.org/10.1111/1365-2745.12705

Grayson, K. L., & Johnson, D. M. (2018). Novel insights on population and range edge dynamics using an unparalleled spatiotemporal record of species invasion. *Journal of Animal Ecology*, 87(3), 581–593. https://doi.org/10.1111/1365-2656.12755

Hayward, J., Horton, T. R., Pauchard, A., & Nuñez, M. A. (2015). A single ectomycorrhizal fungal species can enable a *Pinus* invasion. *Ecology*, 96(5), 1438–1444. https://doi.org/10.1890/14-1100.1

Higgins, S. I., Richardson, D. M., & Cowling, R. M. (2001). Validation of a spatial simulation model of a spreading alien plant population. *Journal of Applied Ecology*, 38(3), 571–584. https://doi.org/10.1046/j.1365-2664.2001.00616.x

Jafari, N., Phillips, A., & Pardalos, P. M. (2018). A robust optimization model for an invasive species management problem. *Environmental Monitoring and Assessment*, 1–10. https://doi.org/10.1007/s10666-018-9631-5

Knape, J., Besbeas, P., & de Valpine, P. (2013). Using uncertainty estimates in analyses of population time series. *Ecology*, 94(9), 2097–2107. https://doi.org/10.1890/12-0712.1

Law, R., Murrell, D. J., & Dieckmann, U. (2003). Population growth in space and time: Spatial logistic equations. *Ecology*, 84(1), 252–262. https://doi.org/10.1890/0012-9658(2003)084[0252:PGISAT]2.0.CO;2

Levin, S. A. (1992). The problem of pattern and scale in ecology: The Robert H. MacArthur Award Lecture. *Ecology*, 73(6), 1943–1967. https://doi.org/doi:10.2307/1941447

Mast, J. N., Veblen, T. T., & Hodgson, M. E. (1997). Tree invasion within a pine/grassland ecotone: An approach with historic aerial photography and GIS modeling. *Forest Ecology and Management*, 93(3), 181–194. https://doi.org/10.1016/S0378-1127(96)03954-0

Melbourne, B. A., & Chesson, P. (2006). The scale transition: Scaling up population dynamics with field data. *Ecology*, 87(6), 1478–1488. https://doi.org/10.1890/0012-9658(2006)87[1478:TSTSUP]2.0.CO;2

Melbourne, B. A., Sears, A. L. W., Donahue, M. J., & Chesson, P. (2005). Applying scale transition theory to metacommunities in the field. In M. Holyoak, M. A. Leibold, & R. D. Holt (Eds.), *Metacommunities: Spatial Dynamics and Ecological Communities* (pp. 307–330). Chicago: University of Chicago Press.

Ministry of Primary Industries. (2014). The right tree in the right place: New Zealand wilding conifer management strategy 2015-2030. Retrieved from http://www.wildingconifers.org.nz/about-us/programme-2/the-national-wilding/

Morel-Journel, T., Hautier, M., Vercken, E., & Mailleret, L. (2018). Clustered or scattered? The impact of habitat quality clustering on establishment and early spread. *Ecography*, 41(10), 1675-1683. https://doi.org/10.1111/ecog.03397

Müllerová, J., Pergl, J., & Pyšek, P. (2013). Remote sensing as a tool for monitoring plant invasions: Testing the effects of data resolution and image classification approach on the detection of a model plant species *Heracleum mantegazzianum* (giant hogweed). *International Journal of Applied Earth Observations and Geoinformation*, 25, 55–65. https://doi.org/10.1016/j.jag.2013.03.004

Müllerová, J., Pyšek, P., Jarošík, V., & Pergl, J. (2005). Aerial photographs as a tool for assessing the regional dynamics of the invasive plant species *Heracleum mantegazzianum*. *Journal of Applied Ecology*, 42(6), 1042–1053. https://doi.org/10.1111/j.1365-2664.2005.01092.x

Ng, K., & Driscoll, D. A. (2015). Detectability of the global weed *Hypochaeris radicata* is influenced by species, environment and observer characteristics. *Journal of Plant Ecology*, 8(4), 449–455. https://doi.org/10.1093/jpe/rtu032

Nuñez, M. A., Horton, T. R., & Simberloff, D. (2009). Lack of belowground mutualisms hinders Pinaceae invasions. *Ecology*, 90(9), 2352–2359. https://doi.org/10.1890/08-2139.1

Nuñez, M. A., & Paritsis, J. (2018). How are monospecific stands of invasive trees formed? Spatio-temporal evidence from Douglas fir invasions. *Annals of Botany Plants*, 10(4). https://doi.org/10.1093/aobpla/ply041

Purves, D. W., Zavala, M. A., Ogle, K., Prieto, F., & Rey Benayas, J. M. (2007). Environmental heterogeneity, bird-mediated directed dispersal, and oak woodland dynamics in Mediterranean Spain. *Ecological Monographs*, 77(1), 77–97. https://doi.org/10.1890/05-1923

Ramaswami, G., Kaushik, M., Prasad, S., Sukumar, R., & Westcott, D. (2016). Dispersal by generalist frugivores affects management of an invasive plant. *Biotropica*, 48(5), 638–644. https://doi.org/10.1111/btp.12343

Roques, K. G., O'Connor, T. G., & Watkinson, A. R. (2001). Dynamics of shrub encroachment in an African savanna: Relative influences of fire, herbivory, rainfall and density dependence. *Journal of Applied Ecology*, 38(2), 268–280. https://doi.org/10.1046/j.1365-2664.2001.00567.x

Spiegel, O., & Nathan, R. (2012). Empirical evaluation of directed dispersal and density-dependent effects across successive recruitment phases. *Journal of Ecology*, 100(2), 392–404. https://doi.org/10.1111/j.1365-2745.2011.01886.x

Theoharides, K. A., & Dukes, J. S. (2007). Plant invasion across space and time: Factors affecting nonindigenous species success during four stages of invasion. *New Phytologist*, 176(2), 256–273. https://doi.org/10.1111/j.1469-8137.2007.02207.x

Thuiller, W., Münkemüller, T., Schiffers, K. H., Georges, D., Dullinger, S., Eckhart, V. M., Edwards Jr, T. C., Gravel, D., Kunstler, G., Merow, C., Moore, K., Piedallu, C., Vissault, S., Zimmermann, N. E., Zurell, D., & Schurr, F. M. (2014). Does probability of occurrence relate to population dynamics? *Ecography*, 37(12), 1155–1166. https://doi.org/10.1111/ecog.00836

Vance, R. R., Steele, M. A., & Forrester, G. E. (2010). Using an individual-based model to quantify scale transition in demographic rate functions: Deaths in a coral reef fish. *Ecological Modelling*, 221(16), 1907–1921. https://doi.org/10.1016/j.ecolmodel.2010.04.014

Walter, J. A., Johnson, D. M., & Haynes, K. J. (2017). Spatial variation in Allee effects influences patterns of range expansion. *Ecography*, 40(1), 179–188. https://doi.org/10.1111/ecog.01951

Walter, J. A., Meixler, M. S., Mueller, T., Fagan, W. F., Tobin, P. C., & Haynes, K. J. (2015). How topography induces reproductive asynchrony and alters gypsy moth invasion dynamics. *Journal of Animal Ecology*, 84(1), 188–198. https://doi.org/10.1111/1365-2656.12272

Wheatley, M., & Johnson, C. (2009). Factors limiting our understanding of ecological scale. *Ecological Complexity*, 6(2), 150-159. https://doi.org/10.1016/j.ecocom.2008.10.011

Yokomizo, H., Takada, T., Fukaya, K., & Lambrinos, J. G. (2017). The influence of time since introduction on the population growth of introduced species and the consequences for management. *Population Ecology*, 59(2), 89–97. https://doi.org/10.1007/s10144-017-0581-6

Zipkin, E. F., Sillett, T. S., Grant, E. H. C., Chandler, R. B., & Royle, J. A. (2014). Inferences about population dynamics from count data using multistate models: A comparison to capture-recapture approaches. *Ecology and Evolution*, 4(4), 417–426. https://doi.org/10.1002/ece3.942

Appendix A

Linear regressions in Chapter 2

A.1 Slope and intercept values from linear regressions

In Chapter 2, linear regressions were done to examine how detection changed with density of trees of different canopy diameters. Table A1 shows the slope and intercept values from these regressions. The p-values are from the one-sample t-tests comparing the slopes and intercepts to the null expectation of one and zero, respectively. The bolded slope values represent values which are not significantly different from one, meaning that the detection of densities using aerial imagery is not significantly different from the densities measured in the field. All of the intercept values were significantly different from zero, meaning that aerial imagery consistently over-estimated the number of trees in sparse densities.

Table A1 Slopes and intercepts of regression lines for different tree canopy diameter groups (± 95% Confidence Intervals).

Canopy Diameter	Slope of regression line	Intercept of regression line
> 1m	0.41 ± 0.10 (p-value = 3.4×10^{-12})	206 ± 112 (p-value = 0.0010)
> 1.5m	0.61 ± 0.13 (p-value = 1.6×10^{-6})	206 ± 102 (p-value = 3.3×10^{-4})
> 2m	0.71 ± 0.18 (p-value = 0.0039)	259 ± 114 (p-value = 1.3×10^{-4})
> 2.5m	**0.88 ± 0.22** (p-value = 0.28)	266 ± 112 (p-value = 7.0×10^{-5})
> 3m	**1.11 ± 0.31** (p-value = 0.513)	266 ±125 (p-value = 2.7×10^{-4})

Appendix B

Solving for the analytic solution in Chapter 3

In Chapter 3, I calculated and examined the results from analytic solutions which included detection bias but not observation error. In this Appendix, I will show how I solved for the analytic solution for the components of the difference between local and regional growth (density dependence and variance of densities) and the difference itself.

B.1 Detection bias in density dependence term

I will start by going back to Equation 3.3 in Chapter 3 which I used to estimate population growth.

$$N_{t+1,i} = (1 + r)N_{t,i} + aN_{t,i}^2 \qquad \text{(Equation 3.3, from Chapter 3)}$$

Substituting biased observations of densities into the N_t and N_{t+1} terms, the equation becomes:

$$N_{t+1,biased} = (1 + r)N_{t,biased} + aN_{t,biased}^2 \qquad \text{(Equation B1)}$$

I know from Equation 3.4 in Chapter 3 that $N_{biased} = (slope)\ N_{true} + intercept$, so I plug this into Equation B1. Equation B1 then becomes:

$$\begin{aligned}(N_{t+1,true}(slope) + intercept) \\ = (N_{t,true}(slope) + intercept) + r(N_{t,true}(slope) + intercept) \\ + a(N_{t,true}(slope) + intercept)^2\end{aligned}$$

Next I multiplied everything out, and the equation becomes:

$$\begin{aligned}(N_{t+1,true}(slope) + intercept) \\ = (N_{t,true}(slope) + intercept) + rN_{t,true}(slope) + r(intercept) \\ + aN_{t,true}{}^2(slope^2) + 2a(slope)(intercept)N_{t,true} + a(intercept^2)\end{aligned}$$

Then I isolated $N_{t+1,\,true}$ on left side of the equation:

$$(N_{t+1,true}(slope)) = N_{t,true}(slope) + rN_{t,true}(slope) + r(intercept) + aN_{t,true}{}^2(slope^2) + 2a(slope)(intercept)N_{t,true} + a(intercept^2)$$

$$N_{t+1,true} = \overbrace{N_{t,true}(1 + r + 2a(intercept))}^{bias\ in\ r} + \overbrace{a(slope)N_{t,true}{}^2}^{bias\ in\ a} + \underbrace{r\left(\frac{intercept}{slope}\right) + a(intercept^2)/slope}_{bias\ in\ intercept}$$

The '*bias in a'* component of the equation represents the bias in the density dependence term. Therefore the biased density dependence term equals the true density dependence divided by the *slope* term.

B.2 Detection bias in variance of densities term

I will start with substituting the equation for $N_{t,\,bias}$ into $Var(N_t)$.

$$Var(N_{t,bias}) = Var(N_{t,true}(slope) + intercept)$$

From identities of the variance function (Ross, 2010), I found that the intercept term disappears and the variance function becomes:

$$Var(N_{t,bias}) = (slope^2)Var(N_{t,true})$$

Therefore the biased variance in densities term equals the true variance in densities multiplied by the *slope* term squared.

B.3 Detection bias in the difference between local and regional population growth

To determine the bias in the difference between local and regional population growth, I will plug in the analytic solutions of bias in the components.

$$Difference_{biased} = -(a_{biased} Var(N_{t,biased}))$$

$$Difference_{biased} = -{}^{a_{true}}/_{slope} \ (slope^2 Var(N_{t,true}))$$

This results in:

$$Difference_{biased} = -(slope) \underbrace{(a_{true} Var(N_{t,true}))}_{true\ parameter\ of\ Difference}$$

Therefore the biased difference between local and regional population growth differs from the true difference by a factor of the *slope* term.

Appendix C

Results from one sample t-tests of density dependence and variance of initial densities in Chapter 3

In Chapter 3, the simulation results were compared to the analytic results. Tables C1 and C2 show these results comparing the simulation and analytic values for the density dependence and variance in densities terms. The analytic values represent the results with detection bias but not observation error. The simulation values represent the results with both detection bias and observation error. I compared these values for when the slope changed and the intercept term was held constant and again when the intercept changed but the slope term was held constant. I did this to test the effects of detection bias from the slope or intercept term.

Table C1 Values of density dependence with changing slope and intercept values from the analytic results and the simulated estimates. When estimating density dependence for changing slope values, a constant value of 4 was used for the intercept value. When estimating density dependence for changing intercept values, a constant value of 0.5 was used for the slope. Asterisks indicate significance from one-sample t-tests.

Slope values	Analytic :: Simulation values of density dependence (± standard deviation)	Intercept value	Analytic :: Simulation values of density dependence (± standard deviation)
0.4	-0.025 :: -0.016 ± 0.009 ***	-4	-0.020 :: -0.015 ± 0.0066 ***
0.6	-0.017 :: -0.014 ± 0.0039 ***	0	-0.020 :: -0.015 ± 0.0056 ***
0.8	-0.013 :: -0.011 ± 0.0026 ***	4	-0.020 :: -0.015 ± 0.0061 ***
1.0	-0.010 :: -0.094 ± 0.0019 **	8	-0.020 :: -0.015 ± 0.0054 ***
1.2	-0.0083 :: -0.0079 ± 0.0013 **	12	-0.020 :: -0.014 ± 0.0059 ***

In Table C1, as the slope values increased, both the analytic and simulation results increased. As the intercept term increased, the analytic and simulation results held constant. This means that when there is detection bias, the slope term influences the values of density dependence, but the intercept term does not.

The simulation results were slightly higher than the analytic results, meaning that observation error tended to slightly increase the values for density dependence. As indicated by the asterisks in Table C1, the difference between the analytic and simulation results was always significant, no matter the value of the slope or intercept terms.

Table C2 Values of variance of initial densities with changing slope and intercept values from the analytic results and the simulated estimates. When estimating the variance for changing slope values, a constant value of 4 was used for the intercept value. When estimating the variance for changing intercept values, a constant value of 0.5 was used for the slope. Asterisks indicate significance from one-sample t-tests.

Slope values	Analytic :: Simulation values of variance(N) (± standard deviation)	Intercept value	Analytic :: Simulation values of variance(N) (± standard deviation)
0.4	82.70 :: 41.05 ± 6.4 ***	-4	51.68 :: 60.90 ± 9.14 ***
0.6	124.04 :: 83.76 ± 12.0 **	0	51.68 :: 60.34 ± 9.13 ***
0.8	165.39 :: 141.18 ± 21.1 ***	4	51.68 :: 60.65 ± 9.22 ***
1.0	206.74 :: 215.16 ± 31.1 **	8	51.68 :: 60.81 ± 8.59 ***
1.2	248.09 :: 306.59 ± 44.5 **	12	51.68 :: 60.56 ± 8.65 ***

In Table C2, as the slope values increased, both the analytic and simulation results of variance increased. As the intercept term increased, the analytic and simulation results held constant. This means that when there is detection bias, the slope term influences the values of the variance, but the intercept term does not.

When the slope values increased, the simulation results switched from being lower than the analytic results to then being higher than them after the slope increased above a value of one. This means that observation error affected the values for the variance of densities differently depending on whether the slope was less than or greater than one. When the intercept values increased, the simulation results were higher than the analytic results, meaning that the observation error tended to increase the value of the variance. As indicated by the asterisks in Table C2, the difference between the analytic and simulation results was always significant, no matter the value of the slope or intercept terms.

Appendix D
Results of Case Study in Chapter 3

In the case study examined in Chapter 3, I used the same values of the slope and intercept of the detection bias equations as found in the linear regressions for the tree canopy size threshold groups in Chapter 2. Using these values, I estimated the biased difference between local and regional population growth excluding and including observation error for different canopy sizes. I compared these results to the calculated unbiased values of the difference between local and regional population growth (Table D1).

Table D1 Size thresholds and unbiased, analytic, and biased values of the difference between local and regional population growth.

Size threshold and detection bias	Unbiased estimate of difference between local and regional population growth (from fieldwork data)	Analytic result of difference between local and regional population growth	Biased estimate of the difference between local and regional population growth (from the aerial imagery data)	Residual Standard Error from linear regression
Trees >1m $N_{bias} = 0.41 * N + 8.8 + \varepsilon_1$	-9.05	-3.71	-2.45	9.083
Trees >1.5m $N_{bias} = 0.61 * N + 8.8 + \varepsilon_2$	-4.43	-2.70	-1.66	7.362
Trees >2m $N_{bias} = 0.71 * N + 11 + \varepsilon_3$	-2.76	-1.96	-1.43	7.943
Trees >2.5m $N_{bias} = 0.88 * N + 11.2 + \varepsilon_4$	-1.801	-1.58	-1.26	7.895
Trees >3m $N_{bias} = 1.1 * N + 11.4 + \varepsilon_5$	-1.10	-1.21	-1.42	8.412

The analytic values in Table D1 represent the effect of detection bias but not observation error on the estimate of the difference between local and regional growth. When the slope of the detection bias was less than one (i.e., for size thresholds of >1m, >1.5m, >2m, and >2.5m), the analytic results were higher than the unbiased values. The biased values of the difference between local and regional growth include both detection bias and observation error, and they represent the values estimated by the aerial imagery data. Similar to the analytic results, when the slope of the detection bias was less than one, the biased results were higher than the unbiased values.

Appendix E

Site Information and Imagery Data for Chapter 4

In Chapter 4, I used imagery data from eight invasion sites for 2-4 time steps. Here I have listed the imagery specifications for each site and time step (Table E1). I also showed the imagery photos for each site as well to demonstrate each site's unique features and location. For each site, I listed the known conifer species present and whether there is any management happening in these areas.

E.1 Site and Imagery specifications

Table E1 Imagery specifications for each site and time step.

Site	Imagery Source	Date Imagery Captured	Pixel Size (m)	Latitude/ Longitude coordinates	Occupied Area (ha)	Number of Trees Detected
Ohau	Google Earth	2011 (4 September)	1	-44.258 / 169.972	515	7,685
Ohau	LINZ	2014 (4 February)	0.4	-44.258 / 169.972	594	28,798
Mt Barker	Google Earth	2010 (18 February)	1	-43.357 / 171.610	484	101,864
Mt Barker	LINZ	2016 (10 April)	0.3	-43.357 / 171.610	598	209,472
S. Pukaki	Google Earth	2006 (11 April)	0.57	-44.207 / 170.136	233	13,523
S. Pukaki	LINZ	2008 (19 March)	0.75	-44.207 / 170.136	230	29,309
S. Pukaki	LINZ	2014 (20 February)	0.4	-44.207 / 170.136	285	59,504
S. Pukaki	Google Earth	2016 (9 April)	0.71	-44.207 / 170.136	330	89,651
Shelterbelt W.	LINZ	2006 (31 March)	0.75	-44.188 / 170.038	24	3,708
Shelterbelt W.	Google Earth	2010 (7 March)	0.4	-44.188 / 170.038	37	5,071
Shelterbelt E.	LINZ	2008 (19 March)	0.75	-44.195 / 170.071	42	5,731
Shelterbelt E.	Google Earth	2010 (7 March)	0.45	-44.195 / 170.071	58	11,331
Shelterbelt E.	LINZ	2014 (4 February)	0.4	-44.195 / 170.071	72	16,905
Quailburn	LINZ	2008 (19 March)	0.75	-44.388 / 169.850	141	29,598
Quailburn	LINZ	2014 (4 February)	0.4	-44.388 / 169.850	169	54,926
Ohau Village	LINZ	2006 (31 March)	0.75	-44.270 / 169.838	128	13,931
Ohau Village	Google Earth	2011 (4 September)	0.57	-44.270 / 169.838	143	38,232
Irishman Creek	LINZ	2008 (19 March)	0.75	-44.144 / 170.224	1299	47,390
Irishman Creek	LINZ	2014 (23 March)	0.4	-44.144 / 170.224	1660	129,725

Across the eight sites, a total of 896,354 trees were detected (Table E1).

E.2 Photos and information of each site and time step

The extent of each site is outlined in bold black lines. If there were any intentionally planted trees in the site such as those trees in a plantation or shelterbelt, the trees were not counted as individuals in the population growth models.

Ohau

Dominant species: *Pinus contorta*
Other species known to be present: *Pseudotsuga menziesii* and *Pinus ponderosa*

Management: Control of the site took place around 2016 to the south of the canal.

2011

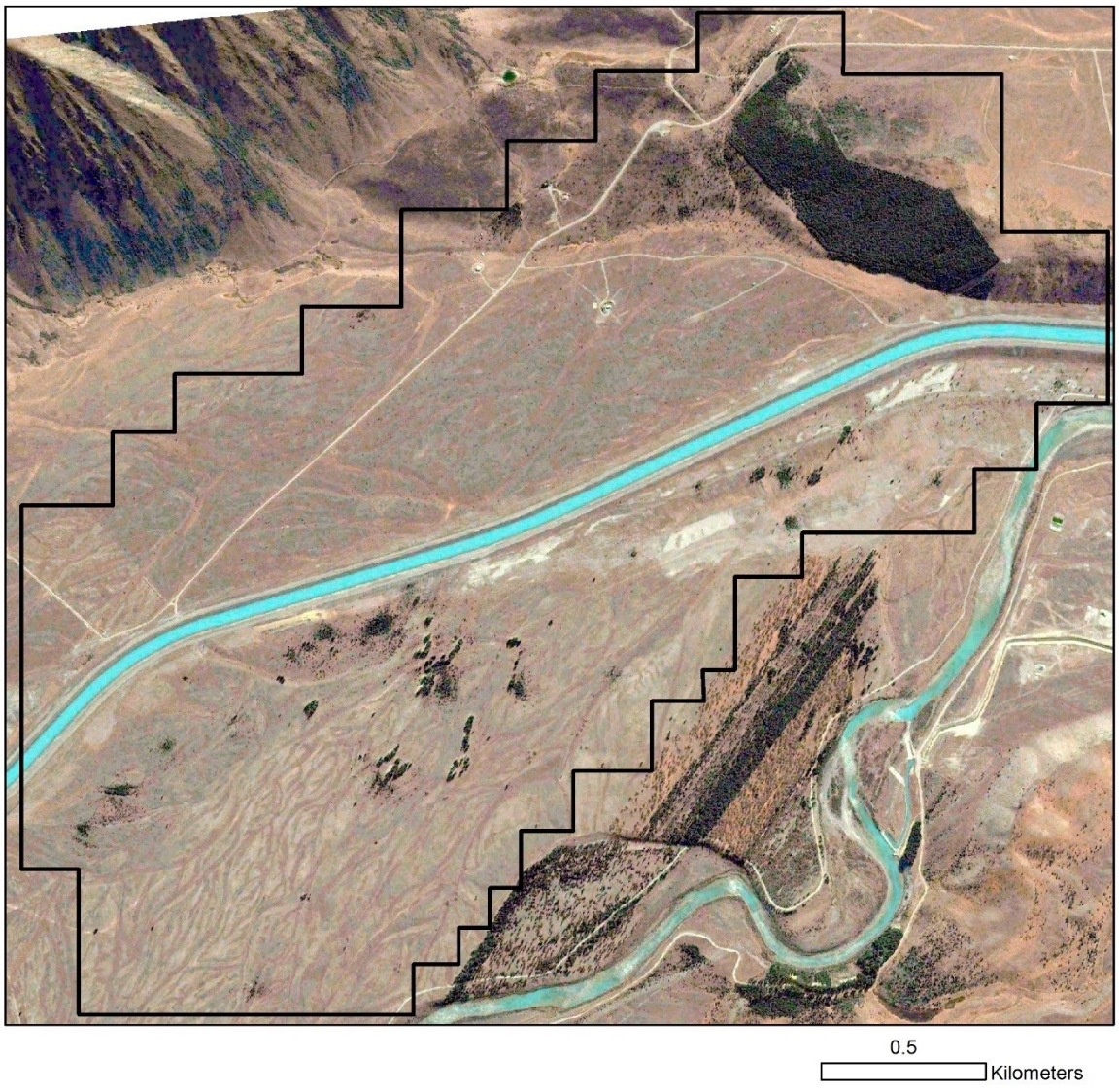

Figure E1 Imagery from Google Earth of the Ohau site in 2011.

2014

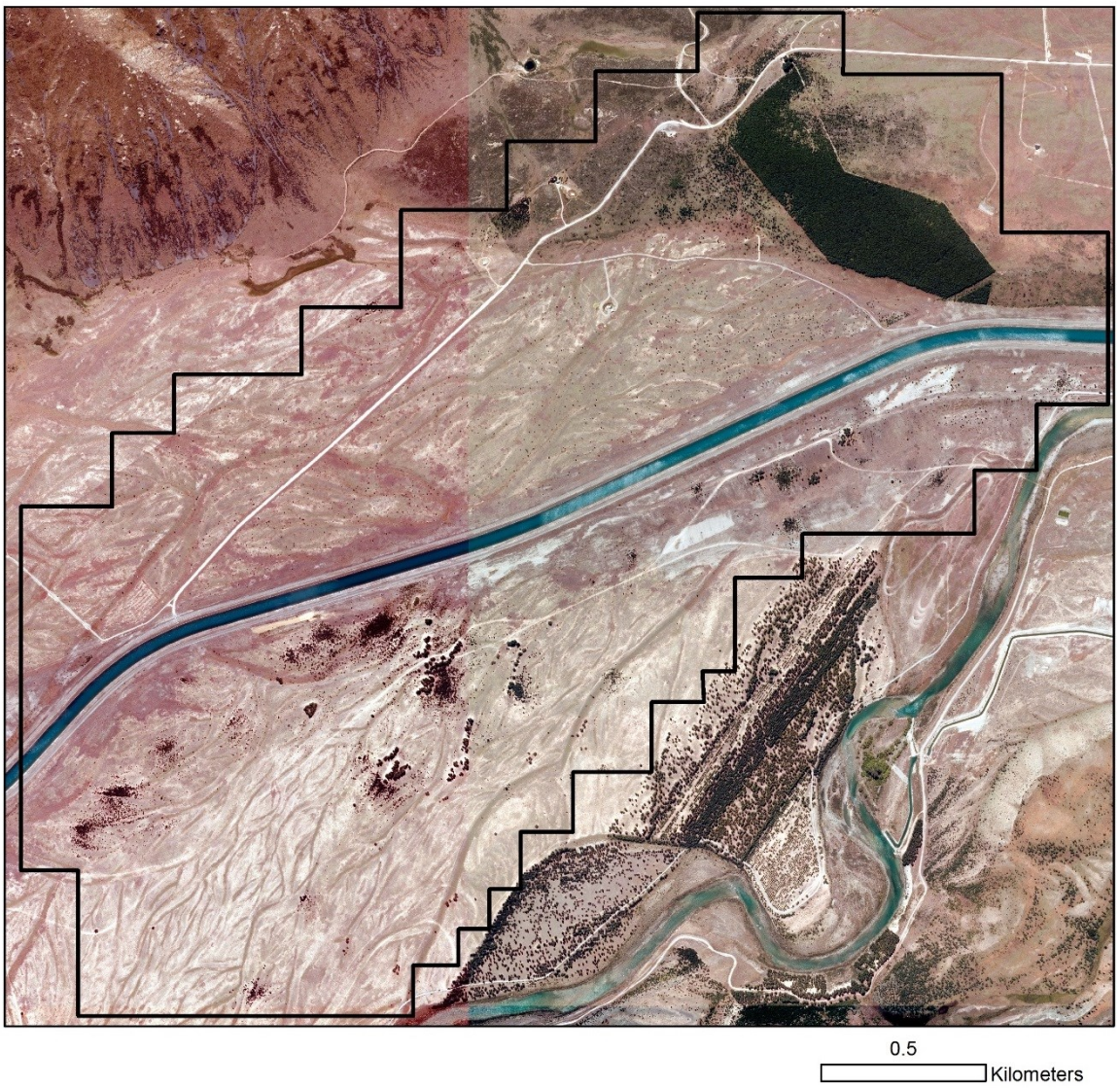

Figure E2 Imagery from Land Information NZ of the Ohau site in 2014.

Mt Barker

Dominant species: *Pinus nigra*
Other species known to be present: *Pseudotsuga menziesii*, *Pinus contorta*, *Pinus sylvestris*, *Pinus ponderosa*

Management: Some localised removal of conifers occurred in 20x20m plots in the south-eastern part of the site. Herbicide trials also were undertaken in localised areas of the site. Trees were removed from the middle of the site between 2010-2016 as well. These removal areas were excluded from the population growth models.

2010

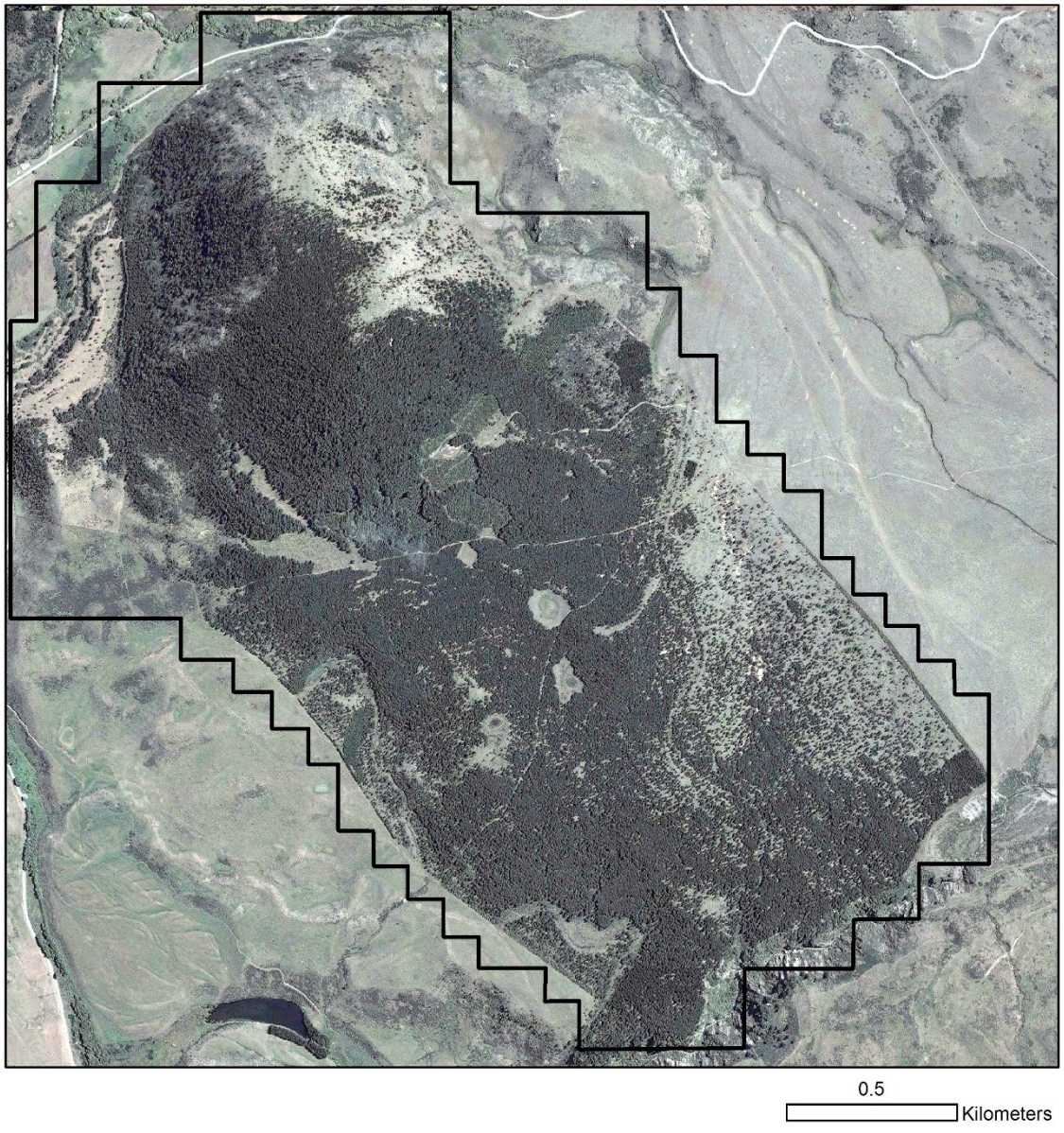

Figure E3 Imagery from Google Earth of the Mt Barker site in 2010.

2016

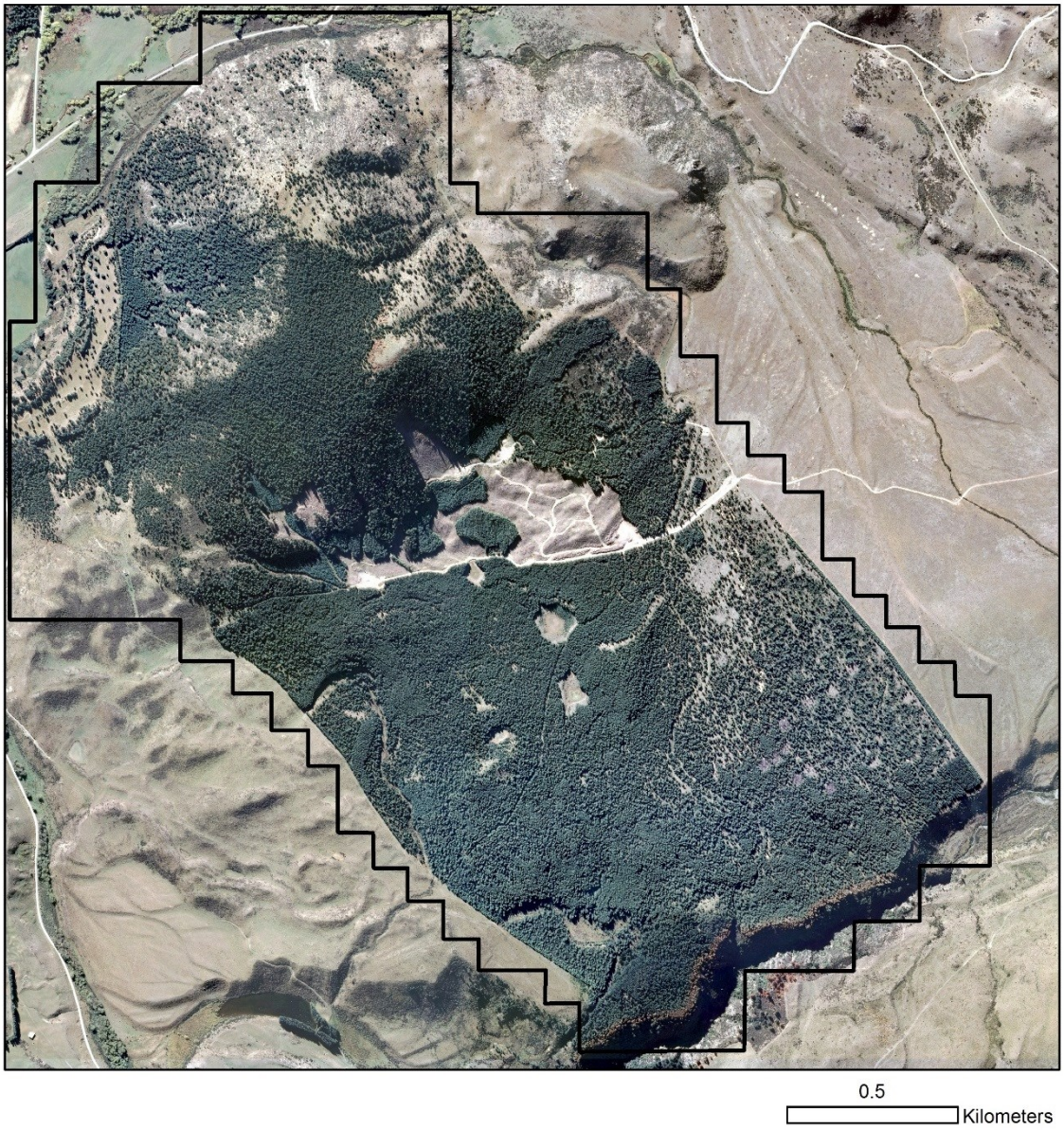

Figure E4 Imagery from Land Information NZ of the Mt Barker site in 2016.

South Pukaki

Dominant species: *Pinus contorta*
Other species known to be present: *Pinus nigra* and *Pinus ponderosa*

Management: Some herbicide trials took place between 2014-2016. No trees were removed during this period and the spray trials did not affect the detection of the trees.

2006

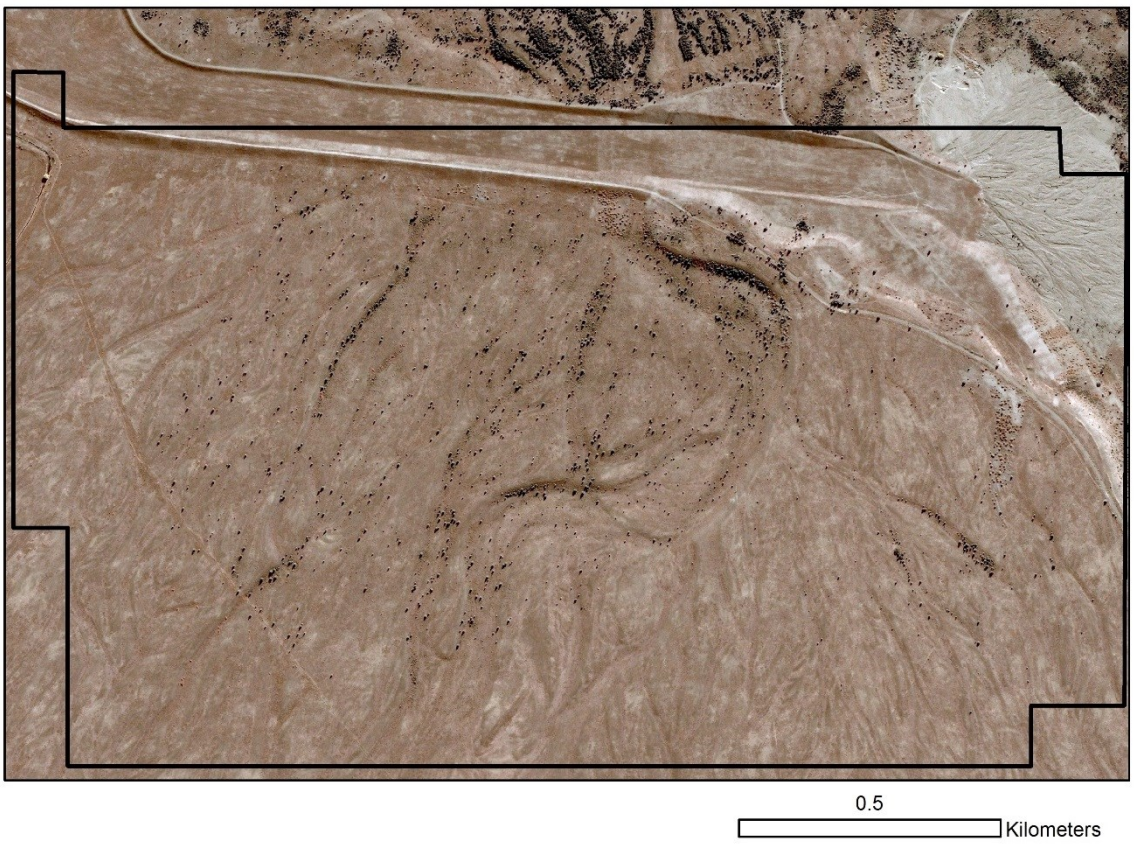

Figure E5 Imagery from Google Earth of the South Pukaki site in 2006.

2008

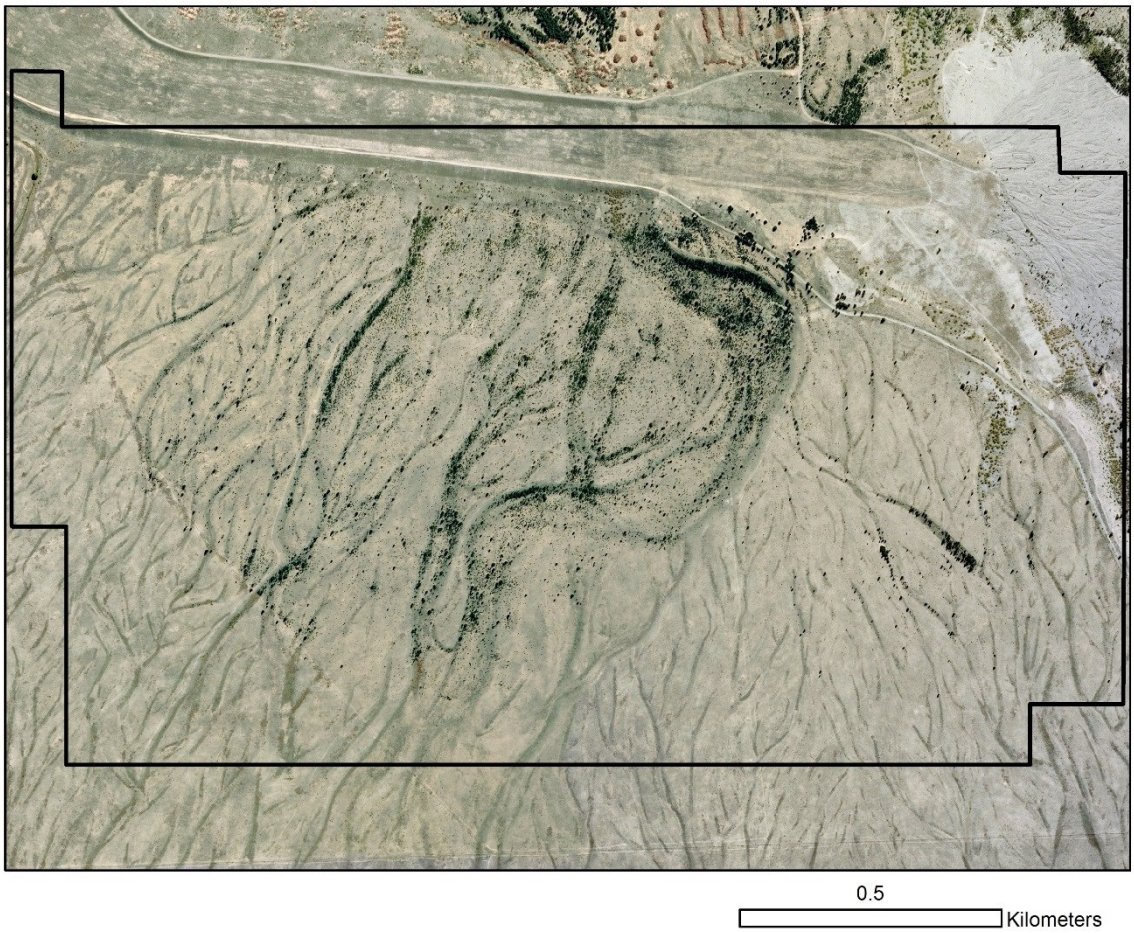

Figure E6 Imagery from Land Information NZ of the South Pukaki site in 2008.

2014

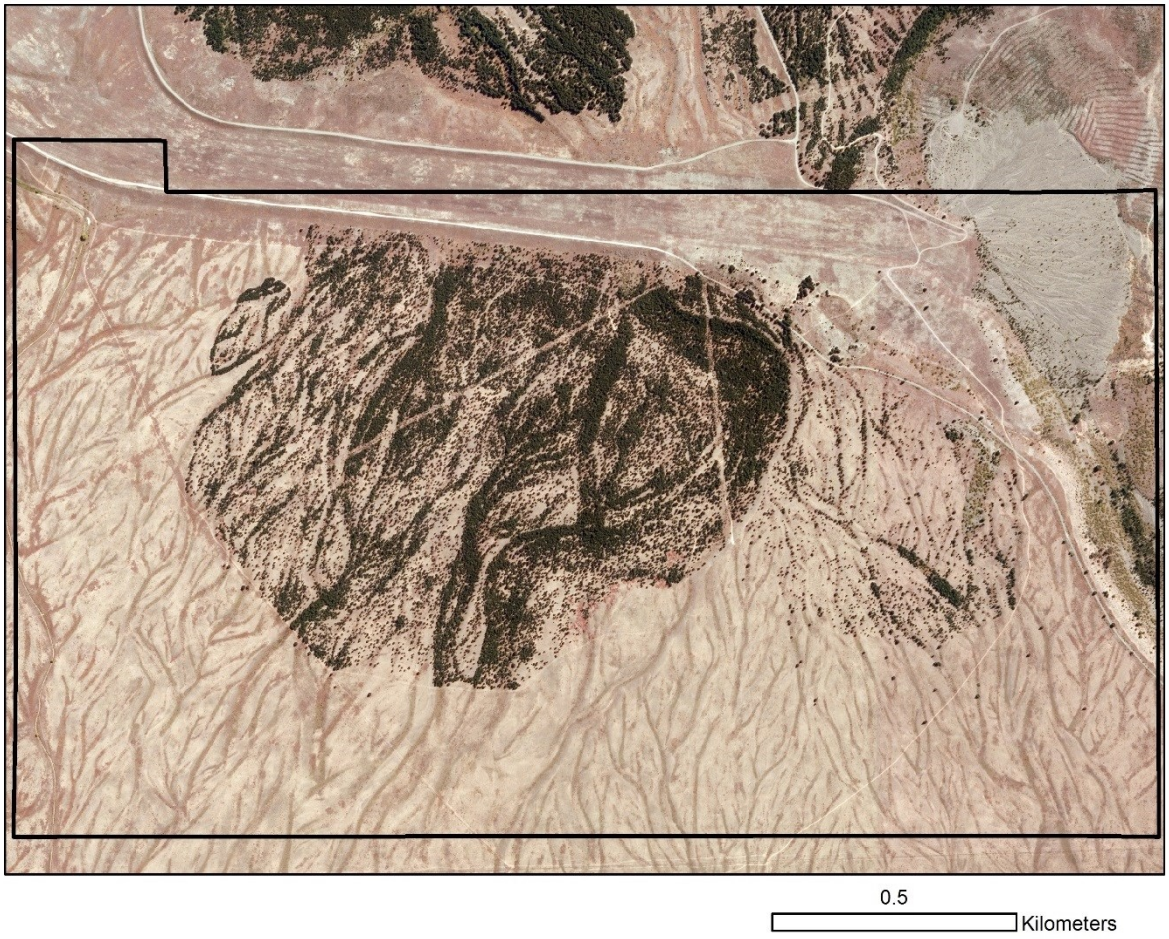

Figure E7 Imagery from Land Information NZ of the South Pukaki site in 2014.

2016

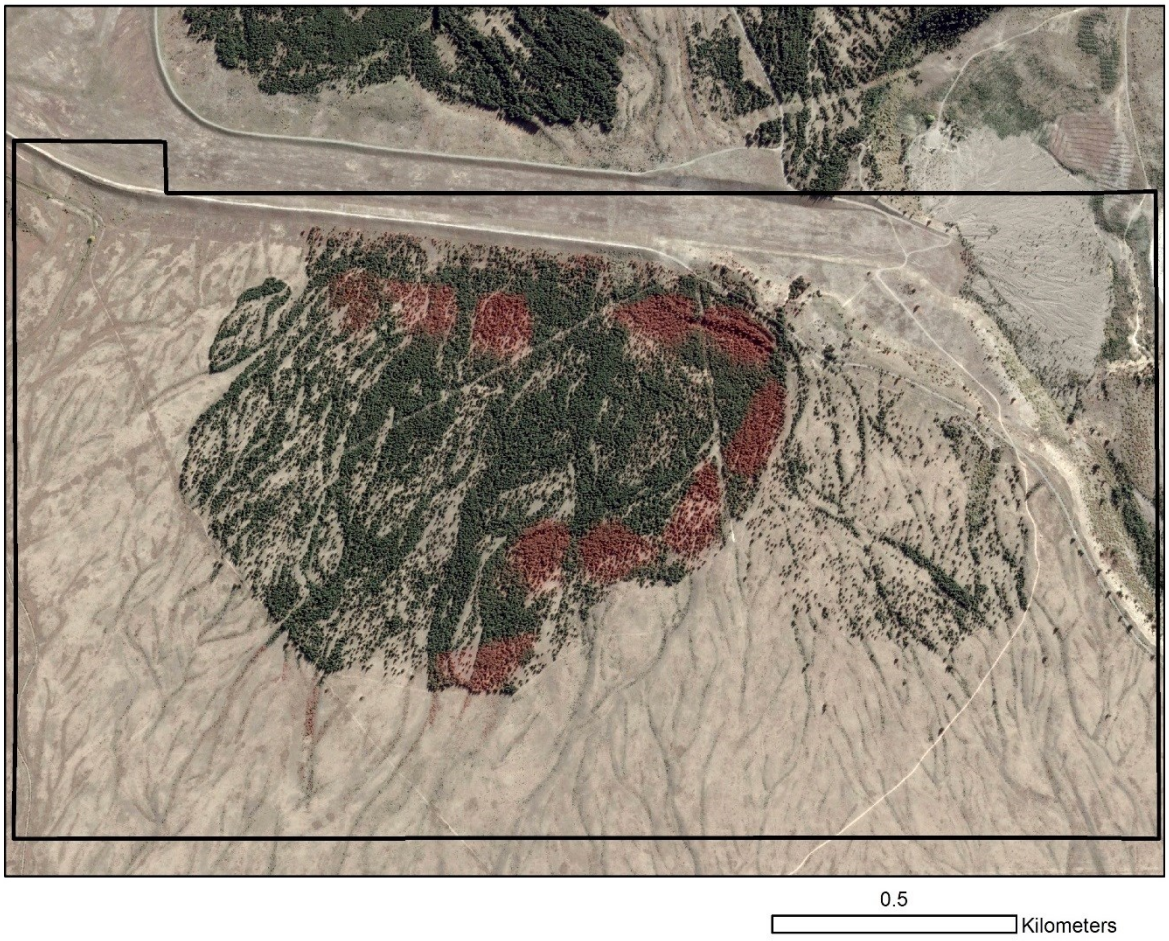

Figure E8 Imagery from Google Earth of the South Pukaki site in 2016. The red-orange areas are where trees were sprayed with a herbicide.

Shelterbelt West

Dominant species: *Pinus contorta*

Other species known to be present: Unknown

Management: Some trees were removed after 2010.

2006

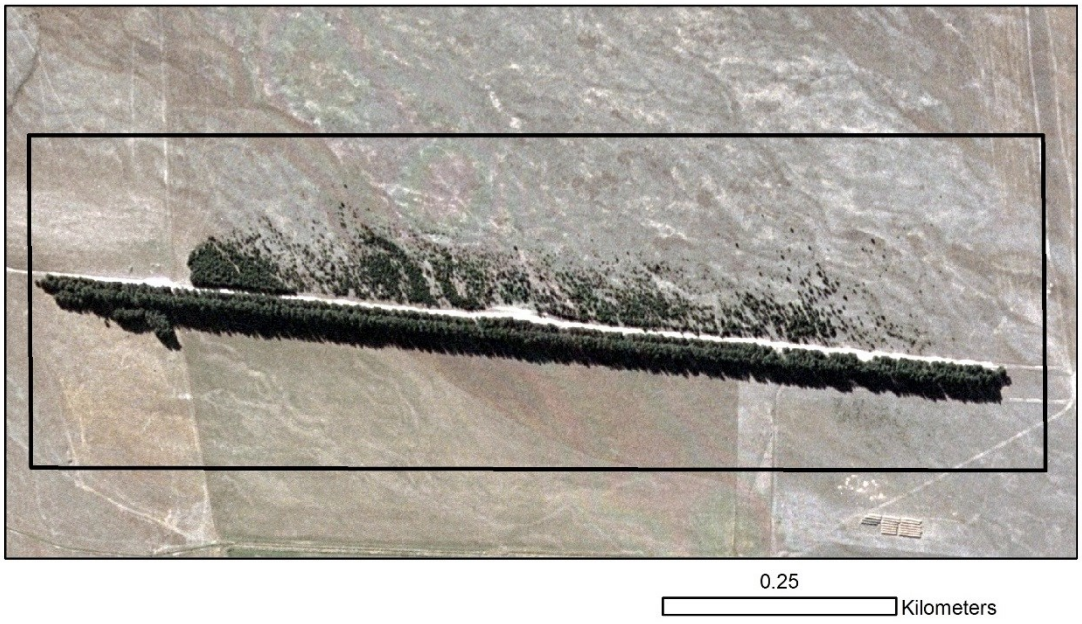

Figure E9 Imagery from Land Information NZ of the Shelterbelt West site in 2006.

2010

Figure E10 Imagery from Google Earth of the Shelterbelt West site in 2010.

Shelterbelt East

Dominant species: *Pinus contorta*
Other species known to be present: Unknown

Management: Some trees were removed in the northern and southern ends of the site, but these areas were excluded from the population growth models.

2008

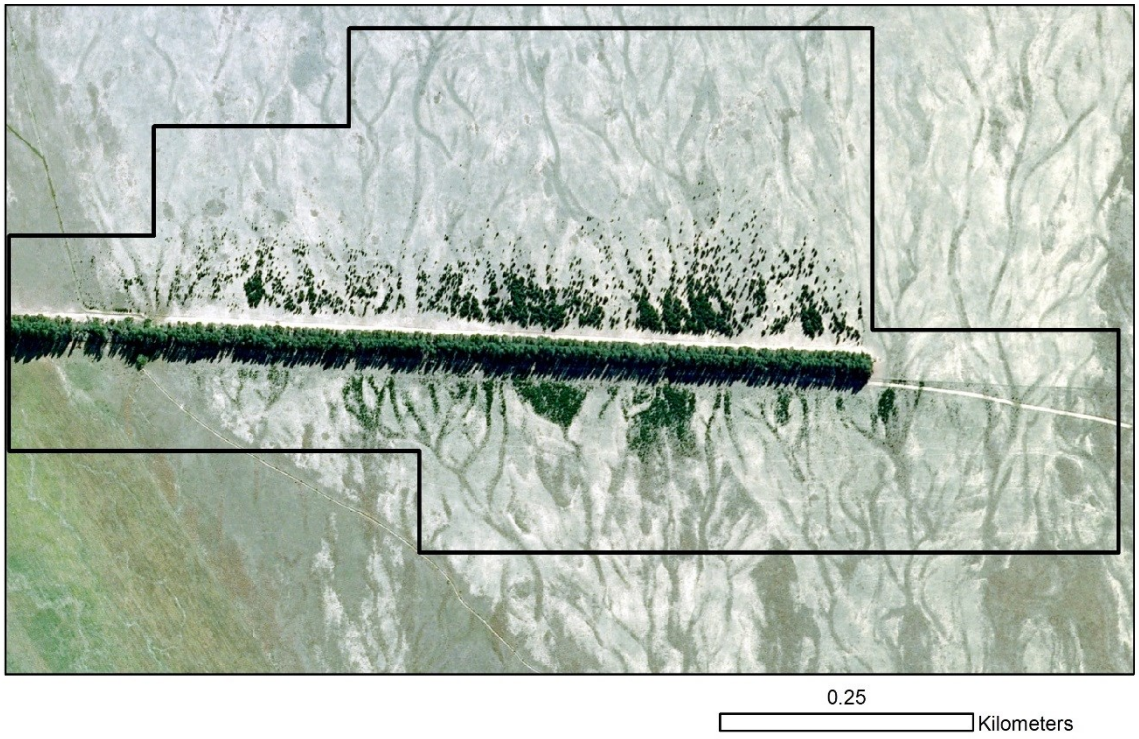

Figure E11 Imagery from Land Information NZ of the Shelterbelt East site in 2008.

2010

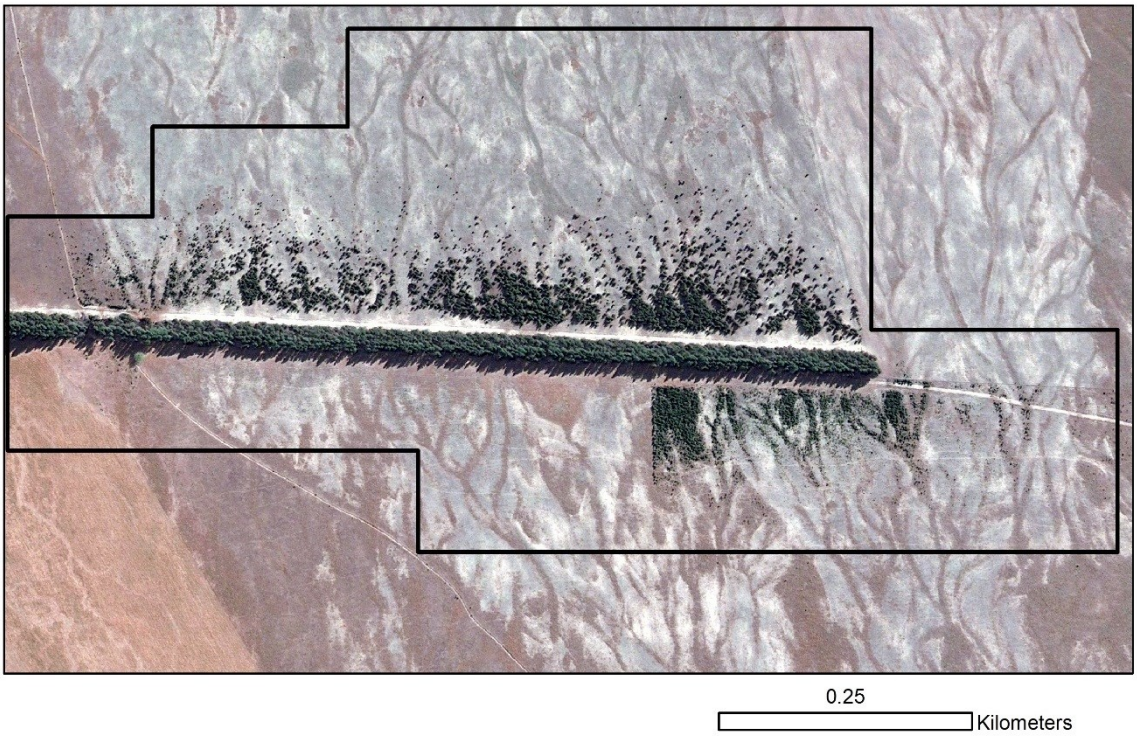

Figure E12 Imagery from Google Earth of the Shelterbelt East site in 2010.

2014

Figure E13 Imagery from Land Information NZ of the Shelterbelt East site in 2014.

Quailburn

Dominant species: *Pinus contorta*

Other species known to be present: Unknown

Management: No known management has occurred here.

2008

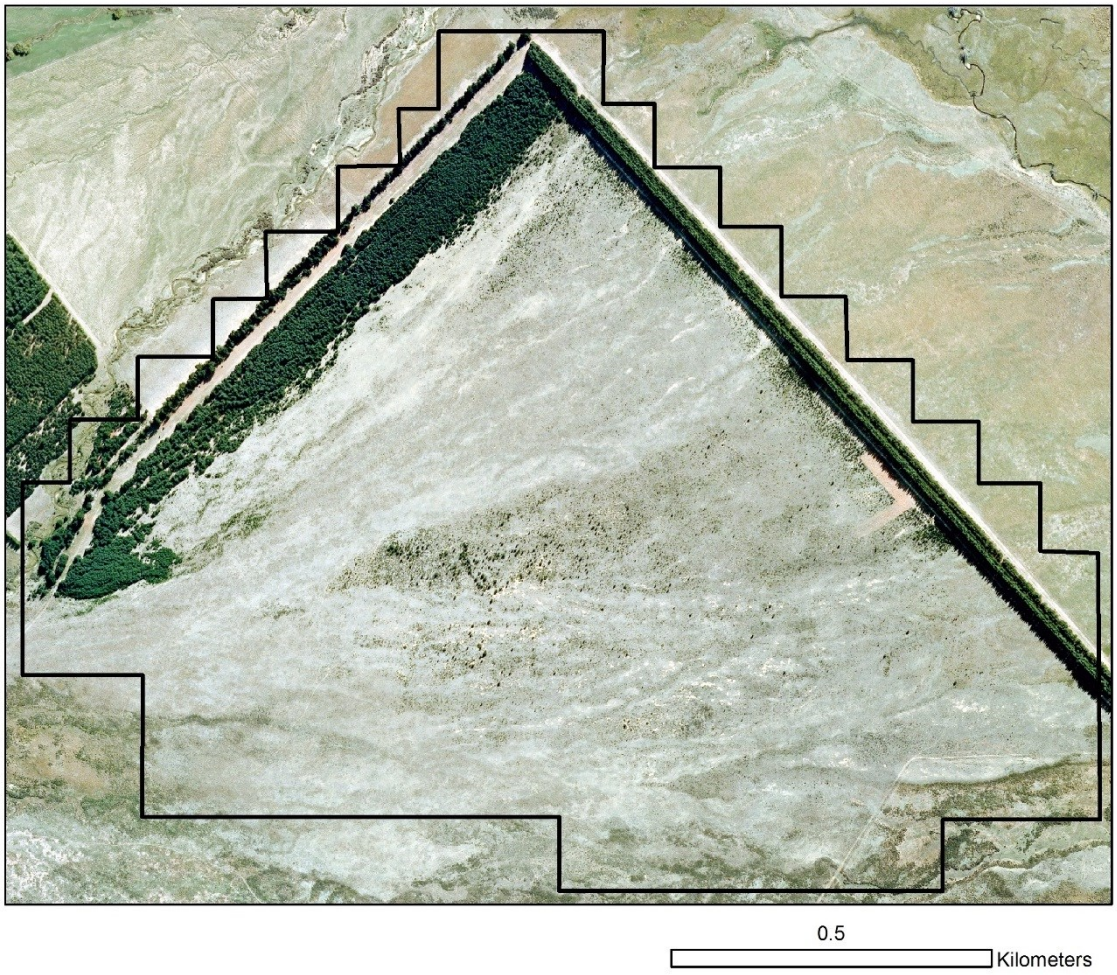

Figure E14 Imagery from Land Information NZ of the Quailburn site in 2008.

2014

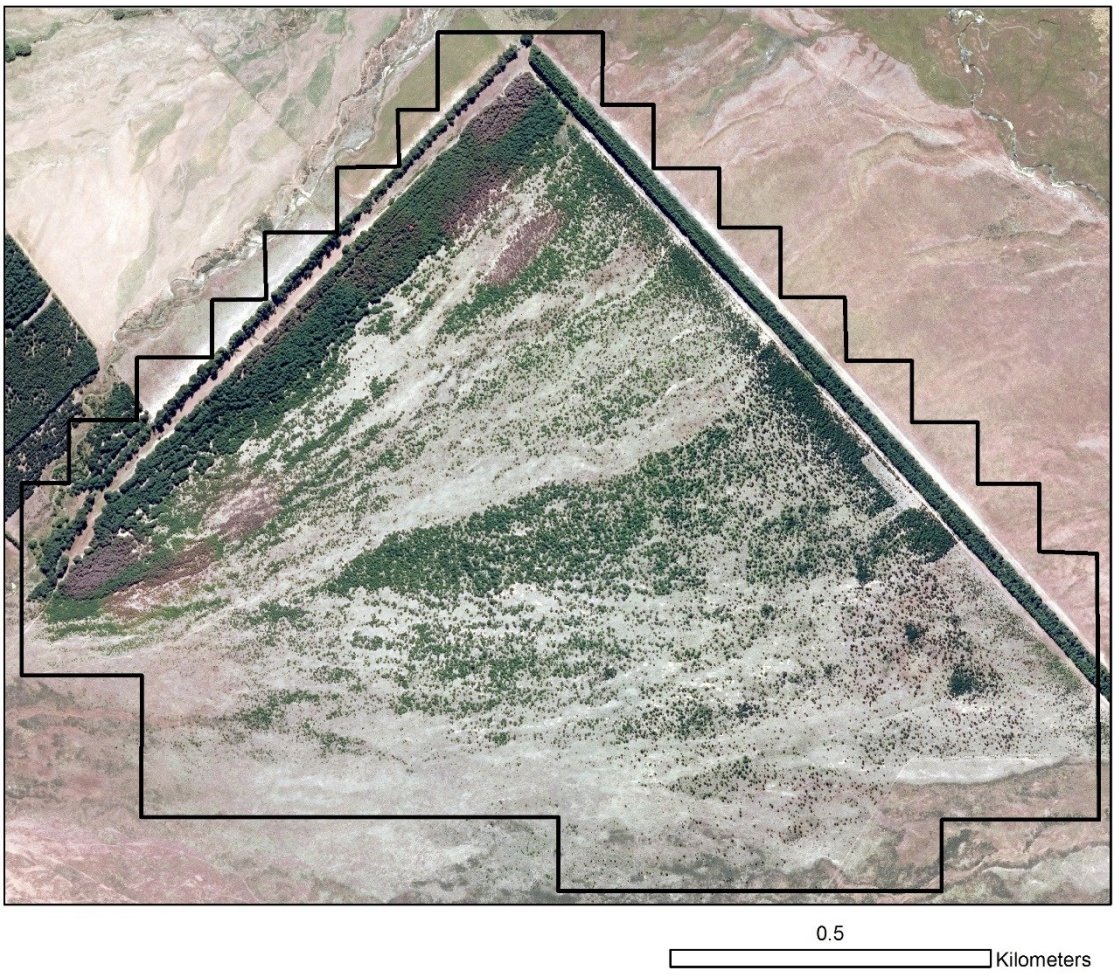

Figure E15 Imagery from Land Information NZ of the Quailburn site in 2014.

Ohau Village

Dominant species: *Larix decidua*

Other species known to be present: Unknown

Management: Some trees were removed between 2011-2014.

2006

Figure E16 Imagery from Land Information NZ of the Ohau Village site in 2006.

2011

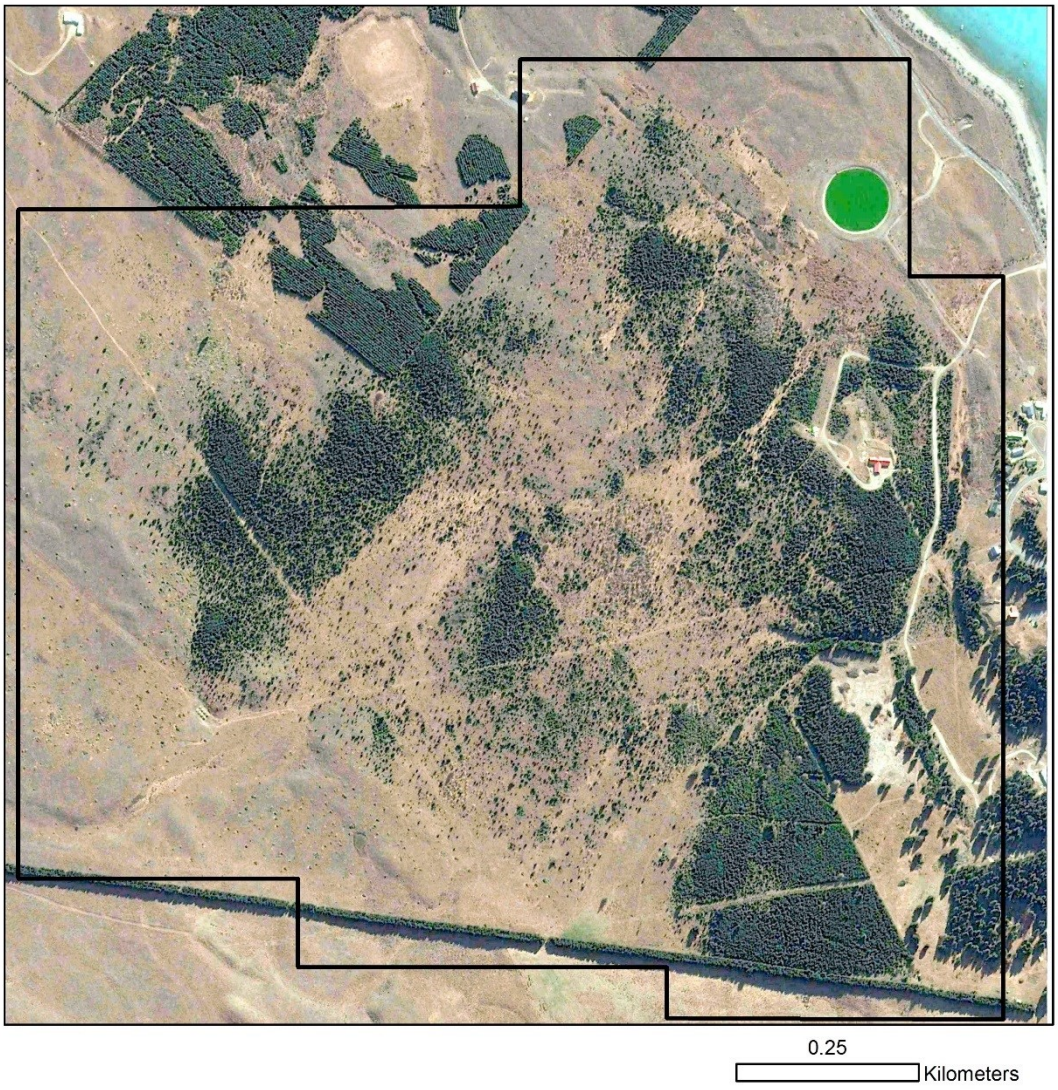

Figure E17 Imagery from Google Earth of the Ohau Village site in 2011.

Irishman Creek

Dominant species: *Pinus contorta*
Other species known to be present: *Pseudotsuga menziesii*, *Pinus nigra*, *Pinus ponderosa*

Management: A few trees were removed along the power distribution lines between 2008-2014. Management has subsequently taken place in March 2018 through aerial spraying at the northern and southern ends of the site.

2008

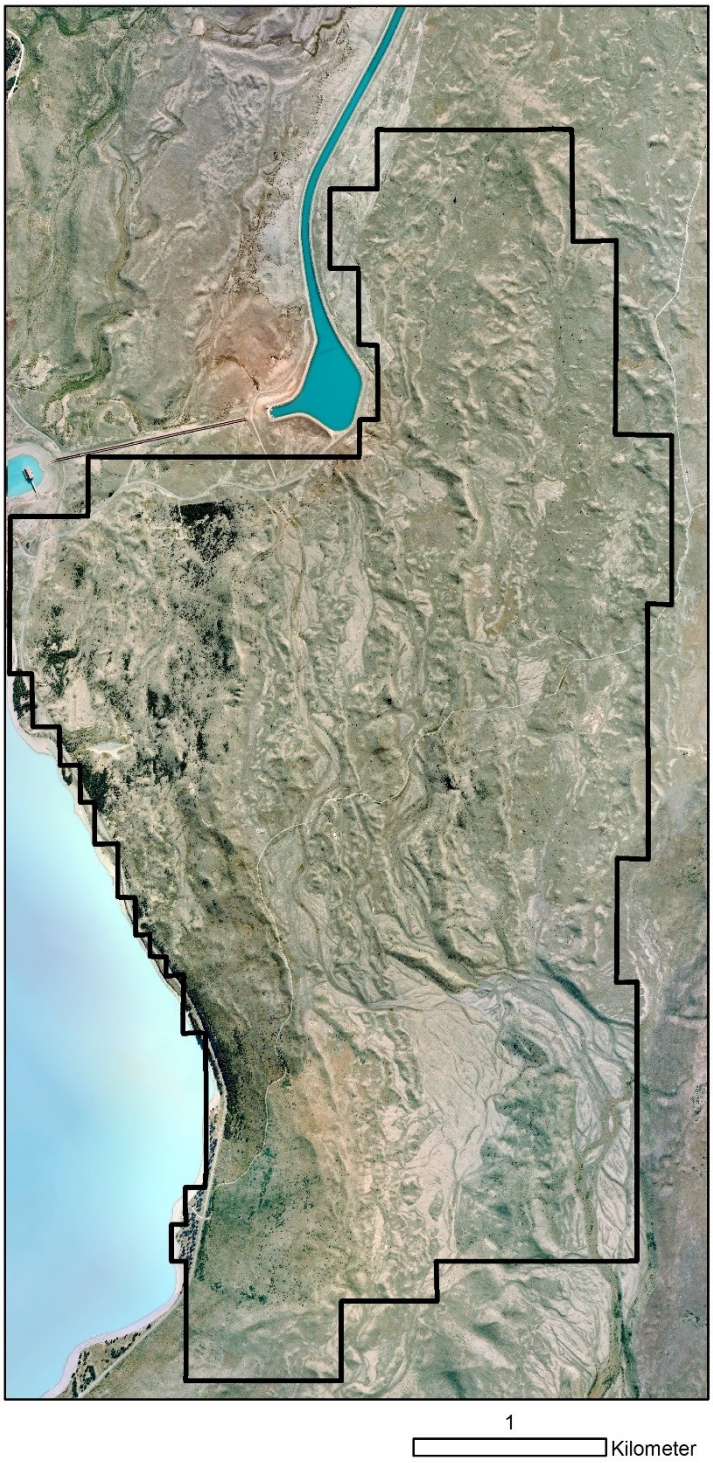

Figure E18 Imagery from Land Information NZ of the Irishman Creek site in 2008.

2014

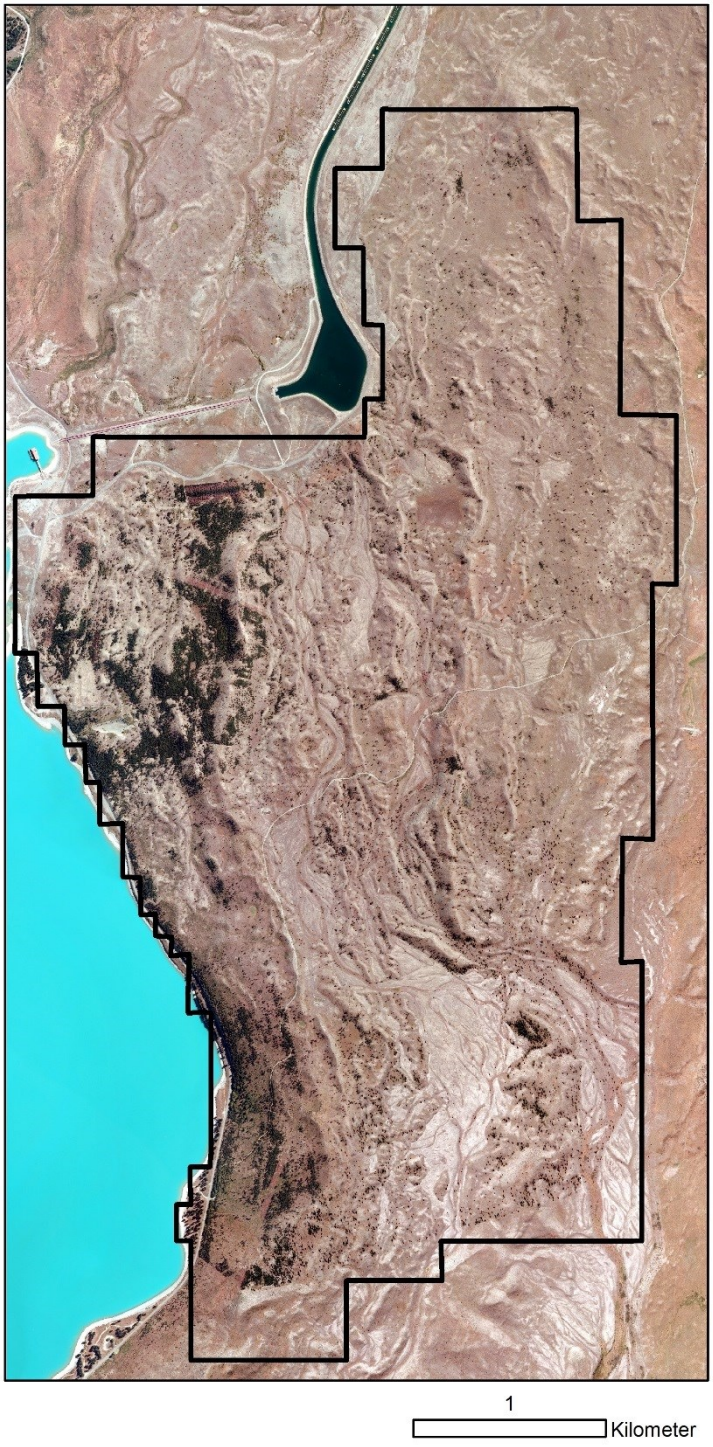

Figure E19 Imagery from Land Information NZ of the Irishman Creek site in 2014.

Appendix F

Information on estimating the STT for Chapter 4

In Chapter 4, I used a Scale Transition Term (STT) from Chesson et al. (2005) to estimate the difference between local and regional estimates of population growth. Here I show the steps to estimate this STT. To do so, I first need to estimate its components. I will start with the equation for the Scale Transition Term from Chesson et al. (2005):

$$STT = \frac{1}{2} Var(N_t) F''(\overline{N_t})$$

To estimate the *Var(N)* term, I need to estimate the variance of densities. This is straightforward because I simply need to calculate the variance in densities of the grid-cells across a site.

Estimating the *F''*($\overline{N}$) term is less straightforward as I need to take the second derivative of the Gompertz population model. I will start with the Gompertz model before having simplified it with taking the natural log of both sides:

$$N_{t+1} = N_t e^{a+(b-1)\log(N_t)}$$

Since $F(\overline{N}) = N_{t+1}$, I will need to take the second derivative of this equation. Taking the second derivative will give:

$$F''(\overline{N_t}) = e^a (b-1) b N_t^{b-2}$$

Thus, to calculate *F''*($\overline{N}$), I need parameter estimates for both intrinsic growth rate (a) and degree of density dependence (b), as well as the mean density of grid-cells ($\overline{N}$). Once these components are calculated, they can be plugged into the STT equation to estimate the STT.

Appendix G

Model Information and Diagnostics for Chapter 4

G.1 Model Code

Below is the code to run the spatial population growth model with the CAR term in R. This code is written as a function, making it easy to run for many sites and time periods. The R package Nimble is needed to run the following code.

The following are inputs into the code:

`Sitet1_gridpts_full_log`: This is the data of the density of trees within each grid-cell for the first time step in the model. The grid-cell order is the same for all time steps for a site.

`Sitet2_gridpts_full_log`: This is the data of the density of trees within each grid-cell for the second time step in the model.

`grid_Site_full`: This is the grid of 100x100m cells for the site. The grid is the same for both time steps.

`Nt_mean`: This is the mean of the tree densities in the grid-cells for the first time step. This mean is used to calculate one of the components of the STT (*F''(N)*).

The code first sets up the model by specifying the distributions of the priors, the CAR term, and the likelihoods for the posteriors. I added in an assessment of model fit by estimating the distribution of the residuals as well. Then the code specifies the constants in the model. Since the model ran three chains, I wrote a function to generate different initial values for the priors for each chain. The code runs the three chains using the model code, constants, data, and initial values. The code ends by returning the MCMC output from the model.

```
spatmodel_run <- function(Sitet1_gridpts_full_log, Sitet2_gridpts_full_log,
grid_Site_full, Nt_mean){


  code_sp1 <- nimbleCode({

    # priors:
    alpha ~ dnorm(0, 0.2)  # alpha is density independent growth
    beta1 ~ dnorm(0, 1)    # beta1 is density dependence
    tau  ~ dgamma(0.1, 0.1) # tau is the precision term for the observed
                              (y) posterior distribution
    tau.sp ~ dgamma(0.1, 0.1) # tau.sp is the precision term for the
                               spatial random effect term
```

```
    # Set up CAR term
    for(k in 1:L)
      weights[k] <- 1   # weights of adjacent cells are set to 1
    b[1:N] ~ dcar_normal(adj[1:L], weights[1:L], num[1:N], tau.sp,
                         zero_mean = 1)  # b = spatial random effect term


    # Likelihood for posteriors
    for (i in 1 : N) {
      y[i] ~ dnorm(mu[i], tau)
      mu[i] <- alpha + beta1 * x[i] + b[i]   # Gompertz equation
    }

    # Assess model fit
    for (i in 1:N) {
      predicted[i] <- mu[i]             # Predicted values
      residual[i] <- y[i]-predicted[i]  # Residuals for observed data
    }

    # Estimate non-linear growth rate F''(N) (2nd Derivative of Gompertz)
    fpp <- exp(alpha)*(beta1^2 - beta1)*Nt_mean^(beta1-2)

  })

# set up adjacency matrix for the site - use matrix in model's CAR term
nb_Site_full <- poly2nb(grid_Site_full)
NumCells_Site_full <- length(nb_Site_full)
num_full <- sapply(nb_Site_full,length)
adj_full <- unlist(nb_Site_full)
sumNumNeigh_full <- length(unlist(nb_Site_full))


# Specify the constants in the model (number of grid-cells, length of
adjacency matrix, mean of Nt)
constants_sp1 <- list(N = length(Sitet1_gridpts_full_log), L =
length(adj_full), num = num_full, adj = adj_full, x =
Sitet1_gridpts_full_log, Nt_mean = Nt_mean)
data_sp1 <- list(y = Sitet2_gridpts_full_log)

# running three chains - so need to specify 3 sets of initial values
# Set up function to generate different initial values within expected
# distribution
  inits_sp2_fxn <- function() list(alpha = rnorm(1,0,1), beta1 =
rnorm(1,0.5, 0.2), tau = 1, tau.sp = 1, b = rep(0, length(num_full)))

  inits_sp2 <- inits_sp2_fxn()


  # put model together
  Rmodel_sp2 <- nimbleModel(code_sp1, constants_sp1, data_sp1, inits_sp2)


  # run MCMC sampling to estimate parameters
  mcmc.out_sp <- nimbleMCMC(model = Rmodel_sp2, monitors = c("alpha",
"beta1", "tau", "tau.sp", "mu", "b", "fpp"), niter = 10000, nchains = 3,
nburnin = 5000, summary = TRUE, WAIC = TRUE)


  # return the output of the model
  return(mcmc.out_sp)

}
```

To compare the spatial and aspatial models for each site and time period, I used the WAIC values (Table G1). The lower of the WAIC values indicates better fit. Therefore the spatial models always fit the data better and thus the parameter distributions from the spatial models were always used.

Table G1 WAIC values to compare the spatial and aspatial models. The lower of the WAIC values (indicating better fit) are in bold for each set of models.

Model	Spatial WAIC Value	Aspatial WAIC Value
Ohau 2011-2014	N/A*	1242
Mt Barker 2010-2016	**605**	970
S. Pukaki 2006-2008	**444**	634
S. Pukaki 2008-2014	**394**	597
S. Pukaki 2014-2016	**503**	677
Shelterbelt W. 2006-2010	**53**	60
Shelterbelt E. 2008-2010	**95**	105
Shelterbelt E. 2010-2014	**104**	159
Quailburn 2008-2014	**255**	350
Ohau Village 2006-2011	**152**	321
Irishman Creek 2008-2014	**2690**	3059

*The spatial model for the Ohau site could not be run because there were unadjacent plots and thus the CAR model could not run.

Table G 2 The number of gridcells included in each model.

Model	Number of gridcells
Ohau 2011-2014	430
Mt Barker 2010-2016	480
S. Pukaki 2006-2008	209
S. Pukaki 2008-2014	226
S. Pukaki 2014-2016	279
Shelterbelt W. 2006-2010	24
Shelterbelt E. 2008-2010	40
Shelterbelt E. 2010-2014	46
Quailburn 2008-2014	140
Ohau Village 2006-2011	128
Irishman Creek 2008-2014	1190

G.2 Model diagnostics for example models

The following model diagnostics will be discussed here: correlation between the estimates of density independence and density dependence; $\hat{R}$ statistics; goodness of fit plots; and estimates for the spatial random effects terms. Three models were chosen randomly to display these diagnostics to represent the work done for all of the models. The correlation and $\hat{R}$ plots were generated by the R package shinystan.

The three models whose diagnostics are shown here are: the model for the S. Pukaki site between 2006-2008; the model for the Shelterbelt W. site between 2006-2010; and the model for the Ohau Village site between 2006-2011.

S. Pukaki 2006-2008

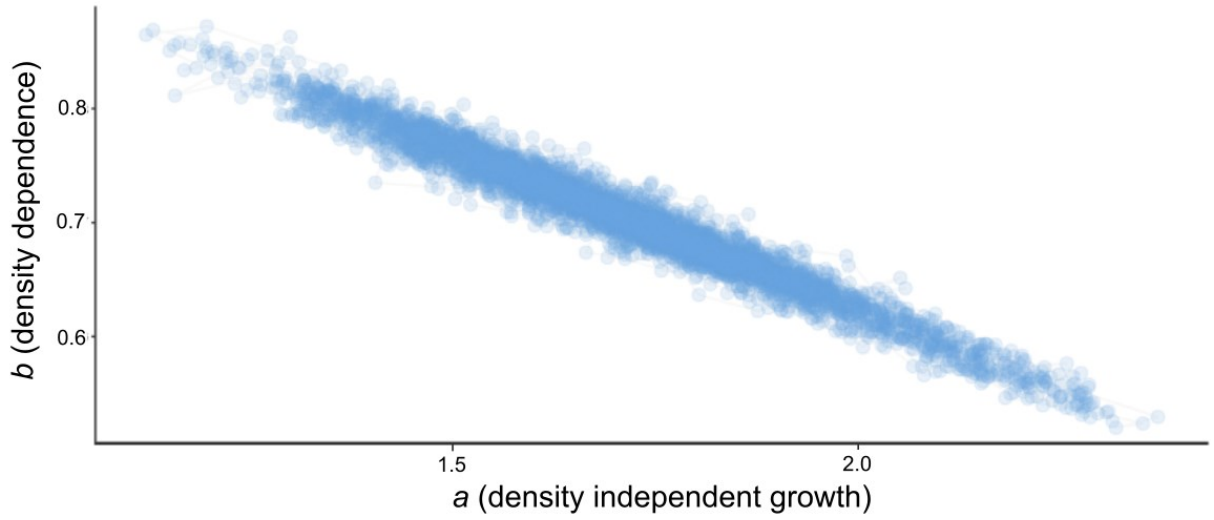

Figure G1 Estimates of density independent growth (*a*) and density dependence (*b*) plotted against each other for the model of the S. Pukaki site from 2006-2008.

These estimates are negatively correlated, meaning that when density independent growth is high, density dependence is low (Fig. G1).

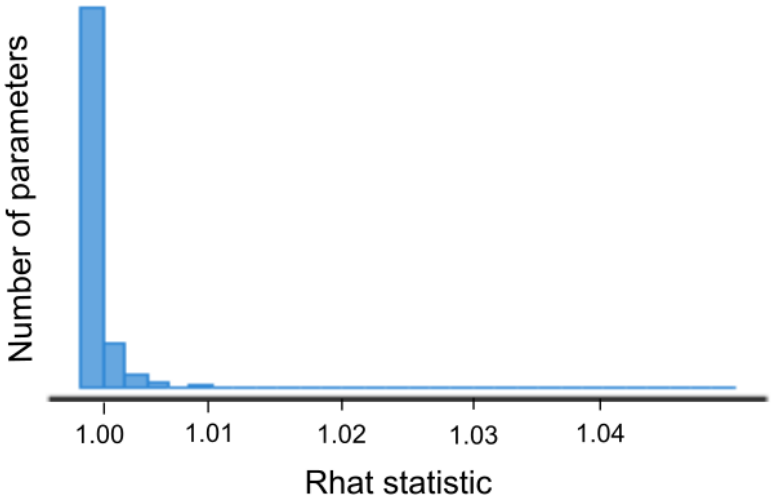

Figure G2 The $\hat{R}$ statistics for all of the model parameter estimates for the S. Pukaki site from 2006-2008.

None of the $\hat{R}$ values for the parameters were above 1.1, meaning that all of the parameter estimates converged (Fig. G2).

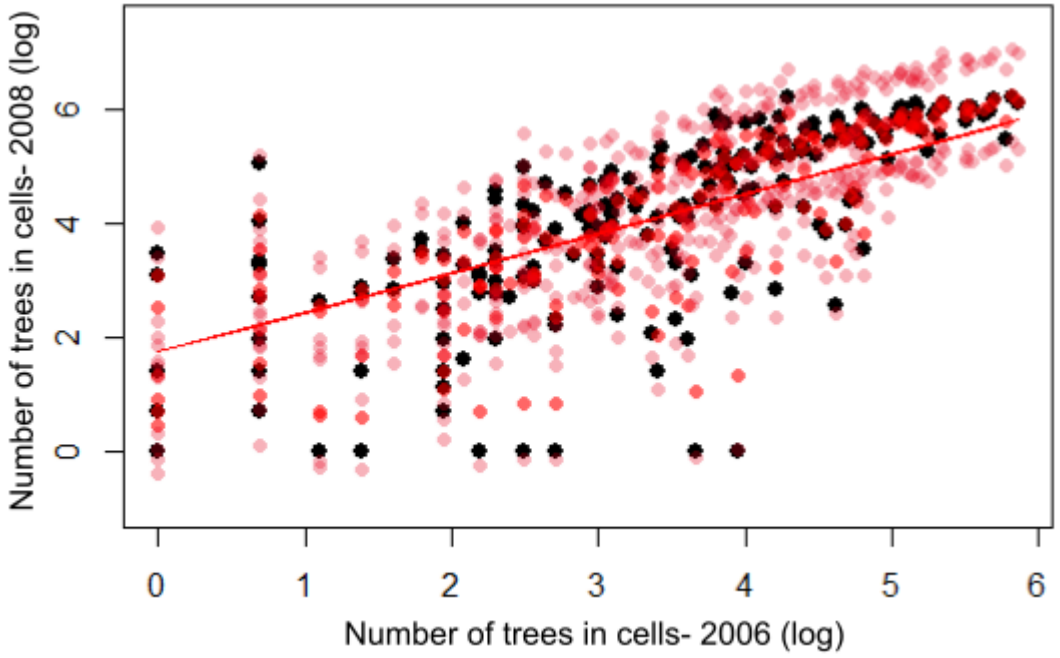

Figure G3 The model predictions for population growth for the S. Pukaki site from 2006-2008 (light red and red points) match closely with the observed population growth (black points). Each point represents the growth in one grid-cell. The light red points indicate the 95% credible intervals for the predictions and the red points indicate the mean predictions. The red line indicates the line of best fit for the model predictions.

All of the observed data (black points) fall within the range predicted by the model (light red and red points), indicating that the population growth model accurately predicted the population growth (Fig.

G3). The red line shows the model's line of best fit through the predicted points.

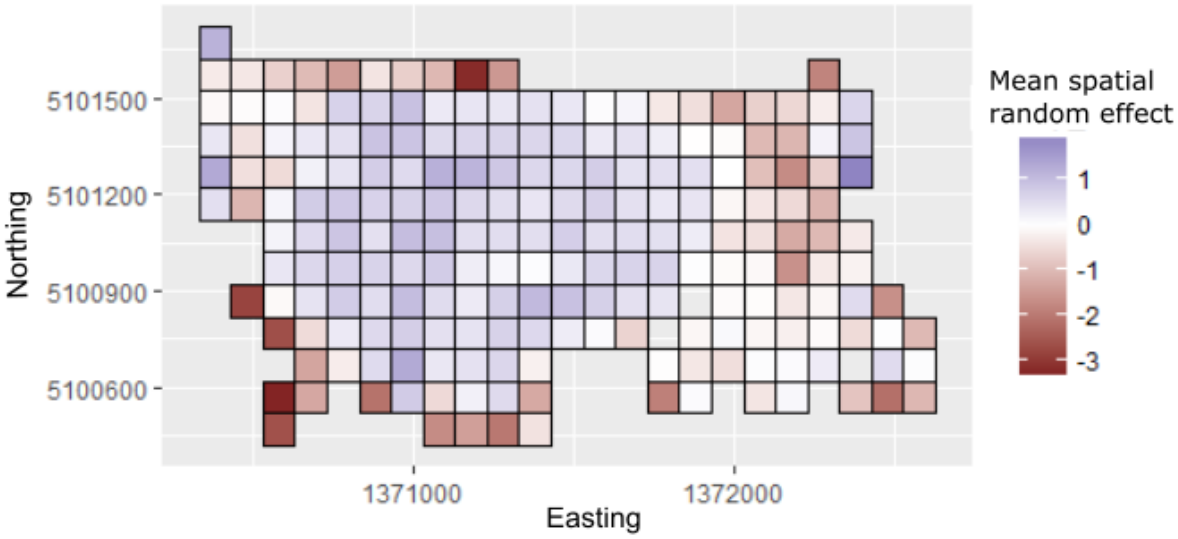

Figure G4 Map of the mean spatial random effects for each grid-cell of the S. Pukaki site from 2006-2008.

The grid-cells with the negative spatial random effect values indicate where the growth in those cells is less than the other cells. This could mean that the neighbouring cells are dispersing less than expected in those negative cells or the environmental conditions are not as favourable, leading to lower growth rates than what would be expected. Many of these negative spatial random effects terms occurred near the edges of the site (Fig. G4) and therefore could be a result of edge effects. Many of the cells in the centre of the invasion exhibited more positive spatial random effects than the other cells. This could indicate that more dispersal occurred into these cells or the environmental conditions were more suitable for conifers.

Shelterbelt W. 2006-2010

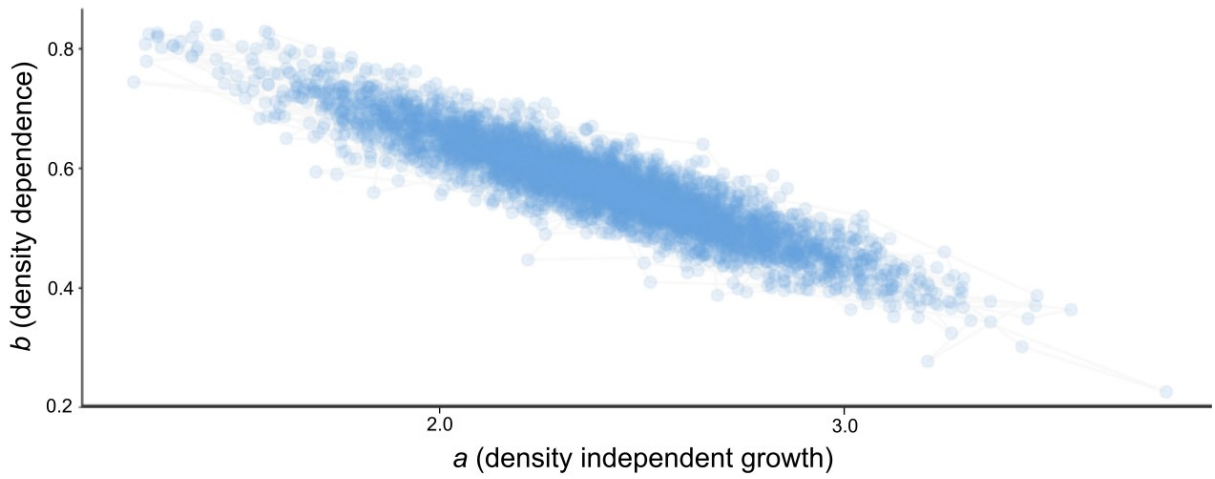

Figure G5 Estimates of density independent growth (*a*) and density dependence (*b*) plotted against each other for the model of the Shelterbelt West site from 2006-2010.

The estimates for density independent growth and density dependence are negatively correlated (Fig. G5).

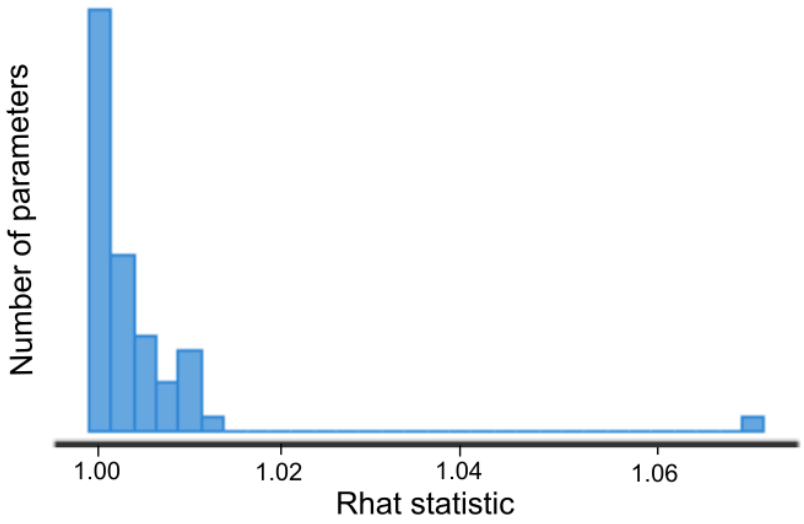

Figure G6 The $\hat{R}$ statistics for all of the model parameter estimates for the Shelterbelt West site from 2006-2010.

None of the $\hat{R}$ values for the parameters were above 1.1, meaning that all of the parameter estimates converged (Fig. G6).

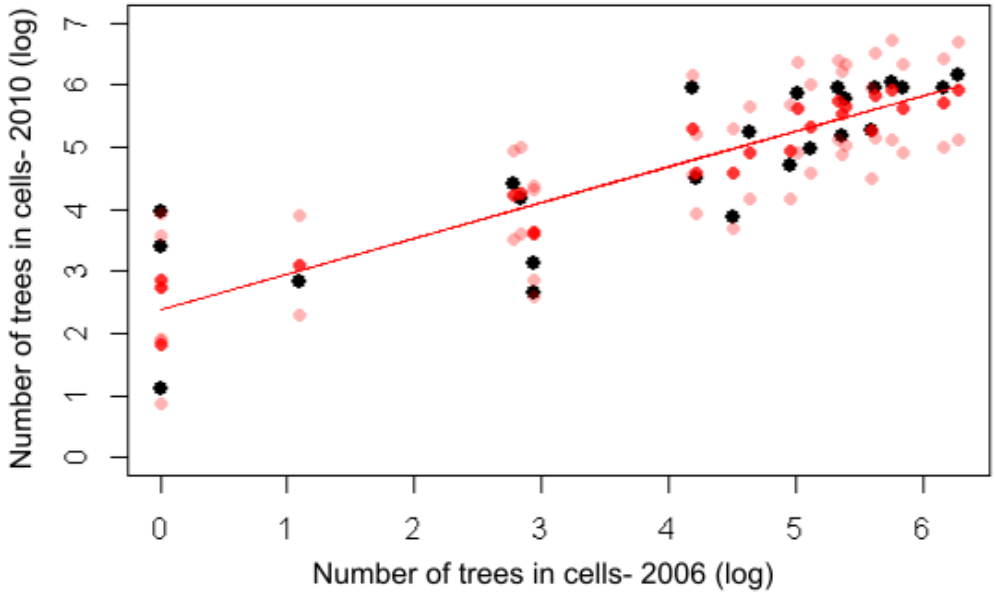

Figure G7 The model predictions for population growth for the Shelterbelt West site from 2006-2010 (light red and red points) align closely with the observed population growth (black points). Each point represents the growth in one grid-cell. The light red points represent the 95% credible intervals for the predictions and the red points represent the mean predicted estimates. The red line indicates the line of best fit for the model predictions.

All of the observed data (black points) fall within the range predicted by the model (light red and red points) (Fig. G7). This signifies that the population growth model accurately predicted the observed population growth. The red line shows the model's line of best fit through the predicted points.

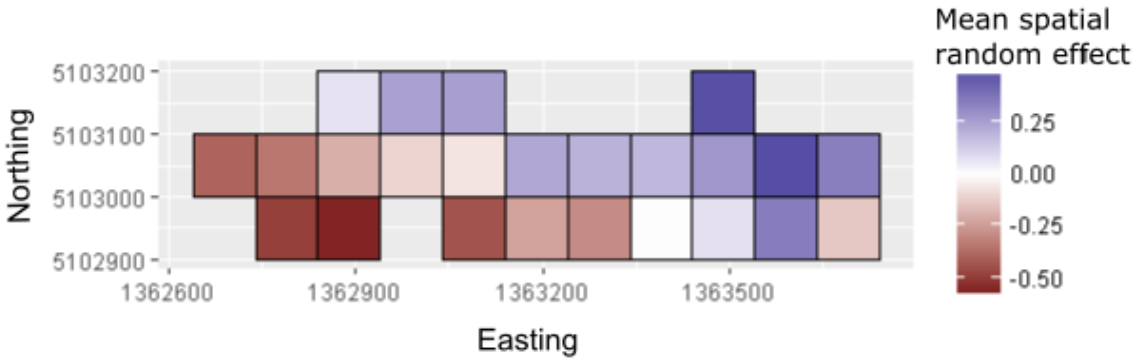

Figure G8 Map of the mean spatial random effects for each grid-cell of the Shelterbelt West site from 2006-2010.

The eastern side of the site had more positive spatial random effects than the western side (Fig. G8). This could mean that more dispersal occurred into the eastern side compared to the western side of the site or that the environmental conditions were more suitable on the eastern side. The spatial random effects terms did not have a large range of variability at this site.

Ohau Village 2006-2011

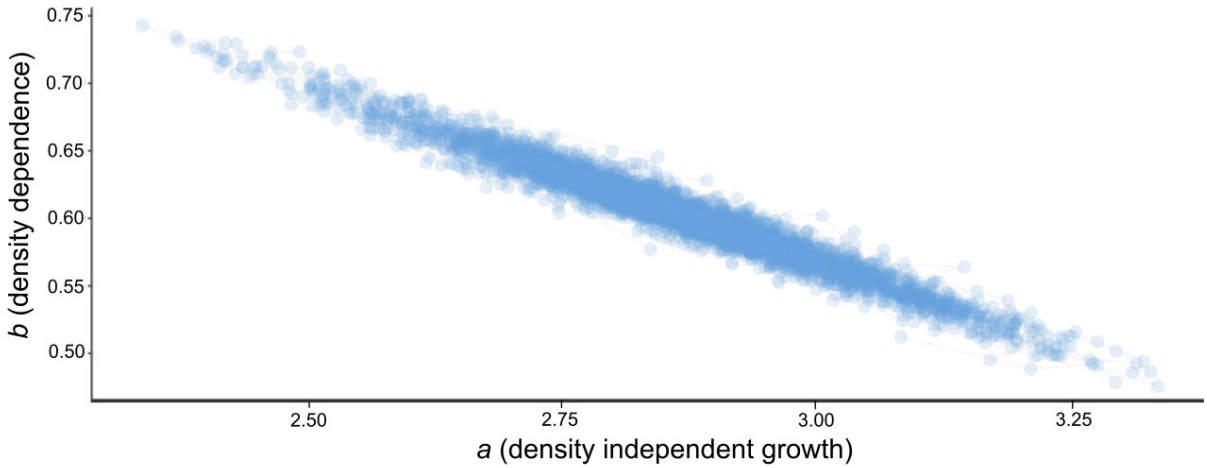

Figure G9 Estimates of density independent growth (*a*) and density dependence (*b*) plotted against each other for the model of the Ohau Village site from 2006-2011.

As with the other sites, the estimates for density independent growth and density dependence are negatively correlated (Fig. G9).

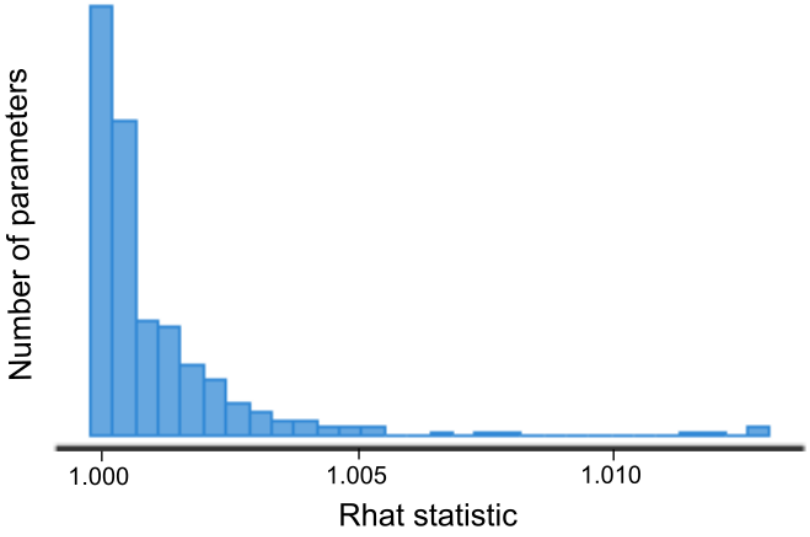

Figure G10 The $\hat{R}$ statistics for all of the model parameter estimates for the Ohau Village site from 2006-2011.

None of the $\hat{R}$ values were above 1.1, meaning that all of the parameter estimates converged (Fig. G10).

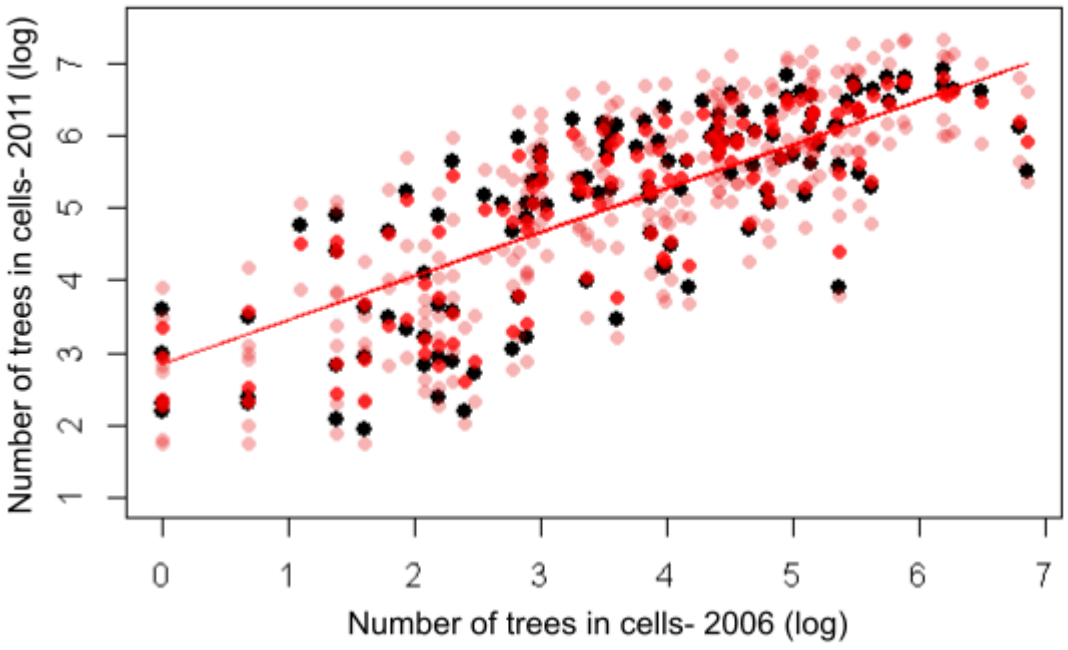

Figure G11 The model predictions for population growth for the Ohau Village site from 2006-2011 (light red and red points) align closely with the observed population growth (black points). Each point represents the growth in one grid-cell. The light red points represent the 95% credible intervals for the predictions and the red points represent the mean prediction estimates. The red line indicates the line of best fit for the model predictions.

All of the observed data (black points) fall within the range predicted by the model (light red and red points) (Fig. G11). This signifies that the population growth model accurately predicted the observed population growth. The red line shows the model's line of best fit through the predicted points.

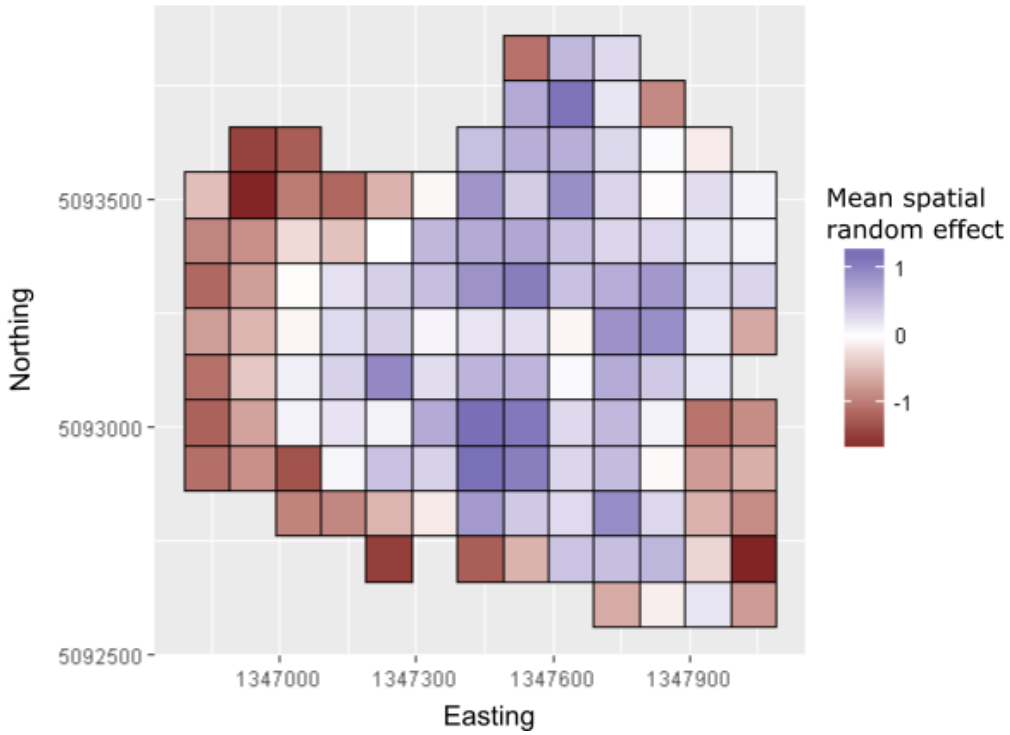

Figure G12 Map of the mean spatial random effects for each grid-cell of the Ohau Village site from 2006-2011.

Many of the negative spatial random effects terms occurred on the edges of this invasion site (Fig. G12), which is possibly due to edge effects. Many of the positive spatial random effects terms occurred in the centre of the invasion site. This could potentially indicate that those cells are being dispersed into more than other cells. It could also potentially indicate that those cells have more suitable environmental conditions for conifers than other cells.

Other Model Checks

I also explored whether the STT estimates were correlated with the area of the site. Plotting the STT against site area (Fig. G13), there did not appear to be any strong correlations in the data, only a slight trend for larger sites having smaller STT values (closer to zero).

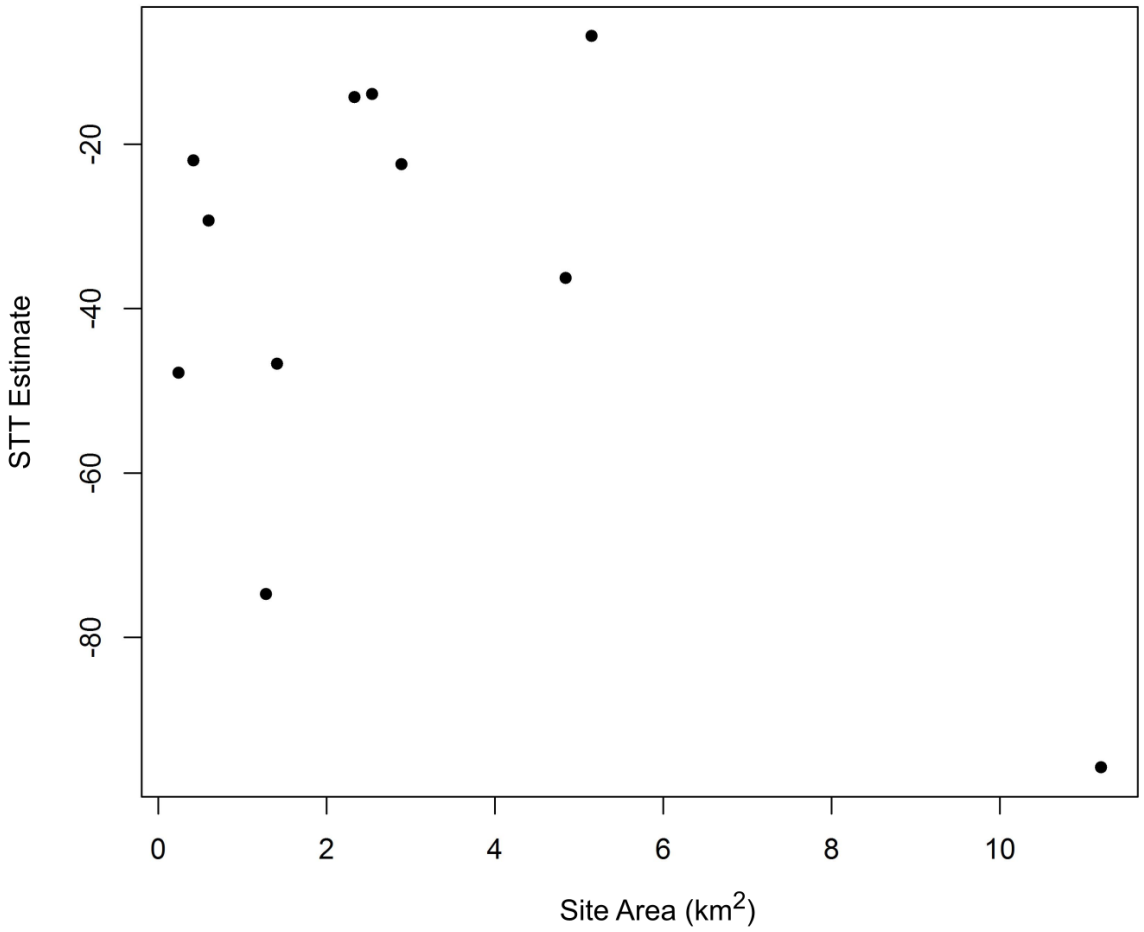

Figure G13 Estimates of STT plotted against the site area for each invasion site and time period examined.